

Functional studies of phototaxis in *Dictyostelium discoideum* mutants

INAUGURAL-DISSERTATION

zur

Erlangung des Doktorgrades
der Mathematisch-Naturwissenschaftlichen Fakultät
der Universität zu Köln



vorgelegt von

Nandkumar Krishna Khaire

aus Solapur, Indien

2003

Referees/Berichterstatter

Prof. Dr. Angelika A. Noegel
Prof. Dr. Siegfried Roth

Date of oral examination/
Tag der mündlichen Prüfung

04.12.2003

The present research work was carried out under the supervision and the direction of Prof. Dr. Angelika A. Noegel in the Institute of Biochemistry I, Medical Faculty, University of Cologne, Cologne, Germany, from October 2000 to December 2003.

Diese Arbeit wurde von Oktober 2000 bis Dezember 2003 am Biochemischen Institut I der Medizinischen Fakultät der Universität zu Köln unter der Leitung und der Betreuung von Prof. Dr. Angelika A. Noegel durchgeführt.

Abstract

Dictyostelium discoideum has proven indispensable to elucidate cytoskeletal dynamics. The cytoskeleton plays a key role in almost all cellular processes, including motility, cytokinesis, cell-to-cell and cell-substrate adhesions and intracellular transport. Several actin binding proteins are also involved in these processes, among them are actin crosslinking proteins (for example, filamin and α -actinin). Filamin (also known as ddfilamin or gelation factor or ABP 120) consists of an actin binding domain and six rod repeats of 100 amino acids, its last repeat being responsible for the formation of the homodimer. Both the domains are necessary for the actin crosslinking activity of filamin. *Dictyostelium* mutants lacking filamin have severe defects in multicellular slug migration towards light, phototaxis, and preferable temperature, thermotaxis. To study the phototaxis defect in filamin⁻ mutants at the molecular level we expressed various domains in the mutant and tested their rescue potential. Expression of C terminally truncated and point mutated (at a putative phosphorylation site) filamin rescued the phototaxis defect partially. Full-length filamin when expressed under the control of the *ecmA* promoter in the anterior tip of the slug rescues the phototaxis, but not when expressed under the control of the *cotB* promoter which allows expression in the posterior $\frac{3}{4}$ th of the slug. Phototaxis is a complex phenomenon, which includes more than 55 genes. To identify genes involved in this process we carried out a microarray analysis. Among 65 genes we selected in microarray analysis, 40 genes were up regulated and 25 genes were down regulated. From the functions of most of these genes, we conclude that the phototactic behaviour of slugs is controlled by extracellular cAMP, Ca²⁺ ions and cell adhesion. To further focus on filamin's function in phototaxis we searched for proteins interacting with filamin by a yeast two hybrid screen and by immunoprecipitation. TipA, GAPA and SapA proteins were pulled down in the immunoprecipitation approach while the FIP, filamin interacting protein, was found earlier in a yeast two hybrid screen. Biochemical studies suggest that FIP is associated with F-actin and may function in vesicle trafficking. Detailed analysis of the mutants of LIM proteins, villidin and filamin for chemotactic migration towards cAMP, led us to conclude that alteration in chemotactic motility of individual cells may not affect the phototactic migration of the slug.

To My Family

ACKNOWLEDGEMENTS

My first, and most earnest, acknowledgment must go to my esteemed advisor, Prof. Dr. Angelika A. Noegel, Institute of Biochemistry I, Medical Faculty, University of Cologne, Cologne, Germany. Her valuable guidance, creative suggestions, constructive criticism and constant encouragement during the course of present investigation are not only praiseworthy but also unforgettable. Her analytical perusal of the manuscript is highly acknowledged. It was indeed a pleasure for me to work under her superb guidance.

I pay my sincere thanks to Dr. Francisco Rivero, who helped me in learning the microscopic work and provided Rac GTPases for checking the interactions with ddfilamin. He has always been the first person I usually run into when I am faced with complicated assays, he always left whatever he was doing to listen to me.

I thank Dr. Ludwig Eichinger, for providing me the lab facilities to carry out microarray analysis and his helpful discussion regarding protein kinases and protein phosphorylation. I also would like to thank Patrick Farbrother, for his help through out the microarray analysis.

I pay my sincere thanks to Dr. Andreas Hasse, Dr. Akis Karakesisoglou and Dr. Budi Tunggal for their suggestions and fruitful discussion during lab meetings and journal clubs.

I am thankful to Rolf for providing technical assistance when required. My thanks are also due to Rosi, for her help during yeast two hybrid screening and monitoring cleanliness in laboratory as well as sitting room. I am also thankful to Monika for introducing the yeast two hybrid system.

The constant cooperation, motivation and nice company provided by Dr. Sonia Ramos, Dr. Michael Leichter, Dr. Somesh Baggavalli and Maria Marko is acknowledged.

My colleagues Henning, Dhamodharan, Hameeda, Sabu, Kumar, Sunil, Deen and Yogikala were very friendly and helpful. Thanks for their company especially during tea and lunchtime.

I also owe a huge debt of gratitude to Bettina Lauss, who made all the necessary official things easy and fast. Far too many people to mention individually have assisted in so many ways during my work at Institute of Biochemistry I can be acknowledged, in particular Maria, Berthold, Kathrin, Bärbel and Roberto.

A penultimate thank-you goes to my wonderful parents for their understanding, endless patience and encouragement when it was most required.

My final, and most heartfelt, acknowledgment must go to my wife Pratibha, for her support, and companionship. For all that, and for being everything I am not, she has my everlasting love. Thanks to little Gouri, my loving daughter for her affection.

Finally, the financial assistance received by me from the DFG is highly acknowledged.

Table of Contents

Chapter	Description	Page(s)
I.	INTRODUCTION	1-8
1.1	<i>Dictyostelium</i> , model organism	1
1.2	Phototaxis in <i>Dictyostelium</i>	3
1.3	Chemotaxis in <i>Dictyostelium</i>	7
II.	MATERIALS AND METHODS	9-41
1	Materials	9
1.1	Laboratory materials	9
1.2	Instruments and equipments	10
1.3	Kits	11
1.4	Enzymes, antibodies, substrates, inhibitors and antibiotics	11
1.5	Chemicals and reagents	13
1.6	Media and buffers	13
1.6.1	Media and buffers for <i>Dictyostelium</i> culture	14
1.6.2	Media for <i>E. coli</i> culture	14
1.6.3	Media and buffers for <i>Yeast</i> culture	15
1.6.4	Buffers and other solutions	16
1.7	Biological materials	18
2	Cell biological methods	19
2.1	Growth of <i>Dictyostelium</i>	19
2.1.1	Growth in liquid nutrient medium	19
2.1.2	Growth on SM agar plates	19
2.2	Development of <i>Dictyostelium</i>	19
2.3	Preservation of <i>Dictyostelium</i>	20
2.4	Transformation of <i>Dictyostelium</i> cells by electroporation	20
2.5	Quantitative Phagocytosis assays	21
3	Molecular biological methods	21
3.1	Purification of plasmid DNA	21
3.2	Digestion with restriction enzymes	22
3.3	Generation of blunt ends in linearised plasmid DNA	22
3.4	Dephosphorylation of DNA fragments	23
3.5	Setting up of ligation reaction	23
3.5.1	Generation of the point mutation	23
3.6	DNA agarose gel electrophoresis	24
3.7	Recovery of DNA fragments from agarose gel	25

Chapter	Description	Page(s)
3.8	RNA formaldehyde-agarose gel electrophoresis	25
3.9	Transformation of <i>E. coli</i>	26
3.9.1	Transformation of <i>E. coli</i> cells by the CaCl ₂ method	26
3.9.2	Transformation of <i>E. coli</i> cell by electroporation	27
3.10	Glycerol stock of bacterial culture	27
3.11	Construction of vectors	28
3.11.1	Vector for the expression of ddfilamin GFP fusion protein	28
3.12	DNA sequencing	28
3.13	Computer analysis	28
4	Methods for Yeast Two Hybrid System	29
4.1	Transformation of Yeast by Lithium Acetate Method	29
4.2	DNA isolation from Yeast	29
4.3	β-galactosidase colony lift assay	30
4.4	Yeast strain maintenance	30
5	Biochemical Methods	31
5.1	Preparation of total protein from <i>Dictyostelium</i>	31
5.2	SDS-polyacrylamide gel electrophoresis	31
5.3	Native or Nondenaturing PAGE	32
5.3.1	Coomassie blue staining of SDS-polyacrylamide gels	33
5.3.2	Silver staining polyacrylamide gels	33
5.4	Immunoprecipitation from <i>Dictyostelium</i> cell lysate	33
5.5	Detection of phosphorylation	34
5.6	Western blotting using the semi-dry method	34
5.7	Immunodetection of membrane-bound proteins	34
5.8	Video imaging and chemotaxis assay	35
5.9	Qualitative phototaxis assay	35
6	Immunological methods	36
6.1	Direct immunofluorescence of <i>Dictyostelium</i> cells	36
6.1.1	Preparation of <i>Dictyostelium</i> cells	36
6.1.2	Methanol fixation	36
6.1.3	Picric acid-paraformaldehyde fixation	36
6.1.4	Immunolabeling of fixed cells	37
6.1.5	Mounting of coverslips	37
6.2	Preparation of heat-killed yeast cells	38
6.3	TRITC-labeling of heat-killed yeast cells	38

Chapter	Description	Page(s)
7	Microscopy	38
7.1	Live cell imaging of <i>Dictyostelium</i> cells expressing RN/GFP	39
7.2	Live cell imaging of RN-GFP during phagocytosis	39
7.3	Microscopy of the fixed preparations	39
8	Microarray analysis	39
8.1	RNA preparation	40
8.2	Spiking of internal mRNA controls	40
8.3	Quantitation, normalization and data analysis	41
8.4	Signal Quantification	41
III.	RESULTS	42-72
1	Biochemical studies	42
1.1	Overexpression of domains of filamin	42
1.2	Localisation and distribution of ddfilamin domains during growth	44
1.3	Expression of full-length ddfilamin GFP fusion protein in GA1 compensates the loss of α -actinin	44
1.3.1	The ddfilamin rod domain GFP fusion protein (RN-GFP) does not localise properly in HG1264 cells	46
1.3.2	Ddfilamin rod domain GFP fusion protein (RN-GFP) forms heterodimers with the endogenous protein	49
1.3.3	A GFP tag located at the C-terminus does not interfere with the dimerisation property of filamin	49
1.4	Detection of phosphorylation and generation of a point mutation	50
1.4.1	Generation of the point mutation	51
1.4.2	Expression and localisation of the mutated protein	51
2	Role of filamin in phagocytosis	52
2.1	Overexpression of the filamin rod domain reduces relative phagocytosis in AX2 as well as in mutant cells	52
3	Phototaxis in mutant strain and rescue experiments	54
3.1	Expression of full-length ddfilamin and full-length ddfilamin with a mutation at the predicted phosphorylation site rescues the phototaxis defect.	55
3.2	Rescue of phototactic defect with filamin domains	56
3.3	The requirement of the dimerisation domain for the rescue behavior of ddfilamin	57
3.4	Expression of full length ddfilamin at the anterior tip of the slug is necessary to rescue the phototactic defect	58

Chapter	Description	Page(s)
4	Identification and characterisation of binding partners for filamin	59
4.1	FIP, a novel protein interacts with filamin	60
4.1.1	Construction of a full-length FIP cDNA	60
4.1.2	Localisation of FIP does not change in HG1264	62
4.1.3	FIP may have a role in vesicle transport	62
4.1.4	FIP is associated with the actin cytoskeleton	63
4.4	Immunoprecipitation revealed the identification of TipA, SapA, and GAPA as ddfilamin associated proteins, suggesting a role for filamin in cell morphogenesis and actin remodeling.	64
4.3	Checking the interaction of filamin with Rho GTPases by yeast two hybrid screening.	65
5	Microarray analysis suggests that mutant slugs have elevated extracellular cAMP levels and lowered cell adhesion.	67
6	Chemotactic motility of mutants in actin binding proteins	69
6.1	Filamin minus cells chemotax normally	69
6.2	LimD ⁻ cells have a defect in chemotaxis but have normal phototaxis	69
6.3	The villidin ⁻ mutant has a defect in chemotaxis as well as in phototaxis	71
IV.	DISCUSSION	73-83
1.	Subcellular localisation of ddfilamin and its domains.	73
2.	F-actin crosslinking by ddfilamin is essential for the rescue of the phototaxis defect in ddfilamin ⁻ mutants.	75
3.	Filamin in the tip region is essential for slug movement and phototaxis.	78
4.	Interaction partners of filamin suggest a diverse function for the protein.	78
5.	FIP may function in membrane traffic.	80
6.	Microarray analysis suggests that the phototaxis defect in ddfilamin ⁻ mutants may be due to reduced cell adhesion and defective cAMP wave propagation.	80

Chapter	Description	Page(s)
V.	SUMMARY/ZUSAMMENFASSUNG	84-88
VI.	BIBLIOGRAPHY	89-102
VII.	ABBREVIATIONS	103
	Erklärung	-
	Curriculum Vitae/Lebenslauf	-

I. Introduction

1. *Dictyostelium* as a model organism for cytoskeletal studies

Dictyostelium discoideum, a soil living social amoeba feeds on yeast and bacteria in its natural habitat and has become an attractive tool for the study of the actin cytoskeleton and related proteins because of the following reasons: (i) The organism can be grown in the laboratory easily on bacterial lawns or in shaking culture (axenically). (ii) It undergoes a developmental cycle, which allows researchers to study a variety of changes that occur during development of a multicellular organism. (iii) Manipulation of genes can be done by homologous recombination or REMI (Restriction Enzyme Mediated Integration) (Kuspa and Loomis, 1992) and is easy because the organism is haploid. Overexpression of gene/s using nonintegrating vectors can be easily achieved, which allows studying the live dynamics of proteins or domains of protein by fusing with Green Fluorescence Protein (GFP). (iv) *Dictyostelium* carries all classes of actin binding proteins, which can be found in all eukaryotes and thus can be compared with mammalian cells. (v) The ongoing *Dictyostelium* genome project, which is likely to be finished by the end of this year and the Japanese cDNA project add great advantage to the study of the organism (Schleicher and Noegel, 1992 and Noegel and Luna, 1995).

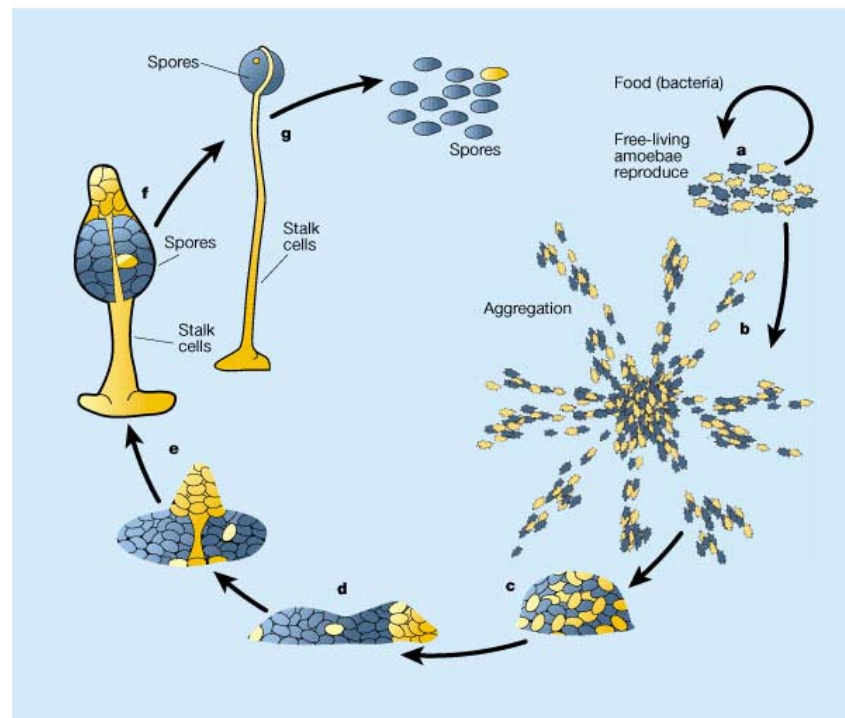


Figure 1: The asexual life cycle of *Dictyostelium discoideum*. **a**, *Dictyostelium* amoebae live off bacteria in the soil. **b**, When the bacteria are consumed and starvation is imminent, the amoebae stop dividing and activate several genes that allow them to aggregate by chemotaxis towards cyclic AMP diffusing from centrally located cells. These aggregates, which can contain up to 100,000 cells, transform into motile slugs (**c**, **d**) and finally into fruiting bodies (**e–g**). The fruiting bodies contain 80,000 viable spores supported by 20,000 dead stalk cells. (Graphic from Kessin 2000.) Blue and yellow colours for the cells indicate two different natural isolates. For a dynamic view of *Dictyostelium* development see <http://dicty.cmb.nwu.edu/dicty/pnd/>

The actin cytoskeleton has a dynamic role in the life cycle of *Dictyostelium*, it gives shape to the cells and controls cell movement, cell division and intracellular vesicle transport. A variety of actin-binding proteins are present in the cells controlling assembly and disassembly of actin. Among these actin-binding proteins are F-actin cross-linking proteins, capping protein, severing proteins, monomer-binding proteins, membrane anchors and motor proteins. The localization and crosslinking of filamentous actin (F-actin) into bundles and networks is mediated by multiple families of cytoskeletal proteins, of which several share an α -actinin-like conserved F-actin binding domain (ABD) (Matsudaira, 1991, Otto 1994 and Troys *et al.* 1999). To date, eleven different actin crosslinking proteins have been identified in *Dictyostelium*, including a filamin-like protein (Hock and Condeelis, 1987), spectrin-like protein (Bennett and Condeelis 1988), ddfilamin (also termed as ddFLN gelation factor or ABP120) (Condeelis *et al.* 1981 and Noegel *et al.* 1989), α -actinin (Brier *et al.* 1983 and Noegel *et al.* 1987), elongation factor 1a (Demma, 1990), comitin (Weiner *et al.* 1993), a 30

kDa bundling protein (Bross, 1985), a 34 kDa protein (Fechheimer and Taylor, 1984, Fechheimer, 1987, Fechheimer *et al.* 1992), cortexellin I and II (Faix *et al.* 1992) and fimbrin (Prassler *et al.* 1997).

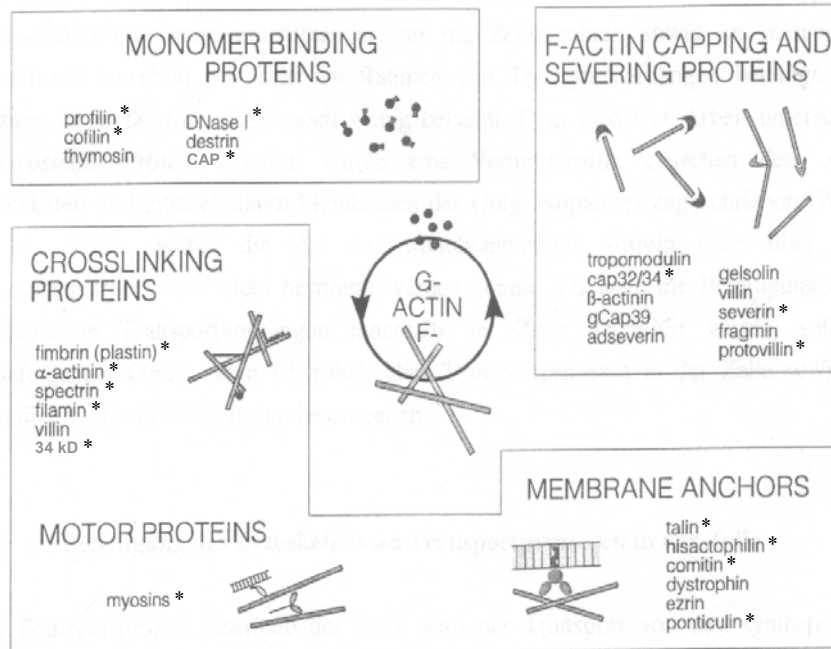


Figure 2: Actin-binding proteins and their function (Schleicher *et al.* 1995). Actin-binding proteins influence the equilibrium between monomeric G-actin and filamentous F-actin as well as the structural organization of the network of actin filaments by either binding to monomeric actin and inhibiting polymerisation, or crosslinking, capping, severing, anchoring or moving the actin filaments by binding to actin filaments. The asterisk indicates actin-binding proteins that have been reported in *Dictyostelium*.

1.2 Phototaxis in *Dictyostelium*

Dictyostelium discoideum is widely used as a simple model organism for multicellular development (Maeda *et al.* 1997 and Gross, 1994). *Dictyostelium* live as individual amoebae in soil, preying on bacteria. But when food runs out and starvation is imminent, the previously independent amoebae form dendritic aggregation streams, which break up into groups of up to 10^5 cells (Shaffer, 1957 and Kessin, 2001) before they form cylindrical migrating slugs. Slugs are sensitive to light, pH, and even slight differences in temperature, which allows them to migrate toward an optimal location for fruiting. Slugs are polar with a tip at the anterior consisting of prestalk cells whereas the posterior consists predominantly of prespore cells. Phototactic turning is initiated in the tip and slugs sense the light only at the anterior prestalk zone (Francis, 1964, Poff and Loomis, 1973 and Fisher *et al.* 1984). Using the tools that are available in *Dictyostelium*, phototaxis and thermotaxis can be addressed at a molecular level.

Several groups isolated membrane bound photoreceptors and analysed the absorption spectrum (Poff and Butler, 1974, Poff *et al.* 1974 and Hader and Lebert, 1994). Schlenkrich *et al.* 1995a isolated a 45.5 kDa putative photoreceptor from *Dictyostelium*, the absorption spectrum of which closely resembled the action spectrum for *Dictyostelium* phototaxis Schlenkrich *et al.* 1995b, leading to the conclusion that this protein might play an important role in the photoreception of *Dictyostelium* amoebae.

Two models have been proposed to explain phototactic turning (Poff and Loomis, 1973, Fisher *et al.* 1984 and Fisher 1997). The optical model assumes that the pseudoplasmodium acts as a cylindrical lens, causing stronger stimulation of light locally and speeding up cell movement in the tip thus leading to bending of the anterior zone toward the light source. The signal transduction or sign reversal model assumes that light acts directly on physiological processes of the cell and cell-cell signalling by shifting the position of the organising centre in the tip. In agreement with both of these hypotheses Miura and Siegert (2001) found that light acts directly on the cAMP-signalling system and cell movement. Upon light irradiation, aggregating cells change their periodicity of cAMP signalling and cells in the slug tip release cAMP. They also found that concomitant changes in cell movement occurred in slug cells. But these results do not explain the thermotaxis (Smith *et al.* 1982), where slugs migrate to a preferred temperature in the dark, neither do they explain data obtained with ddfilamin mutant cells, which have a clear phototaxis deficiency and migrate over shorter distances in the darkness as well as in horizontally directed light (Wallraff and Wallraff, 1997).

The anterior tip of the slug mostly consists of prestalk cells that control the migration of the slug. The tip shows average high concentration of cAMP, while the posterior prespore cells contain lower average concentration (Dormann and Weijer, 2001). Elevated level of cAMP is necessary for the maintenance of the tip, generation of a scroll wave and for the migration of anterior like cells (ALCs) from posterior region cells of the slug. Consistent with these observations, the multicellular aggregates overexpressing extracellular phosphodiesterase do not form a tip. Dormann and Weijer (2001) injected cAMP into the tip of slugs and found that higher concentrations (10^{-2} M) of cAMP are needed to disturb the wave generated at the tip.

Darcy *et al.* (1994) suggested an intermediary role for cGMP in photosensory and thermosensory processing in slugs and amoebae. They found all phototaxis mutant strains

(mutants were derived from the X22 strain with mutation in phototaxis loci) with altered cGMP responses to light and heat were unaltered in their cGMP response to a cAMP pulse, concluding that cAMP and light/heat regulate cGMP via independent pathways.

Several experiments have suggested a role for RasD in the correct proportioning of the prespore and prestalk cells in differentiation (Reymond *et al.* 1986 and Louis *et al.* 1997). Furthermore, RasD⁻ null cells exhibit a phototaxis and thermotaxis defect and were not able to orient correctly, suggesting a role for RasD in the modulation of morphogenetic signaling by the photo- and thermo-receptors (Willkins *et al.* 2000).

Villidin is a novel multidomain protein (190 kDa) containing a N-terminal WD repeat, three PH domains in the middle of the molecule, and five gelsolin-like segments, followed by a villin-like headpiece at the C-terminal end. The protein is prominently expressed in the slug stage (Gloss *et al.* 2003). The villidin-minus slugs exhibited a phototaxis defect. The mutant slugs migrate over a shorter distance and not as directed towards light as wild type slugs. The expression of the WD domain in the mutant background caused a more direct movement of the slugs towards the light source, whereas the gelsolin/villin region did not exhibit any rescuing potential.

Recently, another *Dictyostelium* protein has been described that has some similarity to villidin, GRP125, a new gelsolin-related protein. In the absence of GRP125, slugs fail to readjust their orientation correctly. Analysis of the GRP125-deficient mutant showed that GRP125 is required for coupling photodetection to the locomotory machinery of slugs (Stocker *et al.* 1999).

Li *et al.* (2001) explained the role of Sphingosine-1-phosphate (S-1-P) lyase, an enzyme that functions in fatty acid metabolism and controls the slug migration. S-1-P lyase null mutant show extremely limited directional migration, the slugs developed directly at the site of aggregation. The authors suggest that the phototaxis defect might be due to aberrant actin distribution and abnormal cell morphogenesis in mutant slugs.

Wallraff and Wallraff (1997) tested behavioural deficits in the slugs of three mutant strains of *Dictyostelium* lacking different F-actin binding proteins, among them two were F-actin crosslinking proteins. Two strains, defective in the production of either α -actinin or severin (an actin capping and severing protein), did not show changes in slug behavior. Slugs of the

mutant lacking ddfilamin, however, migrated shorter distances in the darkness as well as in horizontally directed light. More remarkably, they migrated at an angle of approximately 45° to the left or right of the incident light, whereas wild-type slugs migrated on fairly straight paths towards the light. The author concluded that, as these mutants are known to lack a constituent of the cytoskeleton, alterations in the cytoskeletal architecture might cause alterations in the optical properties of cell structures, which are of importance in the specific mechanism underlying slug phototaxis.

Genetic analysis of slug behaviour suggests that as many as 55 genes are involved in phototaxis and that several of the encoded proteins regulate signal transduction pathways involving the intracellular messengers cAMP, cGMP, IP_3 and Ca^{2+} (Darcy 1994, Fisher *et al.* 1997 and Fisher, 1997). But ddfilamin emerged as the only protein directly associated with the actin cytoskeleton, which had a significant role in *Dictyostelium* phototaxis.

Structurally filamins are homodimers with large polypeptide chains that associate at their carboxyl termini (Gorlin *et al.* 1990 and Fucini *et al.* 1999). Their conserved amino-terminal actin binding domains consist of two calponin homology domains common to the members of the α -actinin/spectrin superfamily of actin-binding proteins (Hartwig, 1994). The rest of the polypeptide forms 24 repeated domains of ~ 96 amino acids, each made up of seven antiparallel β -strands that produce an immunoglobulin fold (Fucini *et al.* 1997). The *Dictyostelium* filamin has a shorter elongated domain, consisting of only six rod like repeats of 100 amino acids (Noegel *et al.* 1989). Its dimerisation is mediated via the formation of intramolecular β -sheets between the rod domains 6, leading to an antiparallel arrangement of the two monomer chains (McCoy *et al.* 1999 and Fucini *et al.* 1999). *Dictyostelium* mutants lacking filamin have defects in the structure of the actin cytoskeleton and exhibit reduced cross-linking of actin filaments, leading to reduced size and frequency of pseudopods. This results in a decreased motility, chemotaxis and phagocytosis of the mutant cells (Cox *et al.* 1992 and 1995).

Recent studies suggested that the function of the filamins is not only in maintaining the cortical actin network but also the organisation and stabilisation of these networks by interwebbing them with membrane proteins and receptors. Thus filamins interact with several membrane receptors: the cytoplasmic part of the glycoprotein Ib IX complex, the receptor for von Willebrand factor (Andrews and Fox, 1991 and Takafuta *et al.* 1998), β_1 - and β_2 -integrins

(Sharma *et al.* 1995 and Loo *et al.* 1998) and α - and β -sarcoglycan (Thompson *et al.* 2000) were all identified as ligands for filamin. Filamins also affect intracellular trafficking of proteins and signal transduction. Filamin influences the activity of furin, a protease that is involved in the proteolytic processing of many proproteins, by promoting its internalisation (Zent *et al.* 2000). It binds to presenilin-1, a protein involved in early onset familial Alzheimer's disease and in the notch signalling pathway (Zhang *et al.* 1998, Schwarzman *et al.* 1999) and interacts with caveolin-1, a multifunctional protein with roles in caveolae biogenesis, endocytic events, cholesterol transport and various signal transduction processes (Stahlhut and Deurs, 2000). Furthermore, the involvement of filamin in signal transduction is confirmed by its interaction with several components of the NF κ B pathway (Edwards *et al.* 1997, Marti, 1997 and Leonardi *et al.* 2000) and the small GTPases RhoA, Rac1, Cdc42 and RalA (Ueda *et al.* 1992, Ohta *et al.* 1999, Bellanger *et al.* 2000 and Pi *et al.* 2002).

Human filamin is also strongly phosphorylated *in vivo*, which affects its interaction with several proteins such as GTPases and might also affect the F-actin binding capacity and crosslinking activity. Phosphorylation is mainly on serine and threonine residues and is achieved by a variety of kinases (cAMP-kinase, PKC and CaM-kinase II) (Ohta and Hartwig, 1995 and Tiggs *et al.* 2003).

To understand the role of ddfilamin in phototaxis we performed rescue studies by expressing the actin binding domain, rod domain, C terminally truncated ddfilamin (which can no longer crosslink actin filaments) and point mutated ddfilamin (at suspected phosphorylation site). As the anterior tip of the slug controls its migration, we expressed ddfilamin under the control of cell type specific promoters to test whether it plays a functional role there. We also studied global gene expression pattern in the mutant by microarray analysis in order to identify genes that involved in this process. Furthermore, we checked the interaction of this protein with small GTP binding proteins by using the yeast two hybrid system. With an immunoprecipitation assay we found three proteins interacting with ddfilamin, which might help ddfilamin to perform its role in the phototactic migration.

1.3 Chemotaxis in *Dictyostelium*

Cells sense and respond to signals in the extracellular environment. Many cells have the capacity to detect the direction and intensity of an extracellular chemical gradient and respond by directed migration toward the source of the chemical. This process is called chemotaxis. Chemotaxis results from a localised polymerisation of F-actin leading to the formation of a

new lamellipod or pseudopod, cell polarisation, and the forward protrusion of the leading edge. Phosphoinositide 3-Kinase plays a central role in establishing and maintaining cell polarity by regulating the subcellular localisation and activation of down stream effectors that are essential for regulating cell polarity and proper chemotaxis. In addition, other proteins, among them actin-binding proteins, are crucial for the establishment of polarity and for chemotaxis.

Here we have analysed chemotactic migration of LimC^- , LimD^- , LimC^-/D^- and villidin mutants. LimC and LimD are LIM domain containing proteins that directly associate with F-actin. LimD^- and LimC^-/D^- were found to have a defect in chemotaxis. Reexpression of LimD -GFP in both cells rescued the defect stating that the defect found is due to the loss of function of LimD (Khurana *et al.* 2002). Villidin is a novel protein with WD and PH domains, which are associated with signal transduction and a C-terminal gelsolin like domain followed by a villin headpiece, which normally bundles F-actin very strongly. The headpiece in villidin however, does not bind to F-actin (Vardar *et al.*, 2002). We also studied the migration behaviour of villidin mutants and found that was also altered (Gloss *et al.* 2003).

II. Materials and Methods

1. Materials

1.1 Laboratory materials

Cellophane sheet, Dry ease	Novex
Centrifuge tubes, 15 ml,	Greiner
Coverslips (glass), Ø12 mm, Ø18 mm, Ø55 mm	Assistent
Corex tube, 15 ml, 50 ml	Corex
Cryo tube, 1 ml	Nunc
Electroporation cuvette, 2 mm electrode gap	Bio-Rad
Gel-drying frames	Novex
Microcentrifuge tube, 1.5 ml, 2.2 ml	Sarstedt
Micropipette, 1-20 µl, 10-200 µl, 100-1,000 µl	Gilson
Micropipette tips	Greiner
Multi-channel pipette	Finnigan
Needles (sterile), 18G–27G	Terumo, Microlance
Nitrocellulose membrane, BA85	Schleicher and Schuell
Nitrocellulose-round filter, BA85, Ø82 mm	Schleicher and Schuell
Nuclepore® membrane filter	Nuclepore
Nylon membrane	Biodyne B Pall

Parafilm	American Nat Can
Pasteur pipette, 145 mm, 230 mm	Volac
PCR soft tubes, 0.2 ml	Biozym
Petri dish (35 mm, 60 mm, 100 mm)	Falcon
Petri dish (90 mm)	Greiner
Plastic cuvette, semi-micro	Greiner
Plastic pipettes (sterile), 1 ml, 2 ml, 5 ml, 10 ml, 25 ml	Greiner
Quartz cuvette Infracil	Hellma
Quartz cuvette, semi-micro	Perkin Elmer
Saran wrap	Dow
Scalpels (disposable), Nr. 10, 11, 15, 21	Feather
Slides, 76 x 26 mm	Menzel
Syringes (sterile), 1 ml, 5 ml, 10 ml, 20 ml	Amefa, Omnifix
Syringe filters (Acrodisc), 0.2 µm, 0.45 µm	Gelman Sciences
Whatman 3MM filter paper	Whatman
X-ray film, X-omat AR-5, 18 x 24 mm, 535 x 43 mm	Kodak

1.2. Instruments and equipments

Centrifuges (microcentrifuges):

Centrifuge 5417 C	Eppendorf
Centrifuge Sigma B	Braun
Cold centrifuge Biofuge fresco	Heraeus Instruments

Centrifuges (table-top, cooling, low speed):

Centrifuge CS-6R	Beckman
Centrifuge RT7	Sorvall
Centrifuge Allegra 21R	Beckman

Centrifuges (cooling, high speed):

Beckman Avanti J25	Beckman
Sorvall RC 5C plus	Sorvall

Centrifuge-rotors:

JA-10	Beckman
JA-25.50	Beckman
SLA-1500	Sorvall
SLA-3000	Sorvall
SS-34	Sorvall

Dounce homogeniser, 10 ml

B. Braun

Electrophoresis power supply, Power-pac-200, -300

Bio-Rad

Electroporation unit Gene-Pulser

Bio-Rad

Fluorimeter

PTI

Freezer (-80 °C)

Nunc

Freezer (-20 °C)

Siemens, Liebherr

Gel-documentation unit

MWG-Biotech

Heating block DIGI-Block JR

NeoLab

Heating block, Dry-Block DB x 20

Techne

Hybridization oven

Hybaid

Ice machine

Ziegra

Incubators:

Incubator, microbiological	Heraeus
----------------------------	---------

Incubator with shaker Lab-Therm	Kuehner
---------------------------------	---------

Laminar flow, Hera Safe (HS 12)

Heraeus

Magnetic stirrer, MR 3001 K

Heidolph

Microcontroller	Luigs and Newmann
Microscopes:	
Light microscope, CH30	Olympus
Light microscope, DMIL	Leica
Light microscope, CK2	Olympus
Fluorescence microscope, DMR	Leica
Fluorescence microscope, 1X70	Olympus
Confocal laser scanning microscope, DM/IRBE	Leica
Stereomicroscope, SZ4045TR	Olympus
Oven, conventional	Heraeus
PCR machine, PCR-DNA Engine PTC-200	MJ Research
pH-Meter	Knick
Refrigerator	Liebherr
Semi-dry blot apparatus, Trans-Blot SD	Bio-Rad
Shakers GFL	Kuehner
Sonicator, Ultra turrax T25 basic	IKA Labortechnik
Speed-vac concentrator, DNA 110	Savant
Spectrophotometer, Ultraspec 2000, UV/visible	Pharmacia Biotech
Ultracentrifuges:	
Optima TLX	Beckman
Optima L-70K	Beckman
Ultracentrifuge-rotors:	
TLA 45	Beckman
TLA 100.3	Beckman
SW 41	Beckman
UV-crosslinker UVC 500	Hoefer
UV- transilluminator TFS-35 M	Faust
Vortex, REAX top	Heidolph
Video cameras	
JAI CV-M10 CCD Camera	Stemmer Imaging
SensiCam	PCO Imaging
Waterbath	GFL
X-ray-film developing machine, FPM-100A	Fujifilm

1.3 Kits

FairPlay™ Microarray labeling kit	Stratagene
Nucleobond AX	Macherey-Nagel
NucleoSpin Extract 2 in 1	Macherey-Nagel
Nucleotrap	Macherey-Nagel
Original TA Cloning	Invitrogen
pGEM-T Easy	Promega
Qiagen Midi- and Maxi-prep	Qiagen
Qiagen RNeasy Midi/Mini Kit	Qiagen
Stratagene Prime It II	Stratagene

1.4 Enzymes, antibodies, substrates, inhibitors and antibiotics

Enzymes used in the molecular biology experiments:

Calf Intestinal Alkaline Phosphatase (CIAP)	Roche
Klenow fragment (DNA polymerase)	Roche
Lysozyme	Sigma

Protein A Sepharose CL-4B	Amersham
Proteinase K	Sigma
Restriction endonucleases	Amersham, New England Biolabs
Ribonuclease A (RNase A)	Sigma
S1-nuclease	Amersham
T4 DNA ligase	Roche
<i>Taq</i> -polymerase	Roche

Primary antibodies:

Mouse anti-actin monoclonal antibody Act 1-7 (Simpson <i>et al.</i> 1984)	
Mouse anti-GFP monoclonal antibody K3-184-2 (Gloss <i>et al.</i> 2003)	
Mouse anti-filamin-monoclonal Antibody 82-421-5 (Brink <i>et al.</i> 1989)	
Mouse anti-filamin- monoclonal antibody 82-454-12 (Brink <i>et al.</i> 1989)	
Mouse anti-csA monoclonal antibody 33-294-17 (Bertholdt <i>et al.</i> 1985)	
Mouse anti- α -actinin monoclonal antibody 47-60-8 (Schleicher <i>et al.</i> 1984)	
Mouse anti-FIP230 monoclonal antibody K12-349-7 (Knuth, 2002 Ph. D Thesis)	
Mouse anti-FIP230 monoclonal antibody K12-362-6 (Knuth, 2002 Ph. D Thesis)	
Mouse anti-FIP230 monoclonal antibody K12-454-2 (Knuth, 2002 Ph. D Thesis)	
Goat anti-GST antibody (Amersham).	
Rabbit Phospho-Serine/Threonine polyclonal Antibody (Cell Signaling Technology)	
Rabbit Phospho-Threonine polyclonal Antibody (Cell Signaling Technology)	

Secondary antibodies:

Goat anti-mouse IgG, peroxidase conjugated	Sigma
Goat anti-rabbit IgG, peroxidase conjugated	Sigma
Mouse anti-goat IgG, peroxidase conjugated	Sigma
Sheep anti-mouse IgG, I ¹²⁵ conjugated	Amersham

Inhibitors:

Benzamidin	Sigma
β -glycerophosphate	Sigma
Complete Mini®, Protease inhibitor cocktail tablets	Roche
Diethylpyrocarbonate (DEPC)	Sigma
Leupeptin	Sigma
Pepstatin	Sigma
Phenylmethylsulphonyl fluoride (PMSF)	Sigma
Sodium Fluoride	Sigma
Sodium orthovanadate	Sigma
Sodium pyrophosphate	Sigma

Antibiotics:

Ampicillin	Gruenthal
Blasticidin S	ICN Biomedicals
Chloramphenicol	Sigma
Dihydrostreptomycinsulfate	Sigma
Geneticin (G418)	Life Technologies
Kanamycin	Sigma, Biochrom
Tetracyclin	Sigma

1.5 Chemicals and reagents

Most of the chemicals and reagents were obtained either from Sigma, Fluka, Difco, Merck, Roche, Roth or Serva. Those chemicals or reagents that were obtained from companies other than those mentioned here are listed below:

Acetic acid (98-100%)	Riedel-de-Haen
Acrylamide (Protogel: 30:0,8 AA/Bis-AA)	National Diagnostics
Agar-Agar (BRC-RG)	Biomatic
Agarose (Electrophoresis Grade)	Life Technologies
3-Amino-1, 2, 4-triazol	Sigma
Amino acids	Sigma
Bacto-Agar	Difco
Bacto-Pepton	Difco
Bacto-Trypton	Difco
5-Brom-4-chlor-3-indolyl- β -D-galactopyranosid (X-Gal)	Roth
Bromphenolblue (Na-Salt)	Serva
BSA (Bovine serum albumin)	Roth
Calciumchlorid-Dihydrat	Merck
Chloroform	Riedel-de-Haen
Coomassie-Brilliant-Blue G 250	Roche
Coomassie-Brilliant-Blue R 250	Serva
p-Cumaric acid	Fluka
Cyclohexamide	Sigma
1,4-Dithiothreitol (DTT)	Gerbu
Dimethylformamide	Riedel-de-Haen
Ethanol	Riedel-de-Haen
Ethylen diamine tetraaceticacid (EDTA)	Merck
Ethylenglycolbis [2-aminoethylether]-	
Glycerine	Riedel-de-Haen
Isopropyl-D-thiogalactopyranoside (IPTG)	Loewe Biochemica
Methanol	Riedel-de-Haen
Morpholino propane sulphonic acid (MOPS)	Gerbu
N- [2-Hydroxyethyl] piperazine-N'-2-	
-ethanesulfonic acid (HEPES)	Biomol
Sodium dodecyl sulphate (SDS)	Serva
Sodium hydroxide	Riedel-de-Haen
Triton X-100	Merck
Tween 20	Roth
Yeast Nitrogen Base	Difco
<u>Radiolabelled nucleotide:</u>	
α - ³² P-deoxyadenosine triphosphate, (10 mCi/ml)	Amersham

1.6 Media and buffers

All media and buffers were prepared with deionised water filtered through an ion-exchange unit (Membra Pure). The media and buffers were sterilized by autoclaving at 120 °C and

antibiotics were added to the media after cooling to approx. 50 °C. For making agar plates, a semi-automatic plate-pouring machine (Technomat) was used.

1.6.1 Media and buffers for *Dictyostelium* culture

AX2-medium (Claviez *et al.* 1982), pH 6.7:

7.15 g yeast extract
14.3 g peptone (proteose)
18.0 g maltose
0.486 g KH_2PO_4
0.616 g $\text{Na}_2\text{HPO}_4 \cdot 2\text{H}_2\text{O}$
add H_2O to make 1 litre

Soerensen phosphate buffer (Malchow, 1972), pH 6.0:

2 mM Na_2HPO_4
14.6 mM KH_2PO_4

Phosphate agar plates, pH 6.0:

9 g agar
add Soerensen phosphate buffer, pH 6.0 to make
1 litre

Salt solution (Bonner, 1947):

10 mM NaCl
10 mM KCl
2.7 mM CaCl_2

SM agar plates(Sussman, 1951), pH 6.5:

9 g agar
10 g peptone
10 g glucose
1 g yeast extract
1 g $\text{MgSO}_4 \cdot 7 \text{H}_2\text{O}$
2.2 g KH_2PO_4
1 g K_2HPO_4
add H_2O to make 1 litre

1.6.2 Media for *E. coli* culture

LB medium (Sambrook, 1989), pH 7.4:

10 g bacto-tryptone
5 g yeast extract
10 g NaCl
adjust to pH 7.4 with 1 N NaOH
add H_2O to make 1 litre

For LB agar plates, 0.9% (w/v) agar was added to the LB medium and the medium was then autoclaved. For antibiotic selection of *E. coli* transformants, 50 mg/l ampicillin, kanamycin or chloramphenicol was added to the autoclaved medium after cooling it to approximately 50°C. For blue/white selection of *E. coli* transformants, 10 µl 0.1 M IPTG and 30 µl X-gal solution (2% in dimethylformamide) was spread per 90 mm plate and the plate was incubated at 37°C for at least 30 min before using.

SOC medium (Sambrook, 1989), pH 7.0: 20 g bacto-tryptone
5 g yeast extract
10 mM NaCl
2.5 mM KCl
dissolve in 900 ml deionised H₂O
adjust to pH 7.0 with 1 N NaOH

The medium was autoclaved, cooled to approx. 50°C and then the following solutions, which were separately sterilized by filtration (glucose) or autoclaving, were added:

10 mM MgCl₂·6 H₂O
10 mM MgSO₄·7 H₂O
20 mM glucose
add H₂O to make 1 litre

1.6.3 Media and buffers for *Yeast* culture

YEPD-Medium:

20 g/l Difco Pepton
10 g/l Yeast extract

YEPD-Agar plates:

20 g/l Difco Pepton
10 g/l Yeast extract
18 g/l Agar agar

100 x Adenine solution:

200 mg (1,1 mmol) Adenine in 100 ml water dissolve with addition of little amounts of HCl and filter sterilize.

100 x Tyrosine solution:

300 mg (1,7 mmol) Tyrosin in 100 ml dissolve with addition of NaOH solution and filter sterilize.

100 x Histidine solution:

200 mg (1 mmol) Histidine in 100 ml Water and filter sterilize.

100 x Leucine solution:

1000 mg (7,6 mmol) Leucin in 100 ml Water and filter sterilize.

100 x Tryptophan solution:

200 mg (1 mmol) Tryptophan in 100 ml Water filter sterilize.

100 x Uracil solution:

200 mg (1,8 mmol) Uracil in 100 ml Water dissolve by warming in water bath and filter sterilize.

1 M 3-Amino-1,2,4-triazol solution:

8,4 g 3-Amino-1,2,4-triazol in 100 ml Water, filter once and filter sterilize.

100 x Cycloheximide solution:

1 mg/ml Cycloheximid in Water solution filter sterilize.

10 x Amino acid solutions:

300 mg (2,3 mmol) Isoleucine
1500 mg (1,1 mmol) Valine
200 mg (0,9 mmol) Arginine
300 mg (1,6 mmol) Lysine
200 mg (1,34 mmol) Methionine
500 mg (3 mmol) Phenylalanine
2000 mg (16,8 mmol) Threonine,
make volume to 1l and filter sterilize.

The composition of the selection media and agar plates is indicated in following table. Agar agar and Yeast extract without nitrogen base dissolved in water was autoclaved. The glucose solution was made in water and filter sterilised. The addition of the remaining stock solutions took place after cooling to 55 °C.

Reagents	Selection plates				
	SD/-Leu	SD/-Leu+Cyh	SD/-Leu/-Trp	SD/-Trp	SD/-Leu/-His/-Trp/+3-AT
Yeast Nitrogen Base [g]	6,7	6,7	6,7	6,7	6,7
Agar agar [g]	20	20	20	20	20
Water [ml]	750	750	770	750	745
20% Glucose [ml]	100	100	100	100	100
10 x Amino acid solution [ml]	100	100	100	100	100
100 x Adenine [ml]	10	10	10	10	10
100 x Tyrosine [ml]	10	10	10	10	10
100 x Uracile [ml]	10	10	10	10	10
100 x Histidine [ml]	10	10	10	10	#
100 x Leucine [ml]	#	#	#	10	#
100 x Tryptophane [ml]	10	10	#	#	#
Cycloheximide solution [ml]	#	10	#	#	#
3-AT-solution [ml]	#	#	#	#	25

1.6.4 Buffers and other solutions

The buffers and solutions that were commonly used during the course of this study are mentioned below.

10x NCP-Buffer, pH 8.0:
 12.1 g Tris/HCl
 87.0 g NaCl
 5.0 ml Tween 20
 2.0 g sodium azide
 add H₂O to make 1 litre

PBG, pH 7.4:
 0.5 % bovine serum albumin
 0.1 % gelatin (cold-water fish skin)
 in 1x PBS, pH 7.4

1x PBS, pH 7.4:
 8.0 g NaCl
 0.2 g KH₂PO₄
 1.15 g Na₂HPO₄
 0.2 g KCl
 dissolve in 900 ml deionised H₂O
 adjust to pH 7.4
 add H₂O to make 1 litre, autoclave

<u>1.2 M Phosphate buffer, pH 6.8:</u>	1.2 M Na ₂ HPO ₄ , pH 9.1 was mixed with 1.2 M NaH ₂ PO ₄ , pH 4.02 at the ratio of 2:1.
<u>20x SSC, pH 7.0</u>	3 M NaCl 0.3 M sodium citrate
<u>TE buffer, pH 8.0:</u>	10 mM Tris/HCl, pH 8.0 1 mM EDTA, pH 8.0
<u>10x TAE buffer, pH 8.3:</u>	27.22 g Tris 13.6 g sodium acetate 3.72 g EDTA add H ₂ O to make 1 litre
<u>MES buffer, pH 6.5</u>	20 mM 2-[N-morpholino]ethane sulphonic acid, pH 6.5 1 mM EDTA 250 mM sucrose
<u>Homogenisation buffer, pH 7.4:</u>	30 mM Tris/HCl, pH 7,4 2 mM DTT 2 mM EDTA 4 mM EGTA 5 mM Benzamidin 0,5 mM PMSF 1 Tablet complete [®] mini Protease Inhibitor Mix (Roche) per 10 ml buffer add 30 % sucrose, prepare fresh before use.
<u>Lysis Buffer (phosphorylation):</u>	50 mM Tri-HCl, pH 7.6 150 mM NaCl 1 % Nonidet P-40 1 mM sodium orthovanadate 10 mM sodium fluoride 5 mM sodium pyrpphosphate 10 mM β-glycrephosphate
<u>5 x Immunoprecipitation Buffer:</u>	0.5 m Potassium phosphate buffer 0.375 M NaCl 25 mM EDTA 5 mM Benzamidine 2.5 mM PMSF Adjust the pH to 7.9, prepare fresh.
<u>Hybridisation solution (50 µl):</u>	Hybridisation buffer 48 µl Fish sperm DNA [10 mg/ml] 1µl Oligo dA (18 mer, 100 µM) 1µl mix well
<u>Hybridisation buffer:</u>	1.2M Phosphate buffer, pH 6.8 2mM EDTA 50 % Formamide

	1% Na-Laurylsarcosinate
	0.2 % SDS
	4 x Denhardt's Reagent
<u>100 x Denhardt's reagent:</u>	2 % Ficoll 400
	2 % Polyvinylpyrrolidone
	2 % bovine serum albumin
<u>1.2 M Phosphate buffer, pH 6.8:</u>	2 volumes 1.2 M Na ₂ HPO ₄
	1 volume 1.2 M NaH ₂ PO ₄
Blocking Solution (282 ml):	270 ml 1-Methy-2-pyrrolidinone (solution should be colourless)
	0.4 g Succinic anhydride (store desiccated)
	12.1 ml 1M Sodium borate, pH 8.0 (42mM)

1.7 Biological materials

<u>Bacterial strains:</u>	<i>E. coli</i> JM 38 (Vieira and Messing, 1982)
	<i>E. coli</i> DH5 α (Hanahan, 1983)
	<i>E. coli</i> XL1 blue (Bullock, 1987)
	<i>Klebsiella aerogenes</i> (Williams KL and Newell, 1976)
<u><i>Dictyostelium discoideum</i> strain:</u>	
AX2-214	An axenically growing derivative of wild strain, NC-4 (Raper, 1935). Commonly referred to as AX2.
GHR, Filamin ⁻ Mutant from AX2:	Eichinger <i>et al.</i> 1996
HG1264, Filamin ⁻ mutant from AX2:	Brink <i>et al.</i> 1990
GA1 Filamin ⁻ and α -actinin ⁻ double Mutant:	Rivero <i>et al.</i> 1996
<u>Yeast Strains :</u>	
	Y190 (Flick <i>et al.</i> 1990, Harper <i>et al.</i> 1993)
	Y187 (Harper <i>et al.</i> 1993)

2 Cell biological methods

2.1 Growth of *Dictyostelium*

2.1.1 Growth in liquid nutrient medium (Claviez *et al.* 1982)

Dictyostelium discoideum AX2 and the derived transformants were grown in liquid AX2 medium containing dihydrostreptomycin (40 µg/ml) and other appropriate selective antibiotics (depending upon mutant) at 21°C either in a shaking-suspension in Erlenmeyer flasks with shaking at 160 rpm or on petri dishes. For all the cell biological works, cultures were harvested at a density of 3-5 x 10⁶ cells/ml.

2.1.2 Growth on SM agar plates

In general, *Dictyostelium* cells were plated onto SM agar plates overlaid with *Klebsiella aerogenes* and incubated at 21 °C for 3-4 days until *Dictyostelium* plaques appeared on the bacterial lawns. To obtain single clones of *Dictyostelium*, 50-200 cells were suspended in 100 µl Soerensen phosphate buffer and plated onto *Klebsiella*-overlaid SM agar plates. Single plaques obtained after incubation at 21°C for 3-4 days were picked up with sterile tooth-picks, transferred either to new *Klebsiella*-overlaid SM agar plates or to separate petri dishes with AX2 medium supplemented with dihydrostreptomycin (40 µg/ml) and ampicillin (50µg/ml) (to eliminate the bacteria) and any other appropriate selective antibiotic (depending upon mutant).

2.2 Development of *Dictyostelium*

Development in *Dictyostelium* is induced by starvation. Cells grown to a density of 2-3 x 10⁶ cells/ml were pelleted by centrifugation at 2,000 rpm (Sorvall RT7 centrifuge) for 2 min at 4°C and were washed two times in an equal volume of cold Soerensen phosphate buffer in order to remove all the nutrients present in the culture medium. For development in suspension culture, the cells were resuspended in Soerensen phosphate buffer at a density of 1 x 10⁷ cells/ml and were shaken at 160 rpm and 21 °C for desired time periods. For development on nitrocellulose filters, 0.5 x 10⁸ cells were deposited on nitrocellulose filters (Millipore type HA, Millipore) and allowed to develop at 21 °C as described Newell (Newell *et al.* 1969).

2.3 Preservation of *Dictyostelium*

Dictyostelium cells were allowed to grow in AX2 medium to a density of $4\text{-}5 \times 10^6$ cells/ml. 9 ml of the densely grown culture were collected in a 15 ml Falcon tube on ice and supplemented with 1 ml horse serum and 1 ml DMSO. The contents were mixed by gentle pipetting, and aliquoted in cryotubes (1 ml). The aliquots were incubated on ice for 60 min, followed by incubation at -20 °C for at least 2 hr. Finally the aliquots were transferred to -80 °C for long term storage.

For reviving the frozen *Dictyostelium* cells, an aliquot was taken out from -80 °C and thawed immediately at 37 °C in a waterbath. In order to remove DMSO, the cells were transferred to a Falcon tube containing 30 ml AX2 medium and centrifuged at 2,000 rpm (Sorvall RT7 centrifuge) for 2 min at 4 °C. The cell pellet was resuspended in 250 μ l of AX2 medium and the cell suspension was plated onto SM agar plates overlaid with *Klebsiella*. The plates were incubated at 21 °C until plaques of *Dictyostelium* cells started to appear.

2.4 Transformation of *Dictyostelium* cells by electroporation

The electroporation method for transformation of *Dictyostelium* cells described by de Hostos¹⁴³ was followed with little modifications. *Dictyostelium discoideum* cells were grown axenically in suspension culture to a density of $2\text{-}3 \times 10^6$ cells/ml. The cell suspension was incubated on ice for 20 min and centrifuged at 2,000 rpm (Sorvall RT7 centrifuge) for 2 min at 4 °C to collect the cells. The cells were then washed with an equal volume of ice-cold Soerensen phosphate buffer followed by an equal volume of ice-cold electroporation-buffer. After washings, the cells were resuspended in electroporation-buffer at a density of 1×10^8 cells/ml. For electroporation, 20-25 μ g of the plasmid DNA was added to 500 μ l of the cell suspension and the cell-DNA mixture was transferred to a pre-chilled electroporation cuvette (2 mm electrode gap, Bio-Rad). Electroporation was performed with an electroporation unit (Gene Pulser, Bio-Rad) set at 0.9 kV and 3 μ F without the pulse controller. After electroporation, the cells were immediately spread onto a 100-mm petri dish and were allowed to sit for 10 min at 21 °C. Thereafter, 1 ml of healing-solution was added dropwise onto the cells and the petri dish was incubated at 21 °C on a shaking platform at 50 rpm for 15 min. 10 ml of AX2 medium was added into the petri dish and the cells were allowed to recover overnight. The next day, the medium was replaced by the selection medium containing appropriate antibiotic. To select for stable transformants, selection medium was replaced every 24-48 hr until the control plate (containing cells electroporated without any DNA) was clear of live cells.

Electroporation-buffer:

100 ml 0.1 M potassium phosphate buffer
17.12 g sucrose
add distilled H₂O to make 1 litre adjust to pH 6.1
autoclave

0.1 M Potassium phosphate buffer:

170 ml 0.1 M KH₂PO₄
30 ml 0.1 M K₂HPO₄

Healing-solution:

150 µl 0.1 MgCl₂
150 µl 0.1 CaCl₂
10 ml electroporation-buffer

2.5 Quantitative phagocytosis assays

Phagocytosis was performed according to Maniak et al. (1995). Briefly *Dictyostelium* cells were grown to $<5 \times 10^6$ /ml over 5 generations in axenic medium. Cells were centrifuged and resuspended at 2×10^6 cells/ml in fresh axenic medium at 21 °C. TRITC-labelled yeast cells prepared according to Materials and Method 6.3 were added in a 5 fold excess (10^9 yeast cells/ml stock). Cells were incubated on a rotary shaker at 160 rpm. Samples were taken at different intervals and the fluorescence of non internalized yeasts were quenched by incubating for 3 min with 100 µl trypan blue (2 mg/ml). Cells were centrifuged again, resuspended in phosphate buffer and the fluorescence was measured using a fluorimeter (544 nm excitation / 574 nm emission).

3 Molecular biological methods

3.1 Purification of plasmid DNA

In general, for small cultures (1 ml) of *E. coli* transformants, the alkaline lysis method of Holmes and Quigley (1981) was used to extract plasmid DNA. This method is good for screening a large number of clones simultaneously for the desired recombinant plasmid. Briefly, single transformants were picked up from the culture plate and were grown overnight in 1 ml of LB media containing suitable antibiotic. The *E. coli* cells grown overnight were pelleted by centrifuging at 6,000 rpm in a microcentrifuge for 3-5 min. The pellet was then resuspended completely in 250 µl STET/lysozyme buffer and the suspension was incubated at room temperature for 10 min to lyse the bacterial cells. The bacterial lysate was boiled at 100°C for 1 min and was then centrifuged in an Eppendorf centrifuge at maximum speed for 15 min at room temperature. The plasmid DNA present in the supernatant was precipitated by

adding an equal volume of isopropanol and incubating at room temperature for 10 min. The precipitated DNA was pelleted in the Eppendorf centrifuge at 12,000 rpm for 15 min and the DNA pellet was washed with 70 % ethanol, dried in a speed-vac concentrator and finally resuspended in 40 µl TE, pH 8.0, containing RNase A at 1 µg/ml.

STET/lysozyme buffer, pH 8.0:

50 mM Tris/HCl, pH 8.0

50 mM EDTA

0.5% Triton-X-100

8.0% Sucrose

Add lysozyme at 1 mg/ml at the time of use.

Alternatively, for pure plasmid preparations in small and large scales (for sequencing, PCR or transformations), kits provided either by Macherey-Nagel (Nucleobond AX kit for small scale plasmid preparations) or by Qiagen (Qiagen Midi- and Maxi-Prep kit for large scale plasmid preparations) were used. These kits follow basically the same approach: first overnight culture of bacteria containing the plasmid is pelleted and the cells are lysed by alkaline lysis. The freed plasmid DNA is then adsorbed on a silica matrix, washed with ethanol, and then eluted with TE, pH 8.0. This method avoids the requirement of caesium chloride or phenol-chloroform steps during purification.

3.2 Digestion with restriction enzymes

All restriction enzymes were obtained from NEB, Amersham or Life Technologies and the digestions were performed in the buffer systems and temperature conditions as recommended by the manufacturers. The plasmid DNA was digested for 1-2 hr.

3.3 Generation of blunt ends in linearised plasmid DNA

For many cloning experiments, it was necessary to convert the 5' or 3' extensions generated by restriction endonucleases into blunt ends. Repair of 5' extensions was carried out by the polymerase activity of the Klenow fragment, whereas repair of 3' extensions was carried out by the 3' to 5' exonuclease activity of the Klenow fragment.

Reaction-mix for 5' extensions:

1-4 µg linearised DNA

5 µl 10x High salt buffer

1 µl 50x dNTP-mix (each 4 mM)

2 U Klenow fragment

add H₂O to make 50 µl

Reaction-mix for 3' extensions:

1-4 µg linearised DNA

5 µl 10x High salt buffer

2 U Klenow fragment

add H₂O to make 50 µl

10x High salt buffer:

500 mM Tris/HCl, pH 7.5
1 M NaCl
100 mM MgCl₂
10 mM DTT

The reaction was carried out at 37°C for 25-30 min. After incubation, the reaction was immediately stopped by heat-inactivating the enzyme at 75 °C for 10 min or by adding 1µl 0.5 M EDTA. This was followed by phenol/chloroform extraction and precipitation of DNA with 2.5 volume ethanol.

3.4 Dephosphorylation of DNA fragments

To avoid self-ligation of the vector having blunt ends or that has been digested with a single restriction enzyme, 5' ends of the linearised plasmids were dephosphorylated by calf-intestinal alkaline phosphatase (CIAP). Briefly, in a 50 µl reaction volume, 1-5 µg of the linearised vector-DNA was incubated with 1 U calf-intestinal alkaline phosphatase in CIAP-buffer (provided by the manufacturer) at 37 °C for 30 min. The reaction was stopped by heat-inactivating the enzyme at 65 °C for 10 min. The dephosphorylated DNA was extracted once with phenol-chloroform and precipitated with 2 vol. ethanol and 1/10 vol. 2 M sodium acetate, pH 5.2.

3.5 Setting up of ligation reactions

A DNA fragment and the appropriate linearised plasmid were mixed in approximately equimolar amounts. T4 DNA ligase and ATP were added as indicated below and the ligation reaction was left overnight at 10-12 °C.

Ligation reaction:

Linearised vector DNA (200-400ng)
DNA fragment
4 µl 5x ligation buffer
1µ 0.1 M ATP
1.5 U T4 Ligase
and water to make up to 20 µl.

5x Ligation buffer:

Supplied with the enzyme
by manufacturers

3.5.1 Generation of the point mutation

The point mutation was generated to replace serine 174 in ddfilamin with alanine by using an overlapping PCR approach, involving the following steps.

- i) Two fragments between nucleotides 270-487 and 461-574 were generated, which has 26 nucleotides overlapping end.

- ii) The point mutation was generated by introducing a mismatch nucleotide in the overlapping ends.
- iii) The mutation at the EcoRV site in position 548 bp was made to destroy the restriction enzyme site without changing the amino acid.
- iv) Overlapping PCR was done to join the two fragments using primers at the extreme ends.
- v) The PCR product was cloned into a pGEM-T Easy vector and transformed into *E. coli*.
- vi) DNA obtained from the bacterial transformants was sequenced to confirm the mutation.
- vii) The 290 bp fragment obtained by a EcoRV digestion from the pGEM-T Easy vector was ligated to full-length ddfilamin cDNA with C-terminal GFP tag, digested with the EcoRV.
- viii) The orientation of the cloned fragment was confirmed by PCR using a forward primer at the 5' end of the full-length cDNA and one of the reverse primer used for generation of the 290 bp fragment.
- ix) Clones were further confirmed by sequence analysis.

3.6 DNA agarose gel electrophoresis

Agarose gel electrophoresis was performed according to the method described by Sambrook to resolve and purify the DNA fragments. Electrophoresis was typically performed with 0.7 % (w/v) agarose gels in 1x TAE buffer submerged in a horizontal electrophoresis tank containing 1x TAE buffer at 1-5 V/cm. Only for resolving fragments less than 1,000 bp, 1 % (w/v) agarose gels in 1x TAE buffer were used. A DNA-size marker was always loaded along with the DNA samples in order to estimate the size of the resolved DNA fragments in the samples. The gel was run until the bromophenol blue dye present in the DNA-loading buffer had migrated the appropriate distance through the gel. The gel was examined under UV light at 302 nm and was photographed using a gel-documentation system (MWG-Biotech)

DNA-size marker:

1 kb DNA Ladder (Life Technologies): 12,216; 11,198; 10,180; 9,162; 8,144; 7,126; 6,108; 5,090; 4,072; 3,054; 2,036; 1,636; 1,018; 506; 396; 344; 298; 220; 201; 154; 134; 75 bp

3.7 Recovery of DNA fragments from agarose gels

DNA fragments from restriction enzyme digests or from PCR reactions were separated by agarose gel electrophoresis and the gel piece containing the desired DNA fragment was carefully and quickly excised while observing the ethidium bromide stained gel under a UV transilluminator. The DNA fragment was then purified from the excised gel piece using the Macherey-Nagel gel elution kit (NucleoSpin Extract 2 in 1), following the method described by the manufacturers.

3.8 RNA formaldehyde-agarose gel electrophoresis

The formaldehyde-agarose denaturing electrophoresis (Lehrach *et al.* 1977) is used for separation and resolution of single stranded RNA.

Sample preparation for electrophoresis:

In general, 30 µg of purified total RNA was mixed with an equal volume of RNA-sample buffer and denatured by heating at 65 °C for 10 min. After denaturation, the sample was immediately transferred to ice and 1/10 vol. of RNA-loading buffer was added. Thereafter, the RNA samples were loaded onto a denaturing formaldehyde-agarose gel.

Formaldehyde-agarose gel preparation:

For a total gel volume of 150 ml, 1.8 g agarose (final concentration 1.2%) was initially boiled with 111 ml DEPC-H₂O in an Erlenmeyer flask, cooled to 60 °C and then 15 ml of RNA-gel-casting buffer, pH 8.0 and 24 ml of 36 % formaldehyde solution were added. The agarose solution was mixed by swirling and poured into a sealed gel-casting chamber of the desired size. After the gel was completely set, denatured RNA samples were loaded and the gel was run in 1x RNA-gel-running buffer, pH 7.0, at 100 V until the bromophenol blue dye had migrated the appropriate distance through the gel.

A test gel was sometimes run with 5 µg of total RNA to check the quality of the RNA samples. In such a case, 10 µg/ml ethidium bromide was added to the RNA-sample buffer during sample preparation and after electrophoresis the gel was examined under UV light at 302 nm and was photographed using the gel-documentation system.

10x RNA-gel-casting buffer, (pH 8.0):

200 mM MOPS
50 mM sodium acetate
10 mM EDTA
adjust pH 8.0 with NaOH
autoclaved

10x RNA-gel-running buffer, (pH 7.0):

200 mM MOPS
50 mM sodium acetate
10 mM EDTA
adjust pH 7.0 with NaOH
autoclaved

RNA-sample buffer:

50% formamide
6% formaldehyde
in 1x RNA-gel-casting buffer, pH 8.0

RNA-loading buffer:

50% sucrose, RNase free
0.25% bromophenol blue
in DEPC-H₂O

Internal RNA-size standard:

26S rRNA (4.1 kb)
17S rRNA (1.9 kb)

3.9 Transformation of *E. coli*

3.9.1 Transformation of *E. coli* cells by the CaCl₂ method

Preparation of CaCl₂-competent *E. coli* cells:

Chemical competent cell were prepared according to Hiroaki *et al.* 1990. An overnight grown culture of *E. coli* (0.5 ml) was inoculated into 50 ml LB medium and incubated at 21 °C, with shaking 250 rpm until an OD₆₀₀ of 0.4-0.6 was obtained. The bacteria were then pelleted at 4°C for 10 min at 4,000 rpm (Beckman Avanti J25, rotor JA-25.50) and the bacterial pellet was resuspended in 20 ml of ice-cold TB buffer and incubated on ice for 15 min. The bacterial cells were again pelleted and gently resuspended in 2 ml of ice-cold TB, DMSO was added with gentle swirling to a final concentration of 7 % and aliquoted in 200 µl/tube. The aliquots were then quickly frozen in a dry ice/ethanol bath and immediately stored at -80 °C.

Transformation Buffer (TB): 10 mM Pipes, 55 mM MnCl₂, 15 mM CaCl₂, 250 mM KCl, all the components except MnCl₂ were mixed and pH was adjusted to 6.7 with KOH. Then, MnCl₂ was dissolved, the solution was sterilised by filtration through a prerinsed 0.45 µm filter unit and stored at 4 °C. All salts were added as solids.

Transformation of CaCl₂-competent *E. coli* cells:

Plasmid DNA (~50-100 ng of a ligase reaction or ~10 ng of a supercoiled plasmid) was mixed with 100-200 µl of CaCl₂ -competent *E. coli* cells and incubated on ice for 30 min. The cells were then heat-shocked at 42 °C for 45 s and immediately transferred to ice for 2 minutes. The cells were then mixed with 1 ml of pre-warmed (at 37 °C) SOC medium and incubated at 37 °C with shaking at ~150 rpm for 45 min. Finally, 100-200 µl of the transformation mix, or an appropriate dilution, was plated onto selection plates and the transformants were allowed to grow overnight at 37 °C.

3.9.2 Transformation of *E. coli* cells by electroporation

Preparation of electroporation-competent *E. coli* cells:

An overnight grown culture of *E. coli* (5 ml) was inoculated into 1,000 ml of LB medium and incubated at 37 °C with shaking at 250 rpm until an OD₆₀₀ of 0.4-0.6 was obtained. The culture was then incubated on ice for 15-20 minutes. Thereafter, the culture was transferred to pre-chilled 500-ml centrifuge bottles (Beckman) and the cells were pelleted by centrifugation at 4,200 rpm (Beckman Avanti J25, rotor JA-10) for 20 min at 4 °C. The bacterial pellet was washed twice with an equal volume of ice-cold water and the cells were resuspended in 40 ml of ice-cold 10% glycerol, transferred to a pre-chilled 50-ml centrifuge tube and centrifuged at 4,200 rpm (Beckman Avanti J25, rotor JA-25.50) for 10 min at 4 °C. Finally, the cells were resuspended in an equal volume of 10 % chilled glycerol and aliquoted (50-100 µl) in 1.5 ml Eppendorf tubes that have been placed in a dry ice/ethanol bath. The frozen aliquots were immediately transferred to –80 °C for long-term storage.

Transformation of electroporation-competent *E. coli* cells:

Plasmid DNA (~20 ng dissolved in 5-10 µl ddH₂O) was mixed with 50-100 µl electroporation-competent *E. coli* cells. The transformation mix was transferred to a 2 mm BioRad electroporation cuvette (pre-chilled) and the cuvette was incubated on ice for 10 min. The DNA was then electroporated into competent *E. coli* cells using an electroporation unit (Gene Pulser, Bio-rad) set at 2.5 KV, 25 µF, 200Ω. Immediately after electroporation, 1 ml of pre-warmed (37 °C) SOC medium was added onto the transformed cells and the cells were incubated at 37 °C with shaking at ~150 rpm for 45 min. Finally, 100-200 µl of the transformation mix, or an appropriate dilution, was plated onto selection plates and the transformants were allowed to grow overnight at 37 °C.

3.10 Glycerol stock of bacterial cultures

Glycerol stocks of all the bacterial strains/transformants were prepared for long-term storage. The culture was grown overnight in LB medium with or without the selective antibiotic (depending upon the bacterial transformation). 850 µl of overnight culture was added to 150 µl of sterile glycerol in a 1.5 ml microcentrifuge tube, mixed well by vortexing and the tube was frozen on dry ice and stored at –80 °C.

3.11 Construction of vectors

3.11.1 Vectors for expression of ddfilamin GFP-fusion proteins

Vectors were constructed that allowed expression of full-length ddfilamin-GFP, rod domain-GFP fusion protein and actin-binding domain in *Dictyostelium* cells under the control of the actin-15 promoter and the actin-8 terminator. Ddfilamin rod domain cDNA was generated by PCR using primers I and II listed into the primers list, both the primers add a SmaI site allowing release of the cDNA fragment. The PCR product ligated to pGEM-T Easy vector from the Promega kit (materials and method 1.3) was transformed into bacteria (materials and method 3.9.2), plasmid DNA from bacterial clones was isolated and screened by digesting with SmaI. Clones giving 1.6 kb and 3.0 kb fragment upon SmaI digestion were given for sequencing (Materials and Method 3.12) the sequences were analyzed for PCR mistakes and cDNAs from correct clones were subcloned in-frame at the EcoRI site located at the C-terminus of the coding region of the green fluorescent protein (GFP) in the pDEX-RH expression vector (Scägger, 1994). Sticky ends generated by EcoRI digesion of the vector were made blunt ended by using dNTPs and Klenow enzyme (materials and method 3.3) and dephosphorylated (materials and method 3.4). Full length ddfilamin and the actin-binding domain were cloned as above into the p1ABSr8 vector at the N-terminus of GFP under the control of the A15 promoter. The resulting vectors were introduced into AX2 and HG1264 cells by electroporation (materials and methods 2.4).

3.12 DNA sequencing

Sequence of the PCR-amplified products or plasmid DNA was performed at the sequencing facility of the Centre for Molecular Medicine, University of Cologne, Cologne, by the modified dideoxy nucleotide termination method using a Perkin Elmer ABI prism 377 DNA sequencer.

3.13 Computer analyses

Sequencing analysis, homology searches, structural predictions and multiple alignments of protein sequences were performed using the University of Wisconsin GCG software package (Hiroak *et al.* 1990) and Expasy Tools software, accessible on the world wide web.

4. Methods for ‘Yeast Two Hybrid System’

4.1 Transformation of yeast using the LiOAc method:

The Lithium Acetate method (Elbe, 1992) was used for the yeast transformation. 2-3 medium sized (~3 mm) colonies from the plate were inoculated into the medium and grown till 0.7 to 1.5 OD 600 nm by incubating at 30 °C, and 250 rpm. (For yeast strain grown on YEPD plates, YEPD medium was used, yeast containing pACT2 vector grown on SD-Leu plates, and yeast containing pAS2 vector grown on SD-Trp plates, the corresponding medium was used). 1.0 ml culture was centrifuged in a microfuge tube for 5 sec to pellet down the cells. The supernatant was discarded leaving 50-100 µl in microfuge tube; pellet was resuspended with the help of a microtip. 2.0 µl (from 10 mg / ml solution) of carrier DNA, 1 µg plasmid DNA was added to the cells and vortexed. To this 500 µl of PLATE mixture was added and mixed by vortexing. Finally 50 µl of 1.0 M DTT was added and mixed by vortexing. Tubes were incubated at the room temperature for 6-8 h. Transformation was achieved by giving heat shock for 10 min at 42 °C. 50-100 µl PLATE mixture was removed from the bottom of the tube and plated on the corresponding nutrient agar plate. Plates were incubated at 30 °C till colonies appear in the plate. Colonies of desired size (~3 mm) appeared in three days.

PLATE Mixture:

45 % PEG	9.0 ml
1M LiOac	1.0 ml
1M Tri-Cl (pH 7.5)	100 µl
0,5M EDTA	20 µl

All preparations were sterile.

4.2 DNA Isolation from yeast:

Hoffman’s method (Hoffmann and Winston, 1987) was used for the isolation of plasmid DNA from yeast with little modifications. A saturated yeast culture was prepared by inoculating up to 2-3 medium size (~3mm) colonies into YEPD or selective medium. Cells were pelleted from 5.0 ml culture by centrifuging at 4,000 rpm for 5 min. The pellet was resuspended into 200 µl STET buffer by vortexing briefly and cells were placed into a 1.5 ml tube. About 100 mg 0.45 mm glass beads were added to the cells and vortexed for 5 min. Then the tube was incubated at 100 °C in a heating block for 3 min, cooled briefly on ice and centrifuged at 13,000 rpm, for 10 min at 4 °C. 100 µl supernatant was taken into a fresh tube. To this 500 µl of 7,5 M ammonium acetate was added and mixed by inverting the tube. The mixture was then incubated at –20 °C for 1 h, centrifuged 13,000 rpm, 10 min at 4 °C. 100 µl supernatant was transferred to fresh tube containing 200 µl of 96 % cold ethanol, mixed well and allowed

to stand at room temperature for 5 min 13,000 rpm, 10 min at room temperature, supernatant was discarded and pellet was washed with 70 % ethanol. Ethanol was removed carefully without disturbing the pellet, pellet was air dried and reconstituted in 20 µl of TE buffer, 10 µl of which was used to transform into bacteria (materials and methods 3.9.2).

STET buffer:

8% sucrose in 50 mM Tris, pH 8.0
5 % TritonX-100
50 mM EDTA

7.5M Ammonium Acetate:

28.9 g/50 ml

4.3 β-galactosidase colony lift assay:

Yeast colonies were assayed qualitatively for blue/white selection according to the method described by Schneider *et al.* 1996. Colonies on transformation plate were grown at 30 °C for 2-4 days on (SD/-Trp, -Leu) or (SD/-Trp, -Leu, -His +3AT) agar plates. Few colonies from these plates were streaked on appropriate master replica plate and grown for 1-2 additional days. Clean dry nitrocellulose filter was kept on the surface of plate of colonies to be assayed. Filter was marked for orientation by punching the holes asymmetrically through the filter in to the agar. Filter was lifted carefully and transferred to the pool of liquid nitrogen using forceps and completely submerged for 10 sec. keeping colony side up. Completely frozen filter removed and allow the thaw at room temperature and carefully placed on Z-buffer X-gal solution pre-soaked sterile filter facing colony side up without trapping the air bubble under or between the filters. Filters were incubated at room temperature or at 30 °C and checked periodically for the appearance of blue color. Corresponding blue colony was selected and picked from the plate.

Z-Buffer, pH 7,0:

10,69 g (0,04 mol) Na₂HPO₄ x 7 H₂O
5,5 g (0,04 mol) NaH₂PO₄ x H₂O
0,75 g (0,01 mol) KCl
0,246 g (0,01 mol) MgSO₄ x 7 H₂O
adjust volume to 1l with distilled water and autoclave.

Z-Buffer/X-gal-Solution:

100 ml Z-Buffer, pH 7,0
0,27 ml 14,4 M β-Mercaptoethanol
1,67 ml X-gal-solution (20 mg/ml DMF)

4.4 Yeast Strain Maintenance

Yeast grown to saturation on shaking culture in corresponding medium mixed with glycerol to the final concentration of 25 % and stored at -70 °C. Or isolated colony was picked from the plate by using sterile loop and thoroughly resuspended in 200-500 µl of YEPD medium

(or appropriate SD dropout medium.). Sterile glycerol was added to the final concentration of 25 %, mixed thoroughly and immediately stored at -70°C .

5. Biochemical methods

5.1 Preparation of total protein from *Dictyostelium*

1×10^7 to 5×10^8 *Dictyostelium* cells either vegetative or at different stages of development were washed once in Soerensen phosphate buffer. Total protein was prepared by lysing the pellet of cells in 500 μl 1 x SDS sample buffer. Equal amounts of protein (equivalent to 2×10^5 to 1×10^7 cells/lane) were loaded onto discontinuous SDS-polyacrylamide gels.

5.2 SDS-polyacrylamide gel electrophoresis

SDS-polyacrylamide gel electrophoresis (SDS-PAGE) was performed using the discontinuous buffer system (Laemmli, 1970). Discontinuous polyacrylamide gels (10-15 % resolving gel, 5% stacking gel) were prepared using glass plates of 10 cm x 7.5 cm dimensions and spacers of 0.5 mm thickness. A 12-well comb was generally used for formation of the wells in the stacking gel. The composition of 12 resolving and 12 stacking gels is given in the table below.

Components	Resolving gel			Stacking gel
	10 %	12 %	15 %	5%
Acrylamide/Bisacrylamide (30:0.8) [ml]:	19.7	23.6	30.0	4.08
1.5 M Tris/HCl, pH 8.8 [ml]:	16.0	16.0	16.0	-
0.5 M Tris/HCl, pH 6.8 [ml]:	-	-	-	2.40
10 % SDS [μl]:	590.0	590.0	590.0	240.00
TEMED [μl]:	23.0	23.0	23.0	20.00
10 % APS [μl]:	240.0	240.0	240.0	360.00
Deionised H_2O [ml]:	23.5	19.6	13.2	17.16

Samples were mixed with suitable volumes of SDS sample buffer, denatured by heating at 95°C for 5 min and loaded into the wells in the stacking gel. A molecular weight marker, which was run simultaneously on the same gel in an adjacent well, was used as a standard to establish the apparent molecular weights of proteins resolved on SDS-polyacrylamide gels. The molecular weight markers were prepared according to the manufacturer's specifications. After loading the samples onto the gel, electrophoresis was performed in 1x gel-running buffer at a constant voltage of 100-150 V until the bromophenol blue dye front had reached the bottom edge of the gel or had just run out of the gel. After the electrophoresis, the

resolved proteins in the gel were either observed by Coomassie blue staining or transferred onto a nitrocellulose membrane.

2x SDS-sample buffer:

100 (mM) Tris/HCl, pH 6.8
4 (% v/v) SDS
20 (% v/v) glycerine
0.2 (% v/v) bromophenol blue
4 (% v/v) β -mercaptoethanol

Molecular weight markers:

94, 67, 43, 30, 20.1, 14.4 kDa

5.3 Native or nondenaturing PAGE (Scägger, 1994):

Native gels were prepared as SDS polyacrylamide gel with slight modifications. Briefly, 8 % gels without stacking gel were prepared as shown above. $2-3 \times 10^8$ AX2 cells and AX2 cells expressing FLC-GFP fusion protein were lysed in lysis buffer by passing through nucleopore filter, the filtrate was centrifuged at 13,000 rpm at 4 °C for 30 min. 10 μ l supernatant was mixed with 2x protein sample buffer and loaded on to the gel. The gel was prerun at 140V for 1 h at 4 °C and the electrode buffers were replaced with fresh buffer before loading the samples. A molecular weight ladder was also loaded for the reference molecular weight. The pH of all the buffers and the gel was maintained at 8.2-8.8 at 4 °C, which was well above the isoelectric point of the protein. The gel was allowed to run at 140V at 4 °C till the dye front reached the bottom. The gel was removed and soaked in cold 1 x NCP buffer (section 1.6.4) containing 1 % SDS at 4 °C for 1 h and then transferred to nitrocellulose paper for 1 h at 10V using the semidry blotting device (materials and methods 5.7). The membrane was western blotted using anti ddfilamin mAb 82-421-5.

Lysis buffer:

30 mM Tris/HCl, pH 8.0
2 mM DTT
4 mM EGTA
5 mM Benzamidine
0.5 mM PMSF
2 mM EDTA
30 % sucrose and one complete mini protease inhibitor cocktail tablet/15 ml.

Native protein molecular weight markers:

669, 440, 232, 140 and 66 kDa

Electrode buffer:

1.9 M Glycine, 0.25 M Tris/HCl, pH 8.8
0.1 % Triton X-100, 0.5 mM EGTA and
0,2 mM ATP

2x-sample buffer:

100 mM Tris/HCl, pH 8.8
0.2 % (v/v) bromophenol blue

5.3.1 Coomassie blue staining of SDS-polyacrylamide gels

After electrophoresis, the resolved proteins were visualized by staining the gel with Coomassie blue staining solution at room temperature with gentle agitation for at least 30 min. The staining solution was replaced by destaining solution. The gel was destained at room temperature with gentle agitation. For best results, the destaining solution was replaced several times until protein bands were clearly visible.

Coomassie blue staining solution

0.1 % Coomassie blue R250
50 % ethanol
10 % acetic acid
filter the solution before use

Destaining solution:

7 % acetic acid
20 % ethanol

5.3.2 Silver staining of polyacrylamide gels

Size fractionated proteins on poly acrylamide gel were fixed with 30 % ethanol-10 % acetic acid solution for one hour. The gel was rinsed with 20 % ethanol before sensitizing with 0.02 % sodium thiosulphate for 1 min. After three washings (20 sec each) with MilliQ water, the gel was stained with a 0.2 % silver nitrate solution for 45 minutes. The excess of silver nitrate was removed by washings of the gel three times with MilliQ water. The protein bands were developed with developer solution until they are suitably visible. The reaction was stopped by soaking the gel in stop solution for 5 minutes.

Developer: 0.3 % Sodium carbonate
0.025 % Formaldehyde
10 mg/ml sodium thiosulphate

Stop solution: 50 g Tris base
25 ml glacial acetic acid
Water to 1000 ml.

5.4 Immunoprecipitation from *Dictyostelium* cell lysate

Dictyostelium grown axenially was harvested and washed twice with Soerensen phosphate buffer. Cells suspended in twice the volume of the homogenization buffer were lysed through 'Nuclepore' membrane filters. The complete lysis of the cell was confirmed by visual inspection of a drop of lysate under light microscope. Lysate was centrifuged at 10,000g for 25 min at 4 °C. The supernatant was precleaned by incubating with protein A sepharose beads for 1 h at 4 °C. 600 µl of cleared supernatant was incubated with 100-800 µl of antibody, 325 µl 5 x immunoprecipitation buffer, 0.1 % Triton X-100 and protein A sepharose beads at 4 °C for 3 h to complete the immunoprecipitation. Beads after the immunoprecipitation were washed thrice with 1 x IP buffer. Washed beads were then incubated with 5 x SDS-sample buffer for 5 min at 95 °C. The released proteins were resolved on a 10 % SDS-PA gel. The

size fractionated proteins were stained with silver. The bands shown in figure 23 were analysed by MALDI-MS.

5.5 Detection of phosphorylation

Dictyostelium cells were lysed in lysis buffer (for phosphorylation) as described above. The lysates were subjected to immunoprecipitation with the pSer/Thr antibody. Immunoprecipitated proteins were resolved on the 10 % SDS-PA gel and transferred on to nitrocellulose membrane and probed with mAb 82-421-5.

5.6 Western blotting using the semi-dry method

The proteins resolved by SDS-PAGE were electrophoretically transferred from the gel to a nitrocellulose membrane by the method described by Towbin¹⁴⁹ with little modifications. The transfer was performed using Towbin's buffer in a semi-dry blot apparatus (Bio-Rad) at a constant voltage of 10 V for 45-60 min. The instructions provided along with the semi-dry apparatus were followed in order to set up the transfer.

Transfer buffer: 39 mM glycine,
 48 mM Tris/HCl, pH 8.3
 and 20% methanol

5.7 Immunodetection of membrane-bound proteins

The western blot was immersed in blocking buffer and the blocking was performed with gentle agitation either overnight at room temperature or for 2-3 h at room temperature with several changes of 1x NCP. After blocking, the blot was incubated at room temperature with gentle agitation with either commercially available primary antibody at a proper dilution (in 1x NCP) or hybridoma supernatant or purified antibody for 1-2 h. After incubation with primary antibody, the blot was washed 5-6 times with 1x NCP at room temperature for 5 min each with repeated agitation. Following the washing steps, the blot was incubated for 1 h at room temperature with a proper dilution (in 1x NCP) of horseradish peroxidase-conjugated secondary antibody directed against the primary antibody. After incubation with the secondary antibody, the blot was washed as described above. After washings, the enhanced chemi-luminescence (ECL) detection system was used. For this, the blot was incubated in ECL-detection-solution for 1-2 min and then wrapped in Saran wrap after removing the excess ECL-detection solution. A X-ray film was exposed to the wrapped membrane for 1-30 min and the film was developed to observe the immunolabelled protein.

ECL-detection solution:

2 ml 1 M Tris/HCl, pH 8.0
200 μ l 250 mM 3-aminonaphthylhydrazide in DMSO
89 μ l 90 mM p-Coumaric acid in DMSO
18 ml deionised H₂O
6.1 μ l 30% H₂O₂ (added just before using)

Blocking buffer :

5% milk powder in 1x
NCP

5.8 Video imaging and chemotaxis assay

Vegetative cells were resuspended at 1×10^7 cells/ml in Soerensen phosphate buffer and starved for 6 to 8 h. 25-30 μ l of the cell suspension were diluted in 3 ml of Soerensen buffer and mixed well by pipetting (25-30 times, with occasional vortexing). This is important to dissociate cells from aggregates. 1.5 ml of the diluted cells were then transferred onto a 5 cm glass coverslip with a plastic ring placed on an Olympus IX70 inverse microscope equipped with a 10x UplanFl 0.3 objective. Cells were stimulated with a glass capillary micropipette (Eppendorf Femtotip) filled with 0.1 mM cAMP (Gerisch and Keller 1981), which was attached to a microcontroller. Time-lapse image series were captured and stored on a computer hard drive at 30 second intervals with a JAI CV-M10 CCD camera and an Imagenation PX610 frame grabber (Imagenation Corp., Beaverton, OR) controlled through Optimas software (Optimas Corp., Bothell, Washington). The DIAS software (Soltech, Oakdale, IA) was used to trace individual cells along image series and calculate the cell motility parameters (Soll *et al.* 2001). For processing images, Corel Draw version 8, Corel Photopaint and Adobe Photoshop were used.

5.9 Qualitative phototaxis assay (Wallraff and Wallraff, 1997)

Dictyostelium AX2 cells and derived mutants were cultivated on *Klebsiella* lawns on SM agar plates. Using sterile toothpicks, vegetative cells from edges of the colonies growing on *Klebsiella* lawns were transferred to 90 mm water agar plates. The application point for phototaxis was located in the centre of the plate. The plates were wrapped in an opaque black plastic sheet with a slit of ~ 3 mm and incubated at 21 °C. Approximately 48 h after inoculation, slime trails and cellular material were blotted to nitrocellulose filter (BA85, \varnothing 82 mm, Schleicher and Schuell) by keeping the filter on the plate for 1 h. Thereafter, filters were stained with staining solution for 5 min followed by incubation in destaining solution (with 2 changes) for 10-15 min to remove the excess stain. The filters exhibiting the stained slime trails were photographed using a light microscope (Olympus) equipped with a CCD camera (CVM10, Progressive Scan, Japan). The distance traveled by the slugs towards the source of

light from the point of application and the deviation from the straight line were measured. The angle of deviation was calculated from these two measurements.

Staining solution:

0.1 % amido black

25 % isopropanol

Destaining solution:

25 % isopropanol

10 % acetic acid

6 Immunological methods

6.1 Indirect immunofluorescence of *Dictyostelium* cells

6.1.1 Preparation of *Dictyostelium* cells

Dictyostelium cells were grown in shaking culture to a density of $2-4 \times 10^6$ cells/ml. The desired amount of cells was collected in a centrifuge tube, cells were then resuspended in fresh axenic medium and grown overnight on glass coverslips in axenic medium. Alternatively, cells from the shaking culture were allowed to attach to the coverslips for 20 min. Thereafter, cells attached onto the coverslip were fixed immediately by one of the fixation techniques described below.

6.1.2 Methanol fixation

After the cells had attached to the coverslip, the supernatant was aspirated and the coverslip was dipped instantaneously into pre-chilled (-20 °C) methanol in a petri dish and incubated at -20 °C for 10 min. The coverslip was then taken out from methanol and placed on a parafilm covered glass plate resting in a humid box with the cell-surface facing upwards. This was followed by 2 washings with 500 μ l of PBG for 15 min each and immunolabelling as described in section 6.1.3

PBG, pH 7.4: 0.5 % bovine serum albumin

0.1 % gelatin (cold-water fish skin) in 1x PBS, pH 7.4

6.1.3 Picric acid-paraformaldehyde fixation

After the cells had attached to the glass coverslips the supernatant was gently aspirated from the edge of the coverslip and 200 μ l of freshly prepared picric acid-paraformaldehyde solution was directly added. The coverslip was incubated at room temperature for 30 min. After incubation, the picric acid-paraformaldehyde solution was aspirated, the coverslip was picked up with a fine forceps and swirled in 10 mM PIPES buffer, pH 6.0, followed by blotting off the excess solution with a tissue paper. Now the coverslip was swirled in PBS/glycine and

placed on a parafilm-covered glass plate resting in a humid chamber. The coverslip was then washed with 500 μ l PBS/glycine for 5 min to block free reactive groups followed by post-fixation with 500 μ l 70 % ethanol for 10 min. This was followed by 2 washings with 500 μ l of PBG for 15 min each. After washings, the cells were immunolabelled as described in section 6.1.4.

Picric acid-paraformaldehyde solution:

0.4 g paraformaldehyde was dissolved in 5 ml ddH₂O by stirring at 40 °C and adding 3-4 drops of 2 M NaOH. After dissolving, the volume was adjusted to 7 ml with ddH₂O. To this paraformaldehyde solution, 10 ml of 20 mM PIPES buffer, pH 6.0, and 3 ml of saturated picric acid was added and the pH was finally adjusted to 6.5.

PBS/glycine:

500 ml PBS
3.75 g glycine
filter sterilized
store at -20°C

20 mM PIPES buffer, pH 6.0:

0.605 g PIPES
in 100 ml distilled H₂O
adjust to pH 6.0
filter sterilized

6.1.4 Immunolabelling of fixed cells

Coverslips containing the fixed cells were incubated with 200 μ l of the desired dilution (in PBG) of primary antibody for 1-2 h in a humid box at room temperature. After incubation, the excess unattached antibody was removed by washing the coverslip 6 times with PBG for 5 min each. Now the coverslip was incubated for 1 hr with 200 μ l of a proper dilution (in PBG) of Cy3-conjugated secondary antibody. Following this incubation, two washings with PBG for 5 min each followed by three washings with PBS for 5 min each were performed. After washings, the coverslip was mounted onto a glass slide (see sections, 6.1.5).

6.1.5 Mounting of coverslips

After immunolabelling of the fixed cells, the coverslip was swirled once in deionised water and the extra water was soaked off on a soft tissue paper. Now a drop of gelvatol was placed to the middle of a clean glass slide and the coverslip was mounted (with the cell-surface facing downwards) onto the drop of gelvatol, taking care not to trap any air-bubble between the coverslip and the glass slide. Mounted slides were then stored overnight in the dark at 4 °C. Thereafter, the mounted slides were observed under a fluorescence microscope or confocal laser scanning microscope.

Gelvatol

2.4 g of polyvinyl alcohol (Mw 30,000-70,000; Sigma) was added to 6 g of glycerol in a 50 ml centrifuge tube and mixed by stirring. To the mixture, 6 ml of distilled water was added and the mixture was incubated at room temperature. After several hours of incubation at room temperature, 12 ml of 0.2 M Tris/HCl, pH 8.5, was added and the mixture was heated to 50°C for 10 min with occasional mixing to completely dissolve polyvinyl alcohol. The solution was centrifuged at 5,100 rpm for 15 min. After centrifugation, 2.5 % of diazabicyclo octane (DABCO), an anti-oxidant agent, was added to reduce the bleaching of the fluorescence. The solution was aliquoted in 1.5 ml microcentrifuge tubes and stored at -20 °C.

6.2 Preparation of heat-killed yeast cells

Five grams of dry yeast *Saccharomyces cerevisiae* (Sigma) were suspended in 50 ml of PBS in a 100 ml Erlenmeyer flask and incubated for 30 min in a boiling waterbath with stirring. After boiling, the yeast cells were washed five times with PBS, followed by two washings with Soerensen phosphate buffer. The yeast cells were then finally resuspended in Soerensen phosphate buffer at a concentration of 1×10^9 yeast cells/ml. Aliquots of 1 ml and 20 ml were made and stored at -20 °C.

6.3 TRITC-labeling of heat-killed yeast cells

For labeling, the pellet of 2×10^{10} heat-killed yeast cells were resuspended in 20 ml of 50 mM Na₂HPO₄, pH 9.2, containing 2 mg of TRITC (Sigma) and incubated for 30 min at 37 °C on a rotary shaker. After washing twice with 50 mM Na₂HPO₄, pH 9.2, and four times with Soerensen phosphate buffer, aliquots of 1×10^9 yeast cells/ml were frozen at -20°C.

7 Microscopy

Visual inspection of *Dictyostelium* cells expressing ddfilamin rod domain GFP fusion protein was performed using an inverted fluorescence microscope (Olympus IX70). Confocal images of immunolabelled specimens were obtained with confocal laser scanning microscope TCS-SP (Leica) equipped with a 63x PL Fluotar 1.32 oil immersion objective. A 488-nm argon-ion laser for excitation of GFP fluorescence and a 568-nm krypton-ion laser for excitation of Cy3 or TRITC fluorescence were used. For simultaneous acquisition of GFP and Cy3 fluorescence, the green and red contributions to the emission signal were acquired separately using the appropriate wavelength settings for each photomultiplier. The images from green

and red channels were independently attributed with colour codes and then superimposed using the accompanying software.

7.1 Live cell imaging of *Dictyostelium* cells expressing RN-GFP

To record the distribution of ddfilamin rod domain GFP fusion protein in living cells, cells were grown to a density of $2-3 \times 10^6$ cells/ml, washed in Soerensen phosphate buffer and resuspended at a density of 1×10^7 cells/ml. The cells were then starved for about 1 hr with shaking. Starvation facilitated observation as it allowed the cells to digest endocytosed nutrient medium, which is autofluorescent. For observation, cells were initially diluted in Soerensen phosphate buffer at 1×10^6 cells/ml and then 500 μ l of the cell suspension were transferred onto a 18 mm glass coverslip glued to a plastic rim of the same size. Cells were allowed to adhere to the glass coverslip for 10-15 min and confocal images were obtained and processed as described above.

7.2 Live cell imaging of RN-GFP during phagocytosis

For analysis of dynamics of ddfilamin rod domain GFP fusion protein during phagocytosis, coverslips containing RN-GFP expressing AX2 and HG1264 cells were prepared as described above. After the cells had adhered to the glass coverslips, 5-10 μ l of the heat-killed, TRITC-labelled yeast cell suspension (1×10^9 yeast cells/ml) were carefully added from one edge of the coverslip. Immediately after the yeast cells had settled (in 2-5 min), confocal images were obtained as explained above.

7.3 Microscopy of fixed preparations

To visualize the actin staining in the fixed preparations, an Olympus IX70 inverse microscope equipped with a 40X LCPlanFI 0.6 and a 10X UplanFI 0.3 objective was used. Images were captured either with a JAI CV-M10 CCD video camera or a SensiCam cooled CCD video camera.

8 Microarray analysis

Array Targets

The 34 Mb genome of *Dictyostelium discoideum*, carries about 12,000 genes. A collection of a total of 6,000 genes used as the array targets carries partial sequences of 450 known genes (PCR amplified sequences of an average length of 500 bp) and approximately 5,400 non-

redundant ESTs from the *Dictyostelium* cDNA project (Morio *et al.* 1998) (<http://www.csm.biol.tsukuba.ac.jp/cDNAproject.html>) and appropriate positive (partial genes from *D. discoideum* genomic DNA), negative controls (fish sperm DNA, human Cot-1) and internal control (Sport report Poly A).

8.1 RNA preparation

Wild-type AX2 and ddfilamin minus mutant GHR cells grown axenically to $2-3 \times 10^6$ cells / ml were washed twice with Soerensen phosphate buffer and developed in suspension to the final concentration of 1×10^7 cells per ml in Soerensen phosphate buffer for 10 h at 21 °C before used for extraction of total RNA. The total RNA was extracted with the Qiagen RNeasy Midi/Mini Kit according to the “Protocol for Isolation of Cytoplasmic RNA from Animal Cells” with the modification of washing the cells twice with water after harvesting to remove medium. $2-3 \times 10^7$ cells were used for the extraction. After extraction the RNA concentration is determined by measuring the OD₂₆₀ (should be > 500 µg/ml). The quality of RNA was examined on a gel (materials methods 3.8) should give two bands of 4.1 and 1.9 kb for rRNA without degradation.

8.2 Spiking of internal mRNA controls

Quality control is an important issue of DNA microarray analysis. Therefore we use ten internal mRNA controls from *Arabidopsis thaliana* genes that are added (spiked) to the *D. discoideum* RNA prior to cDNA generation and labelling. These mRNAs are provided in a Spikemix with different known amounts of each mRNA. Two different mixes are used for the two labelling reactions (Cy3 and Cy5) of one microarray experiment. The spiking was done as follows.

The spiking of the RNA was done by mixing equal quantities of Spikemix and *D. discoideum* total RNA. The RNA mixture was precipitated by adding 0.1 volume of 3 M sodium acetate pH 4.8 and 2.5 volume of 100 % ethanol and stored at -20 °C for 2 h. The RNA was precipitated by centrifuging in a tabletop centrifuge at 10,000g for 30 min. Ethanol was removed by aspiration and the pellete was washed with 70 % ethanol, centrifuged for 15 min at 10,000g aspirated and dried. The RNA was dissolved in 12 µl of RNase-free water.

cDNA generation and fluorescent labelling:

The reverse transcription of mRNA to cDNA was done with the protocol from the Stratagene Fair Play Kit with some modifications.

8.3 Quantitation, normalization and data analysis

The fluorescent labelled cDNA targets bound to the spots were detected by the ScanArray 4000XL confocal laser scanner. The microarray is scanned for Cy3 and Cy5 successively with a resolution 10 $\mu\text{m}/\text{pixel}$. The fluorescent dyes were excited by laser-light of pertinent wavelength and emission was detected by a photo-multiplier. To obtain images well suited for signal quantification image brightness has to be adjusted by setting the laser-power (photo-multiplier power should always be set at 70 to 80 %). Signals should be as bright as possible, but spots must not be saturated (indicated by white colouring). It might be necessary to scan at two different laser-power settings. One setting where most spots give bright signals, but a few like some of the positive controls are saturated, and another setting where no saturation is seen, but most spots give weak signals.

8.4 Signal Quantification

The spot and background intensities of the scanned images were quantified by using QuantArray. The two images for the Cy3 and Cy5 scan were aligned first and then an array pattern was laid over the images to support spot detection. In this step the spot identities were also assigned. The signal intensities were then measured and written into an export file, which was used for data analysis.

For the detailed procedure please see

<http://www.uni-koeln.de/med-fak/biochemie/transcriptomics/>

III. Results

1. Biochemical Studies

The filamin binding site on actin has been shown to reside at residues 105-120 and 360-372 in actin subdomain-1 (Mejan *et al.* 1992). These sites over-lap with those of several other actin binding proteins including α -actinin (McGough1998).

1.1 Overexpression of domains of filamin

The cDNA encoding full-length ddfilamin (FLC), the actin-binding domain along with the first five rod domains (Fil5) and the actin binding domain alone (ABD) were cloned in frame at the N-terminus of GFP into the P1ABSr8 vector. The expression was under the control of the actin-15 promoter. The rod domain was subcloned in frame at the N-terminus of GFP into the GFP expression vector pDex79 allowing expression of the fusion protein RN-GFP under the control of the actin-15 promoter (Knecht *et al.* 1986) (Materials and Methods, 3.11.1). The plasmid pDXA-GABD expressing the ABD-GFP fusion was obtained from Dr. David Knecht (Connecticut, USA) (Pang *et al.* 1998). All vectors were introduced into AX2 wild

type cells as well as into the ddfilamin minus mutant HG1264 and into GA1, a mutant lacking ddfilamin and α -actinin by electroporation singly or together. The stable transformants were selected for growth in the presence of 20 μ g/ml G418 (Geneticin) or 10 μ g/ml Blasticidin S (Bsr) or both (in case of cotransformation). The transformants were identified by visual inspection under a fluorescence microscope or by colony blotting followed by immunological detection of the expressed proteins in western blots, which showed that with the exception of FLC-GFP expression in AX2 and Fil5-GFP expression in HG1264 the amounts of fusion proteins produced were comparable or slightly lower than ddfilamin expression in AX2 (Figure 1). The expression level of the ddfilamin rod GFP fusion was higher in AX2 cells expressing the fusion protein than in HG1264 cells expressing the fusion protein. This was shown by western blotting and probing with ddfilamin rod domain specific antibody 82-454-12 and GFP specific antibody K3-184-2 (Figure 2). The strains were used for *in vivo* localization studies and rescue experiments.

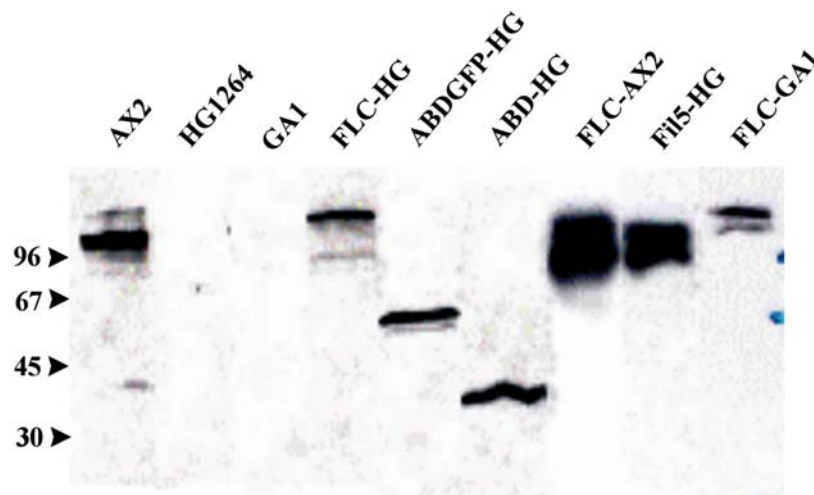


Figure 1: Western blot analysis to test the expression of different domains in AX2 (wild type), HG1264 (filamin minus) and GA1 (ddfilamin and α -actinin minus). 5×10^5 cells were lysed in SDS-sample buffer and the proteins were resolved by SDS PAGE (10 % acrylamide), the proteins were blotted onto a nitrocellulose membrane and probed with mAb 82-421-5, which recognizes the actin binding domain of ddfilamin. HG1264 and GA1 do not express the protein. In AX2 the band appears lower than expected because of the proteolytic degradation of the protein. FLC-AX2, FLC-HG, FLC-GA1, are AX2, HG1264 and GA1 cells expressing full-length ddfilamin fused with GFP at the C-terminal end respectively. ABDGFP-HG, HG1264 cells expressing ABD fused to the C-terminus of GFP. ABD-HG, HG1264 cells expressing ABD. Fil5-HG, HG1264 cells expressing ddfilamin without the dimerization domain with C-terminally fused GFP. Detection was by enhanced chemiluminescence using a peroxidase-coupled secondary antibody. Molecular weight markers are given in kDa at the left.

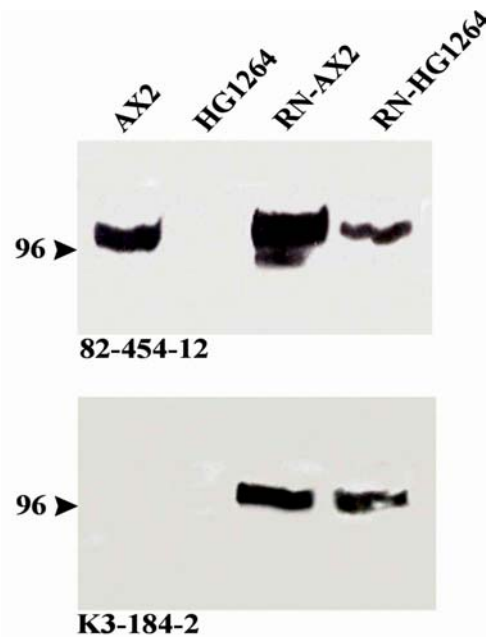


Figure 2: Expression of the ddfilamin rod domain in AX2 and HG1264. 5×10^5 cells were lysed in SDS-sample buffer, the lysates were resolved on 10 % polyacrylamide gels, the proteins were blotted onto a nitrocellulose membrane and probed with mAb 82-454-12 specific for the rod domain and GFP specific mAb K3-184-2. RN-AX2 and RN-HG1264, AX2 and HG1264 cells expressing ddfilamin rod domain with N terminally fused GFP.

1.2 Localisation and distribution of ddfilamin domains during growth

The pattern of the GFP-ABD fluorescence in *Dictyostelium* AX2 cells was reported to coincide with that of dye-labelled phalloidin, indicating that the GFP-ABD colocalises with F-actin (Pang *et al.* 1998). From this information we concluded that the ABD of ddfilamin targets to the F-actin network at the cell periphery (Figure 3A) where the protein might bind to other proteins involved in signal transduction and might control cellular functions like phototaxis. Fil5-GFP shows both a cytosolic staining and enrichment in cell extensions (Figure 3B). The localisation of Fil5-GFP was similar to that of full-length ddfilamin (Figure 3C). Unlike ABD-GFP, FLC-GFP and Fil5-GFP were localised in the cytosol as well.

1.3 Expression of full-length ddfilamin GFP fusion protein in GA1 compensates the loss of α -actinin

Expression of ddfilamin GFP in GA1 (filamin and α -actinin deficient) rescued all the defects of this mutant as described in Rivero *et al.* (1996) including phototaxis. The FLC-GFP when overexpressed in AX2 cells localises in discontinuous patches near the membrane (Figure 3C), however in the GA1 mutant it localises in a rim at the circumference of the cell. The overexpressing cells show numerous filopods, however the fusion protein was not present in

the filopods but only at the base of each filopod, giving a punctate localisation for the fusion protein (Figure 3D and F, arrowhead).

Upon starvation, *Dictyostelium* cells polarise, sense cAMP and start aggregating towards the aggregation centre. Simultaneously they produce cAMP pulses themselves signaling to the other cells in the population and migrate towards the cAMP signaling centre. During this directional movement several proteins reorganise and redistribute. We studied the localisation of ABD-GFP and Fil5-GFP in HG1264 and of ddfilamin-GFP in GA1 developed in suspension for 6 h. The fusion proteins were very prominent at the base of newly extended pseudopods and along the periphery of the cell. The location at the cell periphery occurred discontinuously in a punctate manner. In case of the ABD-GFP we observed a reduced cytosolic staining as compared to Fil5-GFP and FLC-GFP. We also noted a relative increase in fluorescence at the rear end of the cell in ABD-GFP expressing cells (Figure 4a). It has been also observed that the protein rapidly translocates to the rear end upon the change in direction (Laevsky and Knecht, 2003). In case of Fil5- and FLC-GFP expressing cells the relative fluorescence at the rear end was less as compared to that of present at the leading edge of the cell (Figure 4 B and C).

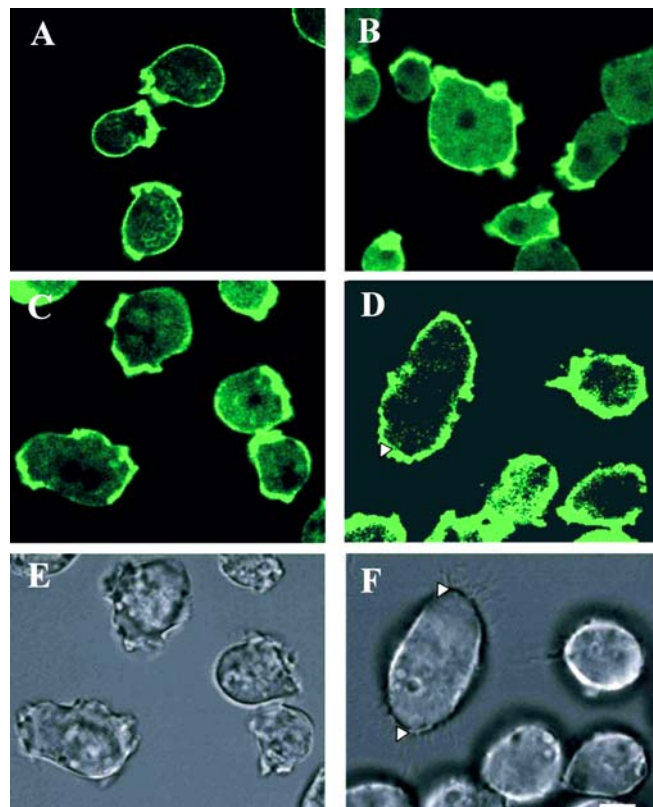


Figure 3: (Opposite page) Localisation and distribution of GFP-tagged full-length ddfilamin(FLC-GFP), the actin binding domain (ABD-GFP) and ddfilamin lacking the dimerisation domain (Fil5-GFP). Cells grown axenically were washed twice with Soerensen phosphate buffer and allowed to settle on coverslips, images of live cells were taken using a confocal laser scanning microscope. (A), HG1264 cells expressing ABD-GFP, (B), HG1264 cells expressing Fil5-GFP, FLC-GFP expressed in AX2 (C) and GA1 (D), respectively. E and F are the corresponding phase contrast images for C and D, respectively. Size bar, 3 μ m. The arrow in D and F indicates the base of the extended filopod.

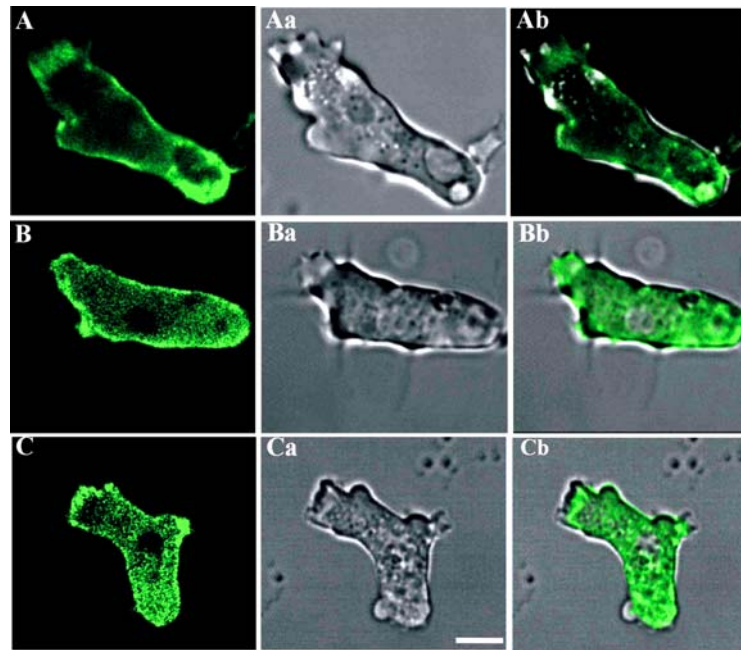


Figure 4: Localisation and distribution of FLC-GFP, ABD-GFP and Fil5-GFP in aggregation competent cells. Cells grown axenically were washed twice with Soerensen phosphate buffer, starved in suspension for six hours and allowed to settle on coverslips. Images of live cells were taken using confocal laser scanning microscopy. The left panels show the GFP fluorescence of (A) HG1264 cells expressing ABD-GFP, (B) HG1264 cells expressing Fil5-GFP, and (C), GA1 cells expressing FLC-GFP. Aa, Ba and Ca are transmission microscopic images of the respective cells. The left panels show the overlay. Bar, 3 μ m.

1.3.1 The ddfilamin rod domain GFP fusion protein (RN-GFP) does not localise properly in HG1264 cells

Filamin is located in the actin cortex at the cell periphery and in cell extensions in *Dictyostelium* cells²¹. When we expressed the GFP-tagged rod domain (RN-GFP) and studied its localisation, we observed RN-GFP exclusively in the cytosol and not in the cell cortex in the mutant, whereas in AX2 cells the fusion protein was present in the cytosol and was also enriched in cell extensions (Figure 5). To determine whether RN-GFP colocalises with the actin cytoskeleton, RN-GFP expressing HG1264 cells were fixed with cold methanol and immunostained with anti-actin monoclonal antibody (Act 1-7) followed by staining with Cy3

conjugated goat-anti mouse IgG as the secondary antibody (as described in Materials and Methods 6.1.4). We found that the distribution of the fusion protein did not coincide with that of actin in the cortical regions (Figure 6). This might well be due to the absence of the actin-binding domain. Surprisingly, in AX2 cells the distribution parallels the one of F-actin. Here the fusion protein can possibly form heterodimers with the endogenous filamin, which targets the fusion protein to the cell cortex.

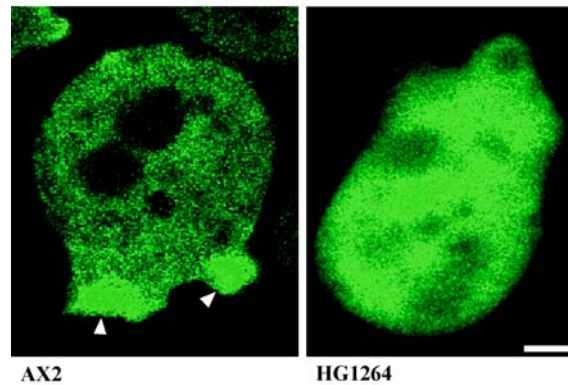


Figure 5: Localisation of the GFP-filamin rod fusion protein (RN-GFP) in wild type and mutant cells. Axenically grown cells were washed twice with Soerensen phosphate buffer and allowed to settle on coverslips, images of live cells were taken using confocal laser scanning microscopy. In case of AX2 cells, the GFP fusion protein is present throughout the cell and accumulates in cell extensions (arrowheads). In the HG1264 mutant the protein is evenly distributed throughout the cells and does not accumulate in cell fronts. Bar, 2 μ m.

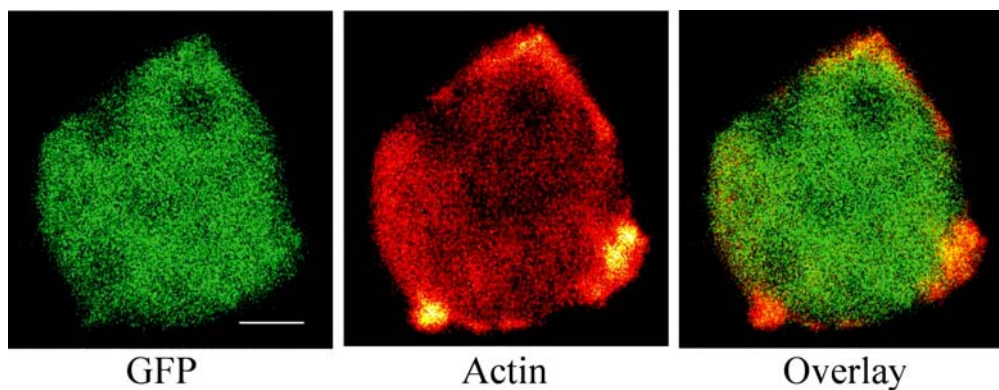


Figure 6: Subcellular Localization of RN-GFP in HG1264. Immunofluorescence studies performed with RN-GFP expressing cells show that the fluorescence pattern of the GFP fusion protein does not coincide with that of the actin staining for most areas of the cells. The cells were fixed with methanol and immunolabeled with actin specific mAb act 1-7 followed by a secondary Cy3-labeled antibody. Bar, 4 μ m.

1.3.2 Ddfilamin rod domain GFP fusion protein (RN-GFP) forms heterodimers with the endogenous protein

To confirm the proposed heterodimer formation of ddfilamin and RN-GFP biochemically, we immunoprecipitated the fusion protein from AX2 cells using mAb K3-184-2 against GFP, resolved the immunoprecipitate by SDS-PAGE and probed the blot with mAb 82-421-5 specific for the ABD of filamin (Figure 7, IP). In this blot we detected a band above 96 kDa, which corresponds to filamin and another band at around 50 kDa, which represents the heavy chain of the antibody used for the immunoprecipitation. The presence of filamin is most likely due to the heterodimerisation, as in control experiments filamin could not be immunoprecipitated with mAb K3-184-2. The amount of immunoprecipitated ddfilamin is around 50 % of the total amount of the protein that was immunoprecipitated. This was confirmed by probing the same blot with mAb 82-454-12 specific for the ddfilamin rod domain after stripping the earlier antibody (data not shown).

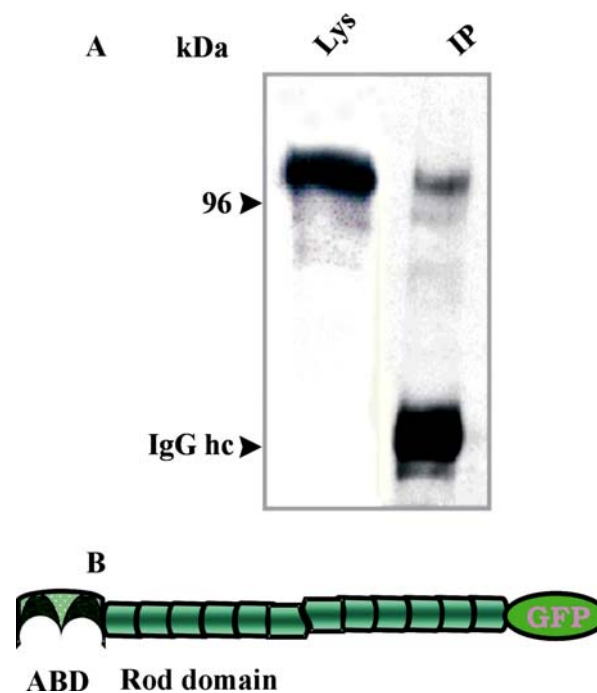


Figure 7: The filamin rod domain GFP fusion (RN-GFP) forms heterodimers in AX2 cells. AX2 cells expressing RN-GFP were lysed in homogenization buffer, the lysate was cleared and incubated with mAb K3-184-2 against GFP to immunoprecipitate the fusion protein followed by addition of protein A sepharose. The cell lysate and sepharose beads were boiled in SDS sample buffer and the proteins resolved on a SDS-PA gel (10 % acrylamide). The proteins were transferred onto a nitrocellulose membrane and probed with mAb 82-421-5 specific for filamin's ABD (A). (B) The schematic representation of the heterodimer.

1.3.3 A GFP tag located at the C-terminus does not interfere with the dimerisation property of filamin

The sixth rod repeat located at the C terminal end of the ddfilamin is responsible for the dimerisation of the protein (Fucini et al., 1999). To find out whether the conjugation of GFP at the C terminal end of the protein interferes with the formation of the dimer in FLC-GFP, we performed native gel electrophoresis. As only a single band was observed with homogenates from AX2 cells as well as from AX2 cells overexpressing FLC-GFP (Figure 8), and as there was no detectable amount of the monomeric form of the protein present in the cell, we concluded that, full-length ddfilamin with a C terminal GFP tag dimerises normally. The formation of the heterodimer (ddfilamin-FLC-GFP) was possible but difficult to detect because of the rather small differences in the molecular weights. In HG1264 cells expressing recombinant Fil5-GFP that lacks the dimerisation domain, we detected only the monomeric form of the protein. The higher bands in the last two lanes might represent a complex of proteins interacting with ddfilamin.

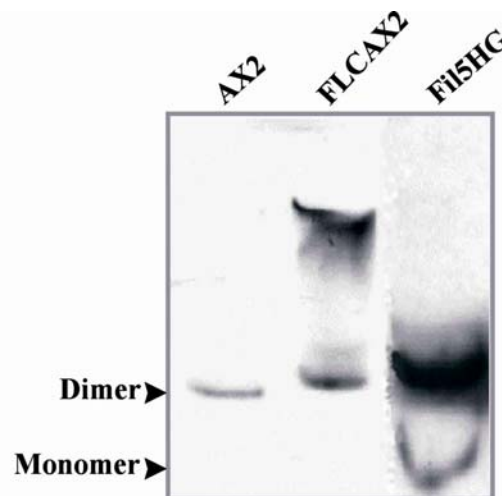


Figure 8: Dimerisation propensity of ddfilamin. To test whether a C-terminally located GFP-tag interferes with the dimerisation of ddfilamin, we performed native polyacrylamide gel electrophoresis. Wild type AX2, AX2 cells expressing full-length ddfilamin fused with GFP at its C terminus (FLCAX2) and mutant cells expressing ddfilamin without its dimerisation domain (Fil5HG) were lysed in lysis buffer and the proteins were resolved on a native polyacrylamide gel with tracking dye. After the dye had reached the bottom, gels were soaked in 1x NCP buffer containing 1 % SDS at 4 °C for one hour before blotting onto nitrocellulose. Blots were probed with mAb 82-421-5 followed by enhanced chemiluminescence. The band indicated by the arrows in each case was in the range of the dimer indicating that there was no interference of GFP with the dimerisation of ddfilamin. The upper band in case of the Fil5 lane seems to be non-specific as in case of FLC-GFP.

1.4 Detection of phosphorylation and generation of a point mutation

It has been shown earlier that ddfilamin can be phosphorylated in vitro by protein kinase A (unpublished data). To detect in vivo phosphorylation of ddfilamin, we immunoprecipitated proteins from a cell lysate from AX2 cells expressing recombinant FLC-GFP with commercial pSer/Thre specific pAb and probed the immunoprecipitate after western blotting with ddfilamin specific mAb 82-421-5. Filamin can be clearly detected proving that the proteins is phosphorylated also in vivo (Figure 9, IP). The bands of slightly smaller mass than 120 kDa are most likely due to proteolysis of the highly protease sensitive filamin.

There are several predicted phosphorylation sites in filamin (for the prediction of phosphorylation we used the NetPhos program, from the Technical University Denmark). Taking into account the specificity of the antibody used, which recognise phosphoserine/threonine with arginine present at the -3 position, we found four probable phosphorylation sites, which are located at S160 and S174 in the Calponin Homology Domain 2 (CH2) of the actin binding domain and T247 and S248 at the -2 and -1 amino acids respectively at the start of the first rod domain. The predicted phosphorylation site S174 is conserved within human skeletal muscle α -actinin 2, *Drosophila* spectrin β -H chain and actin binding protein WO4D2. The CH2 domain harbors the actin binding site 3 (ABS3), which contributes to F-actin binding in such a way that the CH1 and CH2 domains in concert bind to F-actin with higher affinity than the CH1 domain alone (reviewed in Arjan 2001). Therefore we decided to introduce a mutation at S174, which abolishes phosphorylation.

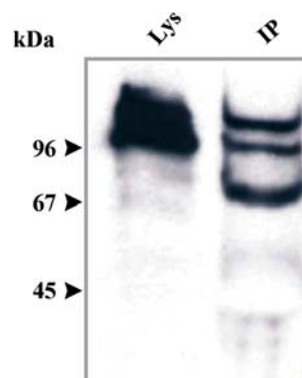


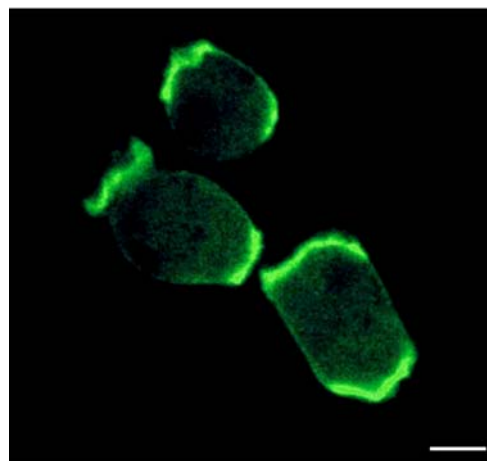
Figure 9: Detection of phosphorylation. Western blot showing phosphorylation of ddfilamin. AX2 cells expressing FLC-GFP were lysed in lysis buffer and subjected to immunoprecipitation with a pSer/Thre specific pAb followed by addition of protein A-sepharose beads. The beads were washed thrice with 1x IP buffer, lysed in SDS sample buffer and proteins were resolved on 10 % SDS-polyacrylamide gels. The proteins were transferred onto nitrocellulose membranes and probed with ddfilamin specific mAb 82-421-5. The lower band in the IP lane is possibly due to the degradation of the ddfilamin. The total cell lysate (Lys) is shown for control.

1.4.1 Generation of the point mutation

To study the significance of the phosphorylation at the detected phosphorylation site, the point mutation was generated by performing the overlapping PCR. Full-length ddfilamin cDNA was used as a template to amplify a fragment between two of the three EcoRV sites (ERV 286, ERV548 and ERV564). ERV548 was mutated at the last nucleotide of the palindrome (5'GATATC3'-5'GATATT3') without changing the amino acid. The amplified fragment was cloned into the EcoRV site of FLC-GFP. The direction of cloning was confirmed by PCR. For detailed procedure please see materials and methods (3.6). The mutated cDNA was used to transform HG1264 cells. The transformed cells were selected by visual inspection for GFP under the UV light.

2.4.2 Expression and localisation of the mutated protein

By confocal microscopy the distribution of FLC(S174A)-GFP appears to be the same as that of the non-mutated protein. The fusion protein accumulates at the front of the cell as well as at the rear end of the cell and discontinuously along the periphery. Like FLC-GFP and Fil5-GFP, FLC(S174A)-GFP also shows the diffused cytosolic staining (Figure 10).



S174AFLC-GFP

Figure 10: Localisation of the FLC (S174A)-GFP in HG1264 cells. Axenically grown cells were washed twice with Soerensen phosphate buffer and allowed to settle on coverslips, images of live cells were taken using confocal laser scanning microscopy. The fusion protein is present throughout the cell and accumulates in cell cortex. The punctuated staining appeared the same as that of FLC-GFP expression in HG1264. Bar, 5 μ m.

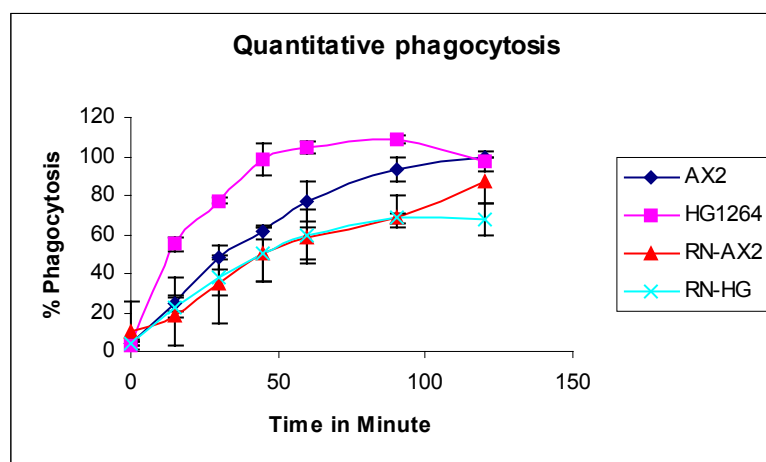
2 Role of filamin in phagocytosis

2.1 Overexpression of the filamin rod domain reduces phagocytosis activity in AX2 as well as in mutant cells

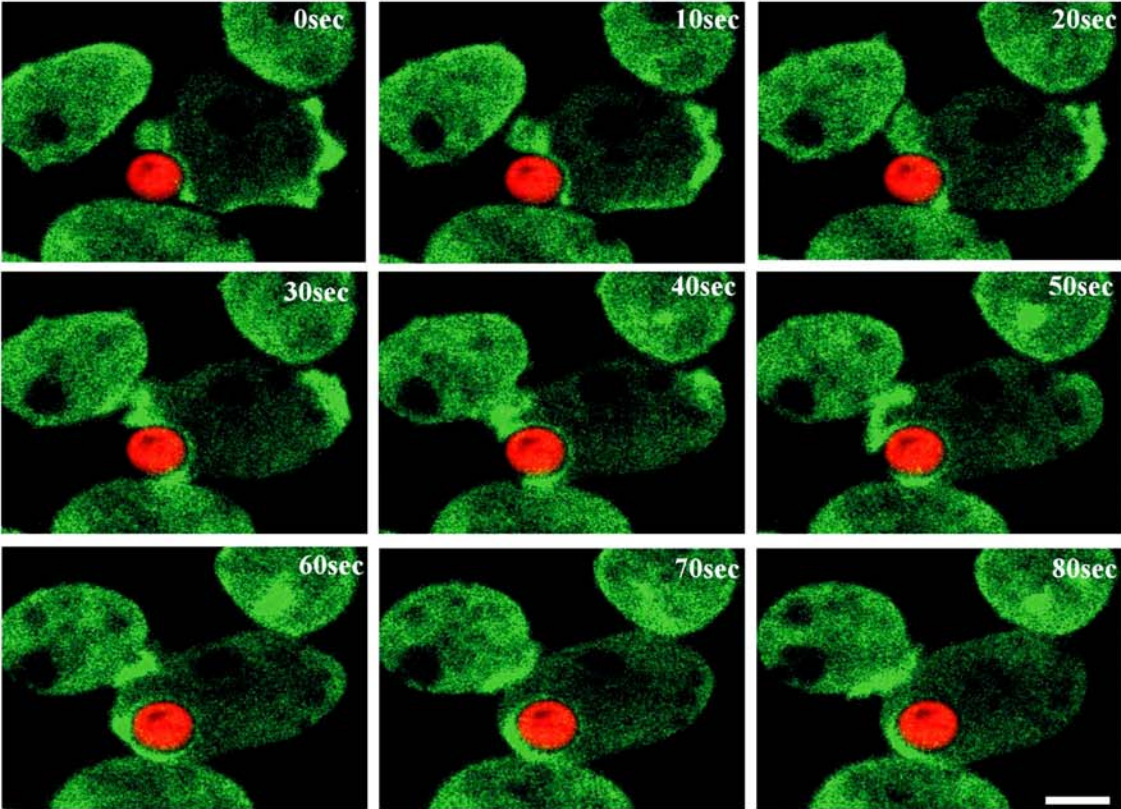
When we studied the localisation and redistribution of RN-GFP in AX2 cells during phagocytosis using confocal microscopy we found that RN-GFP was enriched in the newly formed phagocytic cup (Figure 11A). It was most prominent at the front of the phagosome, where actin also strongly accumulates (Cox *et al.* 1996). During the phagocytic event the fusion protein also accumulated at the rear end of the phagocytic cup and disappeared immediately after the completion of the engulfment (60 sec). In HG1264 cells expressing RN-GFP there was no enrichment observed in the phagocytic cup and the fusion protein remained purely cytosolic at all stages of phagocytosis (Figure 11B).

Our finding that RN-GFP forms heterodimers with the endogenous filamin in vivo led us to perform quantitative phagocytosis assays to test whether an impaired F-actin crosslinking due to formation of heterodimers could affect phagocytosis. To our surprise, we found that HG1264 cells were showing 20-40 % more phagocytosis before reaching a plateau and start exocytosing the TRITC labeled yeast particles used for the assay as compared to the AX2 cells (Figure 11C). These results are contradictory to our earlier finding (Rivero *et al.* 1996), which is most probably due to differences in the assay system used. Not only the AX2 but also the HG1264 cells expressing RN-GFP show 20-40 % reduced phagocytic rate. Therefore reduced phagocytosis was because of the expression of the ddfilamin rod domain. The overexpression of FLC-GFP in AX2 cells also has a similar effect.

C



A



B

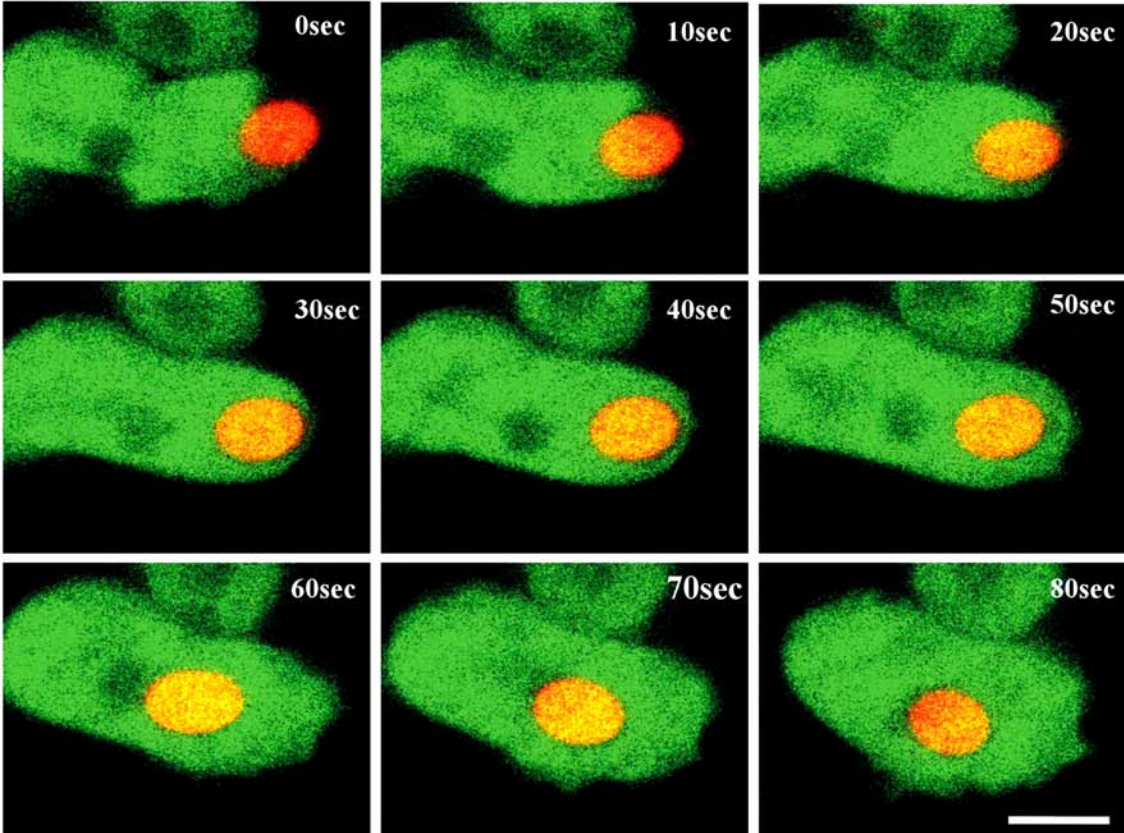


Figure 11 (Opposite page). Localisation and redistribution of RN-GFP in AX2 and HG1264 during phagocytosis. Confocal images of RN-GFP expressing AX2 (A) and HG1264 (B) cells taken at intervals of every 10 sec during phagocytosing the TRITC labelled heat killed yeast particles. In case of AX2 there is enrichment of the protein in the phagocytic cup and at the rear end of the cell but in case of the mutant HG1264 the fusion protein is purely cytosolic. Bar, 5 μm . (C) (please see p 53) Quantitative phagocytosis of TRITC labelled yeast cells. *Dictyostelium* cells were resuspended at 2×10^6 cells/ml in fresh axenic medium and challenged with a five fold excess of fluorescent yeast cells. Fluorescence from internalized yeasts was measured at the designated time points. Values shown are results from three independent experiments.

3. Phototaxis in mutant strains and rescue experiments

Migration of the slug is a complex phenomenon, which involves several proteins controlling various processes like cell-cell adhesion, cell-substrate adhesion, propagation of the cAMP wave to coordinate cell movement in the slug, and the proteins that are involved in the organisation of the tip and in controlling the cell fate. The absence of ddfilamin severely hampers the phototactic migration of the slug. This indicates the necessity of an organised actin cytoskeleton for this process where ddfilamin plays a fundamental. AX2 slugs migrate straight towards the point of light entry (Figure 12 C) while HG1264 slugs move with an angle and exhibit reduced motility as compared to wild type slugs (Figure 12 B). To understand the functional role of the protein at the molecular level, we expressed full-length ddfilamin, different domains and deletion constructs in AX2 and HG1264 cells and analysed the slug behaviour.

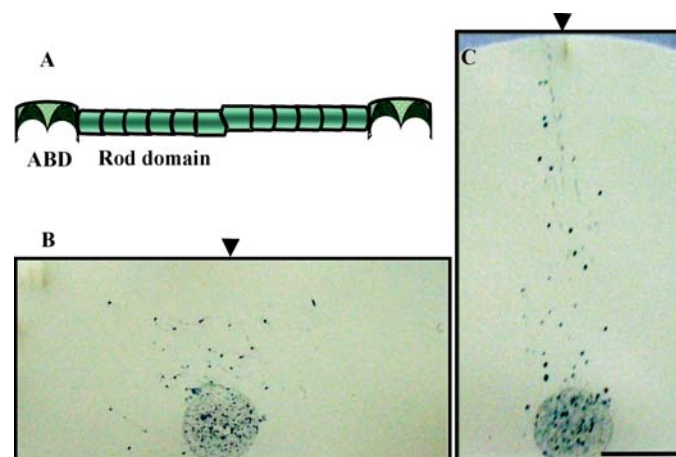


Figure 12. Phototactic migration of the parent strains. Cells grown on *Klebsiella aerogenes* (clearing plates) were harvested and washed with Soerensen buffer to remove the bacteria. About 5×10^5 cells were placed in the centre of a water agar plate. Plates were incubated in a dark chamber with a slit (at the position indicated by a triangle) at 21°C for 48

h. Slugs were blotted onto a nitrocellulose membrane and stained with Amido black. AX2 slugs migrate straight towards the source of the light (C), while HG1264 slugs migrate shorter distances and with an angle towards the light source (B). (A), schematic representation of the ddfilamin showing formation of the homodimer through its sixth rod repeat. Bar, 1 μ m.

3.1 Expression of full-length ddfilamin and full-length ddfilamin with a mutation at the predicted phosphorylation site rescues the phototaxis defect

Expression of full-length ddfilamin GFP (FLC-GFP) fusion protein in HG1264 and GA1 rescues the phototaxis defect completely, suggesting that this protein is fully functional and reverts the phototactic phenotype to the wild type. The phototactic phenotype of AX2 slugs overexpressing FLC-GFP was not only accurate, but the slugs also migrated over longer distances and formed more slugs per plate (data not shown). The overexpression of the rod domain in AX2 cells had a similar effect (see below, section 3.2). We tested the expression of all the GFP fusion constructs by western blot analysis and confirmed that they were present throughout the life cycle (data not shown).

There are several reports describing the *in vitro* phosphorylation of filamin. Vadlamudi et al. (2002) showed that p21-activated kinase 1 (Pak-1) phosphorylates filamin, which in turn regulates the Pak-1 induced cytoskeletal reorganisation of the actin. Goldmann et al. (2002), reported that phosphorylation of filamin regulates its binding to lipid membranes, integrin and actin. We have shown the phosphorylation of ddfilamin *in vivo* and identified two phosphorylation sites, which are located in the CH2 actin-binding domain. We generated a single point mutation (S174A) in full-length ddfilamin and expressed this protein in HG1264 as a GFP fusion protein. The slugs expressing this protein migrate straight towards the light slit, but they travel over shorter distances. Only 12 % HG1264 slugs expressing (S174A) travel distances between 25 mm and 30 mm (33 slugs were analysed), while 40 % of AX2 slugs travelled an equal distance.

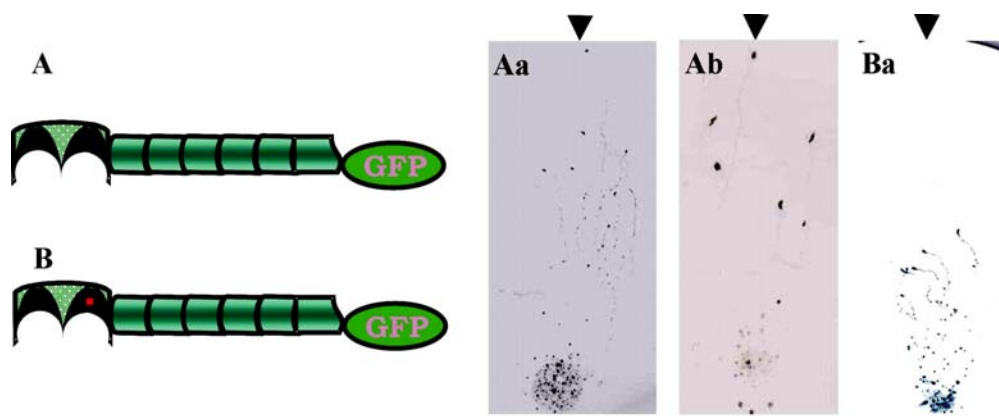


Figure 13: Phototactic rescue with FLC-GFP (Opposite page). (A and B), schematic representation of FLC-GFP and S174A mutated FLC-GFP, respectively. The red dot in the ABD indicates the position of the point mutation. HG1264 expressing FLC-GFP (Aa), GA1 expressing FLC-GFP (Ab) and HG1264 expressing FLC-GFP (S174A) (Ba) are phototactically active and are indistinguishable from wild type AX2 slugs (not shown). Most of the HG1264 slugs expressing FLC-GFP (S174A) migrated over shorter distances as compared to slugs expressing wild type filamin though they migrated straight towards the light. Bar, 1 cm.

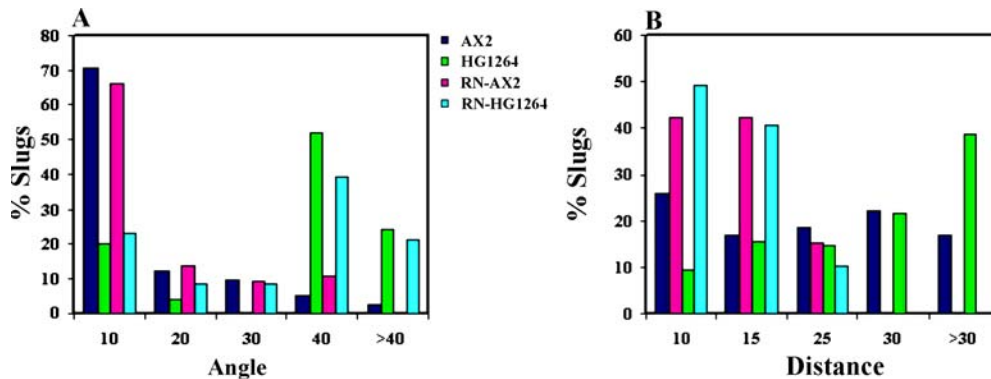


Figure 14: Angle of deviation from the light source and distance travelled by slugs. The angle of the deviation from the light source for slugs travelled more than 10 mm was calculated. About 70 % of AX2 slugs and RN-AX2 slugs migrated with an angle of deviation of 0-10°, while more than 70 % of HG1264 and about 60 % of RN-HG1264 slugs migrated with an angle of 30-40° and more than 40°. Expression of FLC-GFP in the HG1264 mutant rescues the phototaxis defect (A). The distance (in mm) travelled by slugs in 48 h towards the source of the light was measured. More than 40 % of AX2 wild type slugs travel a distance of 25-30 mm and more than 30 mm. About 60 % of RN-AX2 slugs migrate the same distance. But both the HG1264 and HG1264 slugs expressing the GFP-filamin rod fusion protein failed to travel over a distance longer than 25 mm (B). Over 100 slugs in three independent experiments were analysed for each data set.

3.2 Rescue of the phototaxis defect with filamin domains

HG1264 cells expressing the GFP-tagged rod domain (RN-GFP), the actin binding domain (ABD-GFP) or cells coexpressing the actin binding domain (ABD) and RN-GFP (RNGFP+ABD-HG) cultivated on *Klebsiella aerogenes* on SM plates were taken for phototaxis studies. Slugs of all the transformants expressing the fusion proteins moved shorter distances with a wide angle and were indistinguishable from the parent strain HG1264 (Figure 14 and 15).

Overexpression of RN-GFP (Figure 15Ab) and FLC-GFP (Figure not shown) in AX2 led to an increase in the number of slugs formed per plate and also increase in the distance traveled. Wild type slugs migrated over a significant distance of 40.25 ± 2.06 mm in 48 h, where as overexpressors migrated a distance of 43.34 ± 6.44 mm in 48 h. The number of slugs formed per plate in case of RN-GFP expressing AX2 cells were 16.78 ± 4.40 while in case of AX2

cells they were 12.75 ± 5.85 . To study the effect of the expression of separate filamin domains on phototaxis and slug migration in *Dictyostelium* more closely we measured the distance travelled by slugs and the angle of deviation from the incident light (Figure 14). We found that for HG1264 cells expressing RN-GFP only 13 slugs out of 128 analysed travelled over a distance of 25 mm and 63 migrated with an angle more than 30° . Whilst for AX2 cells expressing RN-GFP, 70 slugs out of 116 analysed travelled over a distance of more than 25 mm and 43 with an angle less than 10° . HG1264 cells expressing the actin-binding domain alone or in combination with RN-GFP behaved like HG1264 expressing RN-GFP (data not shown). From these data we concluded that expression of full-length filamin is necessary for the normal phototaxis of *Dictyostelium* cells.

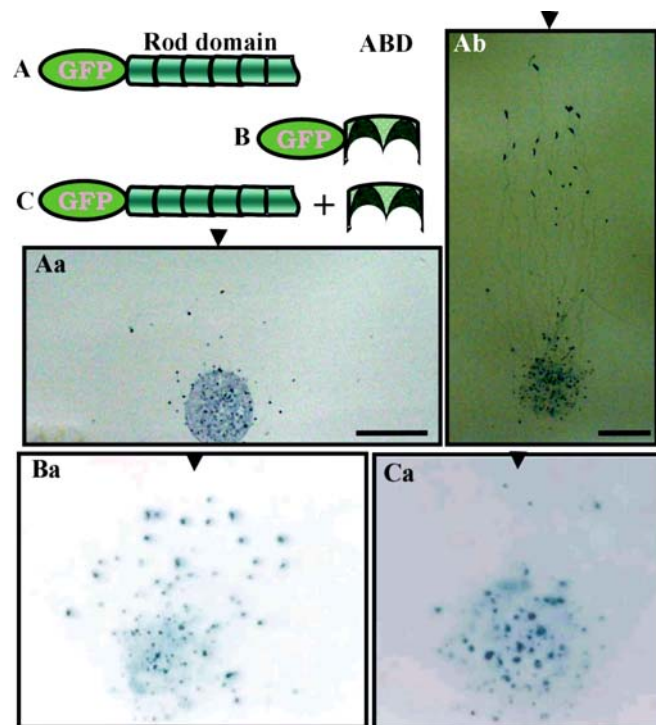


Figure 15. Rescue of the phototactic defect with RN-GFP and ABD. Expression of RN-GFP (A) in HG1264 does not rescue the phototaxis defect (Aa), AX2 slugs expressing RN-GFP (Ab) migrate straight towards the light. HG1264 slugs the expressing ABD-GFP (Ba) or RN-GFP and ABD (Ca) does not rescue the defect. Bar, 1 cm. Bar at Aa is applied for Ba and Ca.

3.3 The requirement of the dimerisation domain for the rescue behavior of ddfilamin

Improper localisation of RN-GFP and the inability of physically separated ABD and rod domains to rescue the phototaxis defect in HG1264 led us to propose that the cortical localisation or the association of ddfilamin with F-actin is essential for rescuing the phototaxis defect. To test this hypothesis we expressed Fil5-GFP, which localises similarly as the wild type protein but does not have the crosslinking function of the protein. We found, that slugs

expressing Fil5-GFP migrated over longer distances as compared to HG1264, however they migrated in a wide angle towards the light, as did the parent strain. Interestingly, the slugs showed a clockwise turn at the end of the trail, which is typical for the mutant strain (Figure 16). These data suggest that for the ability to sense the light, *Dictyostelium* slugs need full-length filamin, which allows the formation of three dimensional F-actin assemblies.

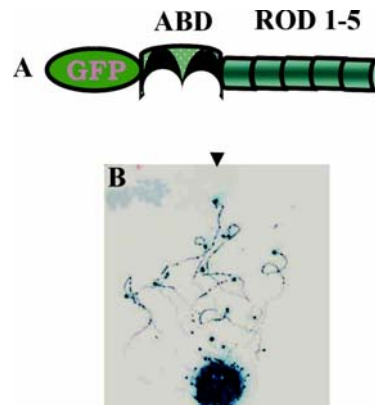


Figure 16: Fil5-GFP rescues slug migration but not phototaxis. Schematic representation of the Fil5-GFP fusion protein (A). Its expression in mutant HG1264 rescues the phototactic defect partially (B). Slugs migrate longer distances but do not migrate straight towards the light and show the typical clockwise turn at the end of the trail as does HG1264.

3.4 Expression of full length ddfilamin at the anterior tip of the slug is necessary and sufficient to rescue the phototactic defect

The slug consists of primarily two cell types, prespore and prestalk cells. We next tested in which cells of the slug the function of filamin in the phototaxis process is needed. For this we used the *ecmA* promoter, a prestalk cell specific promoter (Hong and Loomis 1988 and Morrison *et al.* 1994) and the prespore cell specific *cotB* promoter. In general, cell type specific promoters ensure that the genes under their control are tightly expressed within the boundaries of cell types and within the specific time frame of the developmental cycle. The *ecmA* promoter is strictly expressed at the anterior one-tenth portion of the slug, expression of the *cotB* promoter is restricted to the posterior 3/4th part of the slug. After culmination the cells in this part eventually will form spores. Expression of FLC-GFP in HG1264 cells under the control of the *ecmA* promoter rescued the phototactic defect completely, whereas expression under the *cotB* promoter did not rescue the phototaxis defect (Figure 17).

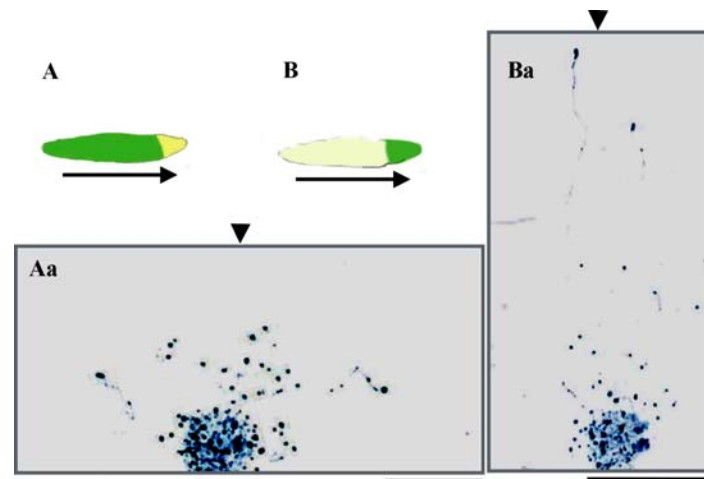


Figure 17: Phototaxis rescue with FL-FLC expressed under the control of cell type specific promoters. A and B are schematic drawings of the slugs expressing full-length ddfilamin under the control of the prespore specific *cotB* and the prestalk specific *ecmA* promoter, respectively. Expression under the control of the *ecmA* promoter rescues the defect (Ba) where the protein is expressed in the anterior one-tenth portion of the slug, whilst expression under the control of the *cotB* promoter, where the protein is expressed in the posterior 3/4 of the slug, does not rescue the defect (Aa). The green portion in the slug indicates the expression of the fusion protein and the arrow indicates the direction of the movement of the slug.

4 Identification and characterisation of binding partners for filamin

Recent studies suggested that filamin functions not only in maintaining the cortical actin network but also in the organisation and stabilisation of the network by interwebbing it with membrane proteins and receptors. In mammalian cells filamins interact with several membrane receptors: the cytoplasmic part of the glycoprotein Ib IX complex, the receptor for von Willebrand factor (Andrews and Fox 1991, Marti *et al.* 1997 and Takafuta *et al.* 1998), β_1 - and β_2 -integrins (Sharma *et al.* 1995 and Loo *et al.* 1998), insulin receptor (He *et al.* 2003) and α - and β -sarcoglycan (Thompson *et al.* 2000). Filamins also affect intracellular trafficking of proteins and signal transduction. Filamin influences the activity of furin, a protease that is involved in the proteolytic processing of many proproteins by promoting its internalisation (Zent *et al.* 2000). It binds to presenilin-1, a protein involved in early onset familial Alzheimer's disease and in the notch signalling pathway (Zhang *et al.* 1998, Schwarzman *et al.* 1999 and Guo *et al.* 2000) and interacts with caveolin-1, a multifunctional protein with roles in caveolae biogenesis, endocytic events, cholesterol transport and various signal transduction processes (Stahlhut *et al.* 2000). Furthermore, the involvement of filamin

in signal transduction is confirmed by its interaction with several components of the NF κ B pathway (Edwards *et al.* 1997, Marti *et al.* 1997 and Leonardi *et al.* 2000), and the small GTPases RhoA, Rac1, Cdc42 and RalA (Ohta *et al.* 1999 and Bellanger *et al.* 2000).

To evaluate the role of ddfilamin in such processes we searched for the interacting partners using a yeast-two hybrid screen. We have screened 97 independent clones, of which 60 clones were found positive for the β -galactosidase assay. DNA obtained from these clones was cotransfected with the rod domain into yeast strain Y190. From this 14 positive clones were isolated of which eight of them were filamin - this was not unexpected as all of them harbour the dimerisation domain -, two clones were autoactive, three were false positive and one contained a short sequence. Twelve other cDNAs were not interacting with filamin. After the failure of searching for new interacting partners for ddfilamin we decided to continue with our laboratory's earlier finding, a novel Filamin Interacting Protein (FIP) (Knuth 2002), which was identified in the yeast two hybrid screen. To evaluate the biochemical significance of the interactions we carried out a set of experiments described in section (4.1). Further in search of new interacting partners we performed also immunoprecipitation experiments, which have been described in section (4.2).

4.1 FIP, a novel protein interacts with filamin

We have reported a novel protein that interacts with ddfilamin, Filamin Interacting Protein FIP (Knuth *et al.* submitted), which was identified using the complete filamin rod domain as bait and a *Dictyostelium* vegetative cDNA library in a yeast two hybrid vector (Ohta *et al.* 1999). FIP is a 230-kDa protein and is composed of mostly coiled coil regions. It is developmentally regulated reaching highest levels of accumulation during development. The protein is present in the cytosol in a punctated manner and is partially associated with membranes. The filamin binding site is located between amino acids 1719 and 1826, a rather serine rich stretch. The FIP binding site resides in ddfilamin rod repeat 3 (Knuth, 2002).

4.1.1 Construction of a full-length FIP cDNA

In continuation of this work, we wanted to uncover the biological significance of the interaction and the biochemical role of FIP in *Dictyostelium*. First we assembled a full-length FIP cDNA from a λ -ZAP library. This DNA included a 3'-untranslated region of 96 bp with a polyadenylation signal and a polyA tail (GeneBank No. AF356600) (Figure 18). The full-length FIP cDNA has been cloned into the yeast two-hybrid vector to confirm its interaction with the filamin rod domain, and into a GFP expression vector for biochemical and further

localisation studies. Full-length FIP interacted with the filamin rod domain in the yeast two-hybrid system. The successful expression of the full-length protein in the yeast was confirmed by western blotting using a monoclonal FIP specific antibody (Figure 19).

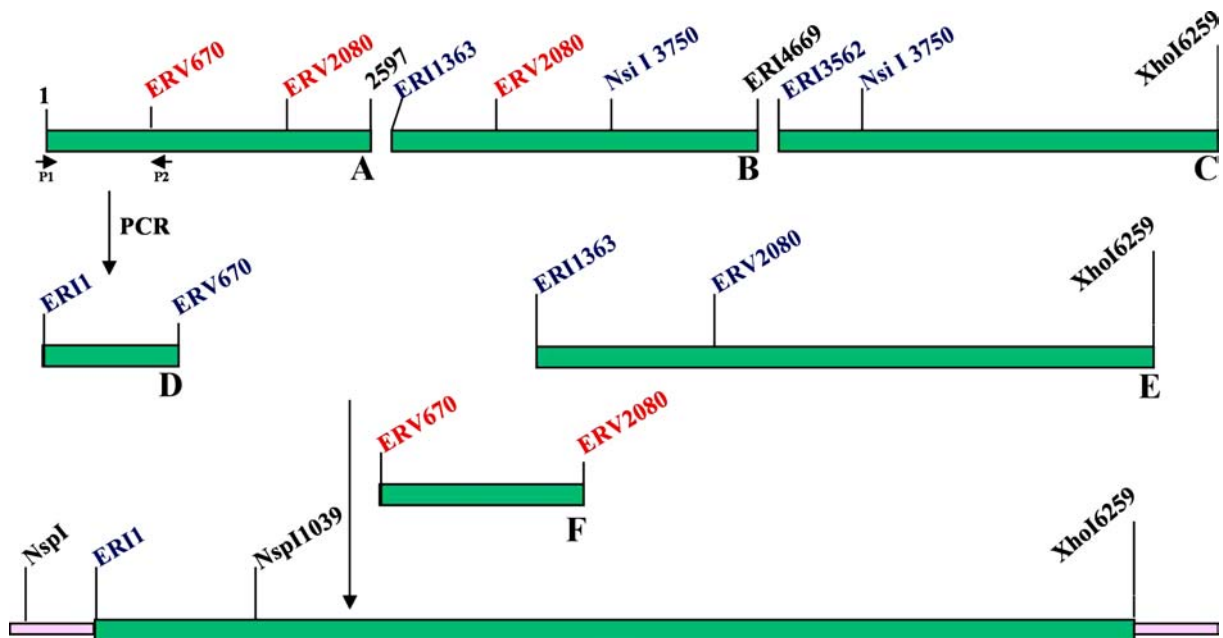


Figure 18. Generation of the full-length FIP cDNA. A full length FIP cDNA was constructed from three cDNA clones (A-C) obtained from a λ Zap *D. discoideum* cDNA library and cloned into the pBluescript cloning vector. The full length FIP cDNA was built on the fragment C (position 3562-6259 of the cDNA), first by cloning the middle EcoRI-NsiI fragment (position 1363-3750) from B. A 670 bp 5' fragment (D) was generated by PCR amplification using genomic DNA with an EcoRI site at the 5' end for cloning into the GFP vector pDex79. Fragment D was ligated to the 4.9 kb fragment (E) in a directed way using EcoRI and EcoRV. Into this product the middle 1.4 kb EcoRV fragment (F) was cloned. The correct orientation was determined by digestion with NspI. The sizes are not given in proportion.

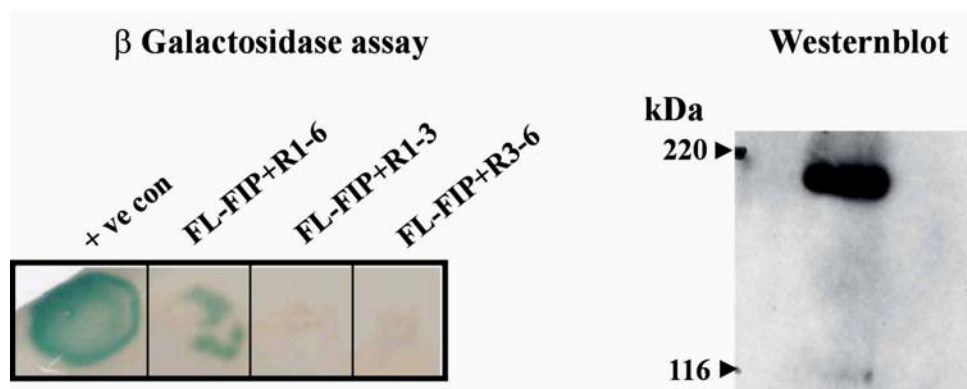


Figure 19: Testing the expression and interaction of FL-FIP with ddfilamin (Opposite page). (A) The Y190 yeast strain was transfected with a Gal4AD vector containing full-length ddFIP cDNA and grown on Leu⁻ plates for selection. A single colony was taken from the plate, the cells were lysed in SDS sample buffer, proteins separated by SDS PAGE (8 % acrylamide) and blotted onto a nitrocellulose membrane. The blot was probed with mAb K12-349-7 specific for ddFIP followed by enhanced chemiluminescence. (B) Interaction of full length FIP with the filamin rod domain was confirmed by the yeast two-hybrid system. Yeast cells co-expressing full length FIP and filamin polypeptides were grown on agar plates lacking histidine, leucine and tryptophan, transferred to nitrocellulose membrane, lysed and assayed for β -galactosidase. The blue color indicates an interaction between the proteins.

4.1.2 Localisation of FIP does not change in HG1264

The localisation of FIP was studied by staining methanol fixed aggregating AX2 and HG1264 cells that had been starved for six hours (t6) with FIP specific antibody K12-363-6. We found that the staining was identical in both AX2 and HG1264. The protein was diffusely present throughout the cytoplasm. The staining appears like a granular one and was concentrated in patches within the cytoplasm (Figure 20). The protein was neither accumulated in the newly formed pseudopods nor at the periphery where the actin cytoskeleton is actively reorganised. The granular and diffuse staining pattern suggests that the protein might be associated with vesicles and might have a role in vesicle transport. To define its role more closely we first performed differential centrifugation studies.

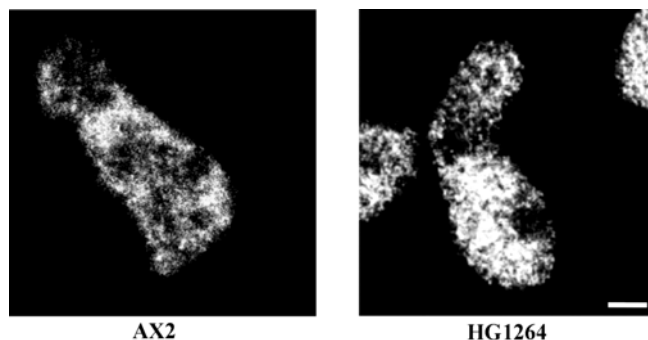


Figure 20. Localisation and distribution of FIP in AX2 and HG1264 cells. Confocal images of methanol fixed AX2 and HG1264 cells (t6) stained with FIP specific monoclonal antibody K12-362-6. The second antibody used was TRITC labelled anti-mouse IgG antibody. The images show that there is no remarkable difference in the localisation of the protein. Bar, 2 μ m.

4.1.3 FIP may have a role in vesicle transport

To confirm whether FIP is associated with membrane vesicles we performed a differential centrifugation using the cell lysate obtained from AX2 cells (t6). The lysate was centrifuged at 2,000 rpm for 10 min to remove unlysed cells and larger aggregates. 10 μ l of pellet and supernatant from every step were resolved on polyacrylamide gels and processed for immunoblot analysis. The staining with the FIP specific antibody K12-362-6 shows that most of the protein is cytosolic, and a thick band of equal intensity was observed in the soluble

fractions of the 10,000g and 100,000g spin. A fainter signal in the 100,000g pellet was an indication of the association of the protein with membrane vesicles. A very faint band was also seen in the first membrane pellet obtained at 10,000g (Figure 21). Probing the blot with an α -actinin specific antibody was used for control. α -Actinin is a purely cytosolic protein.

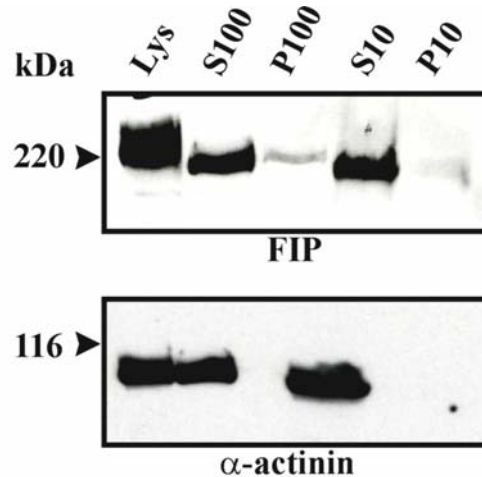


Figure 21: Fractionation of AX2 cell lysates. AX2 cells developed in suspension for six hours (t6) were lysed in lysis buffer containing 1.25 M sucrose. The supernatant after centrifugation at 2,000 rpm was used for differential centrifugation at the speed indicated in the figure (x100). The pellet at every step was resuspended in an equal volume to that of the supernatant at the first step. 40 μ l of lysate from pellet and supernatant at each step were boiled with 5x SDS loading dye and resolved on an 8 % polyacrylamide gel. The proteins were transferred onto a nitrocellulose membrane and probed first with the FIP specific K12-349-7 (upper panel), the antibody was stripped with 0.2 M NaOH and then reprobed with the α -actinin specific mAb 47-62-8 (lower panel) as a control. Detection was with enhanced chemiluminescence.

4.1.4 FIP is associated with the actin cytoskeleton

The treatment of *Dictyostelium* with 5 % DMSO leads to rapid disassembly of the actin network. This process is reversible and the disassembled actin network starts assembling upon further incubation. Within 5 to 15 min of treatment the class I actin network near the plasma membrane rapidly dissociates and forms small actin bundles inside the cytoplasm. After 30 min of incubation with 5 % DMSO microfilaments return to their original location just beneath the plasma membrane (Yumura *et al.* 1983). Since a full-length FIP-GFP fusion protein was not available we followed the staining with the FIP specific mAb using AX2 cells (t6) attached to the coverslips and treated with 5 % DMSO for 0', 5', 10', 20', 30' and 40' min. For the 0 to 10 min treatment there was no remarkable difference in the staining, while at 20 to 30 min the protein assembled into larger and more compact structures in the cytosol and

the granular localisation was lost (Figure 22). After this time it acquired the original staining (data not shown).

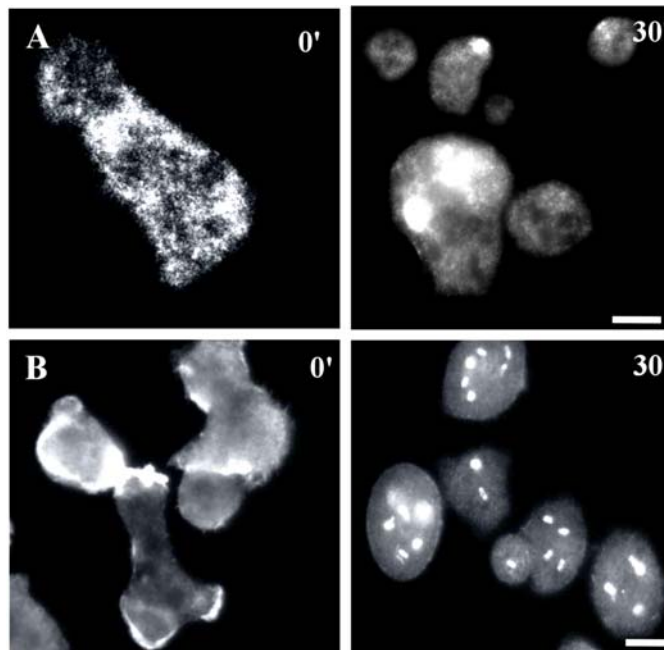


Figure 22. Reorganisation of FIP upon DMSO treatment. AX2 cells after six hours of starvation were allowed to settle on glass coverslips, treated with 5 % DMSO in 17 mM Soerensen phosphate buffer for the indicated time points. They were fixed with cold methanol (-20°C) and immunostained with the FIP specific mAb K12-362-6 (A, 0 and 30 minutes). For control the actin distribution was followed using and the actin specific antibody act 1-7 (B). Detection was with a Cy3-labelled secondary antibody. Bar, 3 μm .

4.2 Immunoprecipitation revealed the identification of TipA, SapA, and GAPA as ddfilamin associated proteins, suggesting a role for filamin in cell morphogenesis and actin remodelling

To identify proteins interacting with ddfilamin we performed an immunoprecipitation with mAb 82-421-5 bound to protein A sepharose beads using AX2 whole cell lysate. In this experiment we were able to coimmunoprecipitate several proteins ranging in molecular weight from 96 down to 30 kDa. The protein bands indicated by arrows were cut out from the gel and processed for MALDI-MS. They were identified as filamin, TipA, actin, a putative cell division factor, SapA, discoidin and GAPA. The proteins indicated in black letters in Figure 23 (lane T) were not considered for further studies. Filamin and actin were expected to be pulled down, whereas discoidin I based on its lectin activity binds to the sepharose beads. The proteins indicated in blue letters were selected for further studies. The band for TipA appeared at the theoretical molecular weight of 90 kDa and also as presumably proteolytic

break down products, whilst SapA and TipA represent break down products of the respective proteins.

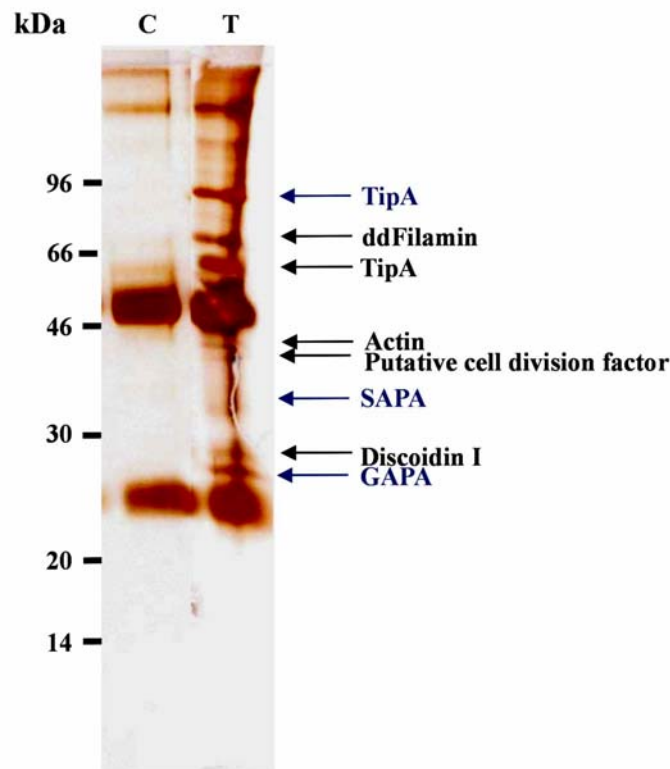


Figure 23: Identification of interaction partners for ddfilamin. Axenically grown AX2 cells were harvested at growth phase, washed twice with Soerensen phosphate buffer and lysed in homogenisation buffer as mentioned in materials and method, and centrifuged at 13,000 rpm for 30 min. The supernatant was precleared by incubating with protein A sepharose beads for 1 h at 4 °C, and the cleared supernatant was used for immunoprecipitation with mAb 82-421-5. Beads after immunoprecipitation were washed thrice with 1x IP buffer and boiled with SDS-sample buffer and the proteins resolved on a 10 % SDS polyacrylamide gel. The gel was stained with silver. Lane C shows the antibody and in lane T the proteins eluted from the beads after incubation with the cell lysate. The bands indicated by arrows were analysed and identified by MALDI-MS.

4.3 Checking the interaction of filamin with Rho GTPases by yeast two hybrid screening

Rho-GTPases related to the Ras superfamily are molecular switches that participate in a myriad of cellular activities like regulation of actin assembly and myosin activation (Bishop *et al.* 2000). Human filamin A binds to RhoA, Rac1, Cdc42 and RalA (Marti 1997, Ohta 1999 and Bellanger *et al.* 2000). *Dictyostelium* contains an unexpectedly large number of Ras superfamily proteins (Reymond *et al.* 1984, Robbins *et al.* 1989, Daniel *et al.* 1993 and 1994).

Interestingly, *Dictyostelium* RasD⁻ mutants have a partial defect in phototaxis (Wilkins *et al.* 2000). This might be a hint that ddfilamin is located upstream of the Ras signaling pathway because ddfilamin mutants have a severe defect in phototaxis while other actin cross linking protein do not have any effect on this phenomenon. We have tested the interaction of Rac proteins and mutated Rac proteins such as Rac 1a, 1a(N17), 1a(L61), 1b, 1c, A, B, C, C(L64), C(N20), D, E, F1, F1(V12), F1(V17), F2, G, G(V12), G(N17), H (auto active), I, J and L, RhoA (mammalian), RhoGDI, RabD and RasG with Rod1-6 using a yeast two hybrid screen. Of the above listed GTPases RacB, RacC, RacC (N20), RacD, RacE, RacF1, RacF1(V12), Rac F2, RacG, RacG(N17), RacG(V12) and RhoA are likely to be a positive integrator (Figure 24). However, we were not able to support our results from yeast two hybrid assays by cosedimentation of GST-Rac fusion proteins and bacterially expressed purified filamin rod domain 1-6. A failure to obtain cosedimentation may be because of weak interactions (Figure 25).

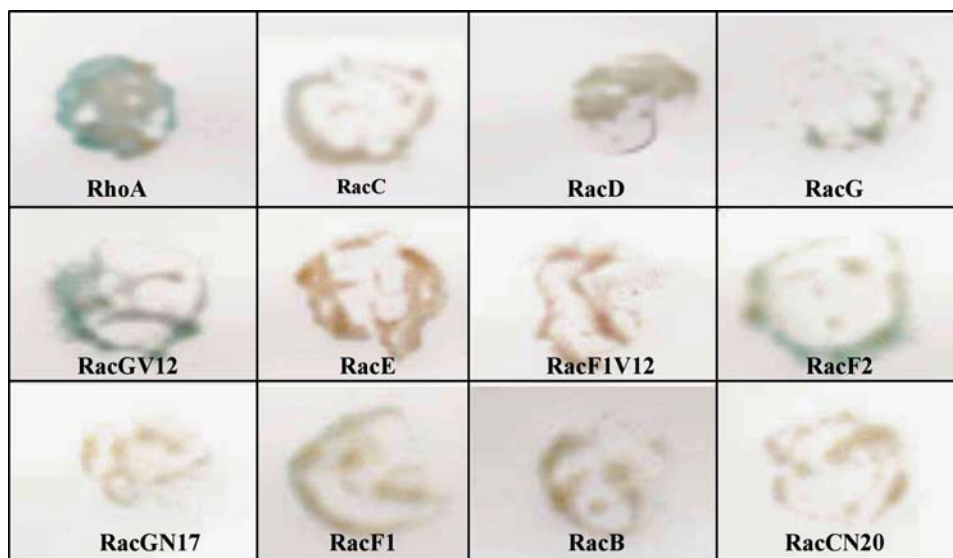


Figure 24: Rho superfamily proteins have direct interactions with *Dictyostelium* filamin. The Figure shows the direct interaction of Rac proteins with the filamin rod domain. Y190 yeast strain cotransformants containing Gal4BD-Rac as indicated in the figure and Gal4AD-filamin rod 1-6 were selected on a medium lacking tryptophane, leucine and histidine, and containing 20 mM 3-amino-1, 2, 4-triazole. Individual colonies were patched onto filters and assayed for β -galactosidase activity. The histidine reporter allows colonies to grow on the nutrient agar and the β -galactosidase reporter gives blue color in the filter lift β -galactosidase assay. Blue color of the colony represents the positive interaction and intensity of the color indicates the strength of the interaction.

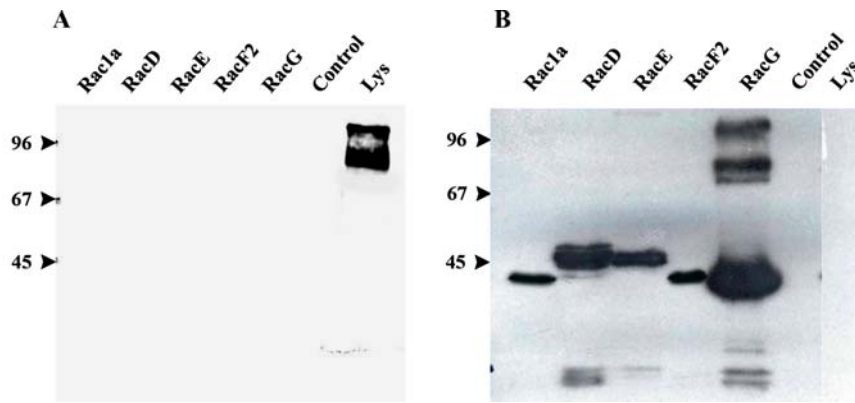


Figure 25: The interaction of Ras superfamily proteins with ddFilamin rod domain does not occur in vitro. Bacterially expressed recombinant ddfilamin rod domain (rod1-6) was allowed to cosediment with GST fusion proteins bound to beads. The bound proteins were resolved on a SDS polyacrylamide gel (10% acrylamide) and transferred to a nitrocellulose membrane. The membrane was probed with filamin specific mAb 82-454-12 (A) and commercially available polyclonal antibodies specific for GST, (B). There was no detectable cosedimentation of rod1-6 with GST fusion protein. ‘Lys’, AX2 cells lysed in SDS-sample buffer. In ‘control’, recombinant rod1-6 was incubated with GST beads.

5. Microarray analysis suggests that mutant slugs have elevated extracellular cAMP levels and lowered cell adhesion

To get an impression of global gene expression in late development, we performed a microarray analysis. Total RNA from AX2 and GHR cells developed in suspension for 10 h was isolated and used for the preparation of cDNA. Three independent experiments were carried out. cDNAs were labelled with cy3 and cy5 separately and mixed together. Six slides containing an array of 6,000 independent expressed sequence tags were probed with different combinations of the labelled cDNAs from the three batches of RNA. A total of 65 genes with a delta value (Delta is a tuning parameter used to determine the cut off significance chosen by the users based on false positive rate. One can also choose ‘fold change’ parameter) more than +/- 1.467 was considered for the study. 40 genes were found up regulated while 25 genes were down regulated. Up regulated genes can be broadly grouped into three groups depending upon the function of the proteins. First, they are acting binding proteins, second, proteins involved in protein/aminoacid metabolism and the third group functions in cell migration and development. The down regulated genes are mostly calcium binding/sequestering proteins, proteins regulating adhesion, a class II cAMP phosphodiesterase and the actin sequestering protein profilin I. All the genes that are up or down regulated are listed in Table 1 and 2.

Table1: List of up regulated genes.

Gene ID	Gene name	ScoreD	Ratio	Gene function
SLJ671	Hypothetical Protein	5,70513015	1,59	Not known
SLD607	Elongation factor 2	5,68526136	1,51	Protein synthesis
SLE817	Major vault protein beta	5,09546962	1,62	Vault formation
SSI137	<i>Dd</i> ring finger protein	4,98797613	2,07	developmentally regulated and present in spore
SSL239	Hypothetical protein	4,59229829	1,73	No homology
SSC778	Flavonoid 3'-5'-Hydroxylase	4,56168491	1,46	Not known
SSH379	ADP/ATP translocase	4,45227964	1,37	catalyses the exchange of ATP and ADP between the mitochondria and the cytosol
SLJ337	DG2044 gene product	4,42987694	1,44	Unknown gene
SSB372	Unknown gene	4,29494618	2,44	Unknown gene with homology with <i>Dd</i> culmination specific protein 45D
SLF771	Ribosomal protein L2	4,17006234	1,54	Unknown
SLE471	Hypothetical Protein	4,13496814	1,52	Unknown
VSE173	Major vault protein beta	4,12032618	1,55	Vault formation
SSD184	Homologous to Actobindin	4,05956253	2,08	bivalent affinity for monomeric actin.
SLC458	Acetylornithine deacetylase	4,05526801	1,94	Arginine biosynthesis
VSC841	Hypothetical Protein	4,02390596	1,51	Unknown
SSM847	Hypothetical Protein	3,98919303	1,52	Unknown
SLI631	Mitochondrial Porin	3,98672339	1,44	Ion channel protein
SLE621	Fatty Acid Desaturase	3,8879746	1,43	fatty acid desaturase
U23957	Acetylornithine deacetylase	3,82519009	1,87	Arginine biosynthesis
X15710	Ribosomal protein L2	3,71327065	1,34	Not known
SSB153	Hypothetical Protein	3,68865704	2,24	Not known
SLB276	Cystein protease	3,67619492	1,54	Unknown
SSB377	Hypothetical Protein	3,65783498	1,42	Homology with Homo species ribosomal protein L9
VSC467	Hypothetical Protein	3,59838188	1,36	No homology
SSD488	Hypothetical Protein	3,57575463	1,63	Homology with Root hair elongation protein
SSD382	Hypothetical Protein	3,46412476	1,48	homology with Cytochrome P450 71A9
SLB855	Discoidin I chain C	3,38789777	2,18	cell-substratum attachment and ordered cell migration
SLD730	Alfa-actinin	3,3755551	1,48	Calcium dependent actin crosslinking
SSE751	Hypothetical Protein	3,36381733	1,77	Not known
VSH695	cAMP PDI	3,35376269	1,81	Expression is highly regulated by cAMP concentration
SSI635	Hypothetical Protein	3,1756571	1,28	Homology with drosophilla HABP4 domain
SLJ823	DIF inducible, prestalk	3,07770474	1,32	extracellular protein containing signal peptide but without TM domain
SSC685	calcium binding protein	3,02203401	1,36	Homology with Annexin
SSC656	Vegetative specific protein H5	3,00014301	1,44	Nutrient responsive promotor element
SLE683	Hypothetical Protein	2,9972458	1,33	Homology with protein that localized in nucleoli
VSI349	Hypothetical Protein	2,95141134	1,54	Unknown
SSL840	Hypothetical Protein	2,93484744	1,28	Unknown
SLC529	gp64 and disintegrin-like,	2,92429264	1,61	Unknown
U13671	hisactophilin II (hsII)	3,71327065	1,61	pH sensitive actin binding
SSL471	Hypothetical Protein	2,87872516	1,29	Unknown

Table 2: List of downregulated genes.

Gene ID	Gene name	score(d)	Fold expn	Gene function
SLH576	gelation factor	-12,39100089	0,15	Actin crosslinking
SLB425	calcium binding protein; CBP3	-5,882301015	0,11	calcium binding/seqeustering
SSE536	ORFVEG106 protein	-4,98366159	0,41	?
X15430	gelation factor	-4,730139009	0,72	Actin crosslinking
J02628	cAMP phosphodiesterase, PDEase_ II,	-4,669827595	0,21	Extracellular phosphodiesterase
SSG484	ORFVEG106 protein	-4,481525352	0,67	?
SSJ161	developmental protein DG1148	-4,471864721	0,64	phosphatase, distruption of gene results morphological defects
SSD437	calcium binding protein; cbp2	-4,391065691	0,75	calcium binding/seqeustering
X82784	calcium binding protein; cbpA	-4,19786585	0,65	calcium binding/seqeustering
SSK273	hypothetical protein	-4,143187512	0,73	?
X04004	contact site A (csA)	-4,023797261	0,64	calcium independent cell-cell adhesion
SSH355	<i>Dd</i> putative adhesion molecule CAD2	-3,744898633	0,68	Putative adhesion molecule
SSA595	hypothetical protein	-3,739166747	0,72	?
X61581	Profilin I	-3,707053674	0,75	G-actin seqeustering protein
SLG145	hypothetical protein	-3,680231984	0,61	?
SSE551	hypothetical protein	-3,44770139	0,86	?
SSL818	calcium binding protein; 4a	-3,421989632	0,62	calcium binding/seqeustering
M16039	pst-cathepsin	-3,368683708	0,7	Regulate cell differentiation
SLG775	pst-cathepsin	-3,106973069	0,71	Regulate cell differentiation
M27588	gp24	-3,056758552	0,77	cell-cell adhesion
SLH549	hypothetical protein	-3,048031563	0,83	?
SSJ883	calcium binding protein; CBP7	-3,044425949	0,8	calcium binding/seqeustering
SLC626	GTP-binding protein SAS2	-3,037234375	0,8	Not known
SSM450	Ddrap1	-3,021501665	0,79	Not known

6. Chemotactic motility of mutants in actin binding proteins

Chemotaxis towards the cAMP plays the pivotal role throughout the *Dictyostelium* development. Mutants defective in cAMP generation and sensing do not complete the developmental cycle. cAMP plays a crucial role to maintain the slug polarity. Unlike *Drosophila* there are no fixed boundaries formed during the development, cells are continuously in motion, mostly in response to cAMP. Therefore it was important to study whether cells having defect in chemotaxis have a defect in phototaxis. To this end we studied mutants of Lim D and villidin.

6.1 Filamin minus cells chemotax normally

Rivero et al. 1997 reported that HG1264 cells perform normal chemotaxis. We analysed the effect of expression of RN-GFP in AX2 and HG1264 cells and found that it does not alter the chemotactic response. This indicates that the behavior of the mutants is normal at the onset of the development.

6.2 LimD^- cells have a defect in chemotaxis but have normal phototaxis

Chemotaxis of starving cells towards cAMP was analysed in the capillary assay, where cells are stimulated with a micropipette filled with cAMP (10^{-3} M), and the velocity was determined. LimC^- cells migrated with an average velocity of 10.19 ± 1.63 $\mu\text{m}/\text{min}$ towards the pipette, which is similar to wild-type velocity (11.32 ± 1.23 $\mu\text{m}/\text{min}$). For LimD^- we observed a slightly lower velocity (8.07 ± 2.93 $\mu\text{m}/\text{min}$) and the double mutant was impaired even more (7.65 ± 1.86 $\mu\text{m}/\text{min}$).

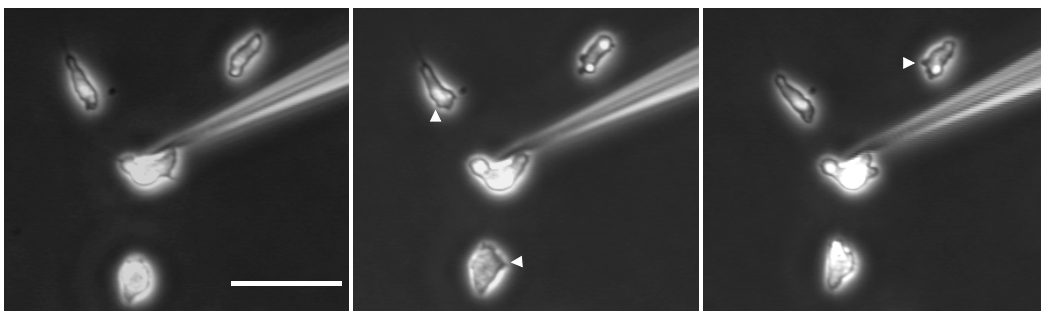


Figure 26: Chemotactic migration of LimD^- mutants. Axenically grown cells were starved in Soerensen phosphate buffer for 6 h at 21° and allowed to migrate towards the microtip filled with 1 mM cAMP. The images obtained with the Olympus IX70 inverse microscope equipped with a 20x UplanFl 0.3 objective were recorded on a computer hard disk. Arrows indicate the lateral pseudopod extended by cells. LimD^- cells form a higher number of pseudopods (Table 3).

To analyse motile cells in more detail we used a chemotaxis assay and followed the cells with time-lapse video microscopy. Wild type as well as LimC^- cells were polarised and migrated in a rapid and directed way towards the micropipette filled with cAMP (Table 3). Furthermore, they extended their pseudopods mainly in the direction of the micropipette and formed very few lateral pseudopods. LimD^- cells also moved to the cAMP source (Figure 26). However, they did not migrate as fast as wild type (Table 4) and formed lateral pseudopods in addition to the main pseudopod extended in the direction of cAMP (Table 3), whereas persistence and directionality were only slightly impaired. LimD^- cells re-expressing LimD protein as a GFP fusion rescues the chemotaxis defect.

Table 3. Lateral pseudopods formed during migration towards a cAMP gradient or crawling in buffer

	Cell type	Number of cells	0-2 lateral pseudopods per 10min (%)	3-5 lateral pseudopods per 10min (%)	>5 lateral pseudopods per 10min (%)	Avg. frequency of lateral pseudopods/cell/10min
Buffer	AX2	28	15	53	30	5,3
	LimD^-	23	5	60	34	4,9
Gradient	AX2	22	81	18	-	1,45
	LimD^-	25	40	60	-	2,7

Images were taken at 20x magnification every 30 sec. Cells in all cases were analysed for 10 minutes. A Chi square test was performed between AX2 and LimD^- cells on the combined data of the three categories of lateral pseudopods formed. The difference between AX2 and LimD^- in the cAMP gradient was found to be highly significant (1×10^{-3}).

Table 4. Motility and chemotaxis parameters in a spatial gradient of cAMP

Cell Type	Cell number	Velocity $\mu\text{m}/\text{min}$	Persistence $\mu\text{m}/\text{min-deg}$	Roundness %
AX2	47	11,32 \pm 1,23	4.40 \pm 0,80	75,04 \pm 3,43
LimC^-	14	10,19 \pm 1,63	4.22 \pm 1,28	74,02 \pm 0,31
LimD^-	27	8,07 \pm 2,47	2,93 \pm 1,05	80,22 \pm 3,97
LimC/D^-	66	7,65 \pm 1,86	2,73 \pm 0,94	79,51 \pm 4,19
Rescue	12	8,96 \pm 1,06	3,11 \pm 0,77	72,83 \pm 5,57

Images were taken at 10x magnification for every 30 sec. Cell in all cases were analysed for at least 10 minutes. The parameters velocity is distance travelled roundness are described in materials and method, persistence is essentially speed divided by the direction change; if the object is not turning its persistence is the same as speed.

LimC and LimD interact directly with F-actin and comprise Zinc fingers of the LIM domain type. LIM domains can form homo- or heterodimers and interact with proteins involved in signalling and the cytoskeleton (Khurana *et al.* 2002). We have found that the LIM proteins have a role in cell polarity and chemotaxis. The observed defect in chemotaxis in LimD^- mutant and LimC^-/D^- is mainly due to changes in cell morphology and cell shape. The morphological analysis showed that the mutants form a higher number of lateral pseudopods, which may often lead to changes in direction. Reexpressing the Lim D-GFP fusion protein in the mutant rescues the phenotype suggesting that the defect in chemotaxis resides in the loss of the function of this particular protein. After cells sense the chemoattractant there are spatial-temporal changes in actin polymerization and myosin II assembly. These changes are mediated by the cyclic AMP receptor (cAR) which activates heterodimeric G proteins, which in turn initiate a signaling cascade involving several proteins such as Pleckstrin Homology (PH) domain containing proteins, kinases, Ras family GTPases and enzymes like adenylyl cyclase A (ACA) and guanylyl cyclase (GC). Actin is predominantly polymerised at the front of cells for anterior pseudopod propulsion through a chemoattractant gradient, and myosin II is assembled at the sides to suppress lateral pseudopod formation and at the rear for retraction (Kimmel and Parent 2003). Cells with reduced levels of cGMP (sGC and GCA mutants) exhibit decreased myosin II phosphorylation and cytoskeletal association in response to chemoattractants. These cells do not move efficiently directionally in chemoattractant gradients (Bosgraaf *et al.* 2002 and Roche *et al.* 2003). Like LimD^- mutant cells Lim2^- , a Lim domain containing protein (Chien *et al.* 2000), have motility as well as a cell polarity defect however, Lim2^- does not bind actin directly. Therefore both the proteins might work in different pathways. Though LimD^- mutant exhibit reduced chemotactic migration, the phototaxis phenotype of mutant slugs was indistinguishable to that of wild type slug (Khurana, 2001).

6.3 The villidin⁻ mutant has a defect in chemotaxis as well as in phototaxis

Villidin is a novel multidomain protein (190 kDa) from *Dictyostelium* containing at its N-terminus a WD repeat, three PH domains in the middle of the molecule, and at the C-terminus only five instead of typically six gelsolin-like segments which are followed by a villin-like headpiece. Villidin mRNA and protein are present in low amounts during growth and early aggregation, they increase during development and reach highest levels at the tipped

aggregate stage. The protein is present in the cytosol as well as in the cytoskeletal and membrane fraction³¹. Villidin protein accumulation is most prominent during development.

The villidin gene has been inactivated by homologous recombination and several mutants were obtained and examined. Growth under several conditions was unaltered. An analysis of the development of the mutants on phosphate agar or on nitrocellulose revealed that the mutants were moderately delayed in development by about 2-3 hours in early development. Analysis of the expression pattern of late development specific proteins and mRNAs did not indicate significant alterations (Gloss *et al.* 2003).

Here we have analysed the chemotactic motility behaviour during development and observed that villidin-minus cells moved significantly slower ($8.84 \pm 1.6 \mu\text{M}/\text{min}$) in a cAMP gradient than wild type cells ($13.53 \pm 1.3 \mu\text{M}/\text{min}$). In later development villidin minus cells exhibited a phototactic defect.

IV. Discussion

1. Subcellular localisation of ddfilamin and its domains

Filamin localises predominantly in new pseudopods of a *Dictyostelium* cell. The ABD however, although derived from this protein behaves differently. Pang et al. (1997) suggested GFP-ABD as a general probe to visualise all known F-actin rich structures such as the cortex, pseudopods, filopods, crowns, and contractile furrows. They also showed that GFP-ABD rapidly relocalised to sites of new actin accumulation. These data in parallel with biochemical data led them to suggest that GFP-ABD bound only weakly to F-actin in contrast to phalloidin, a commonly used probe to reveal F-actin. Phalloidin is a drug that binds very tightly to F-actin and inhibits its depolymerisation. Pang et al. reported also that in cells phalloidin-bound filaments accumulate over time into an aggregate at the rear end of the cell whereas GFP-ABD behaves differently which was taken as further indication for its weak F-actin binding and rapid relocalisation. Our observation with HG1264 cells expressing ABD-GFP suggest that in the absence of endogenous ddfilamin, the fusion protein also relocalises at the rear end of the cAMP stimulated cells, which were moving directionally.

At the biochemical level, the actin incorporation into the cytoskeleton is usually resolved into three peaks after cAMP stimulation. The second and third peak occurs during the resumption of the pseudopod formation. Pseudopod protrusion is a process that is presumed to require new F-actin polymerization and changes in the localisation of existing filaments (Mc Robbie

and Newell, 1983). In case of the ddfilamin minus mutant there is significant reduction in the amount of actin incorporated into the cytoskeleton in the second and third peaks (Brink et al., 1990). The reduced amount of the ABD-GFP at the anterior as compared to the rear end of the cell could underline this finding. The localisation of the ABD-GFP is also delayed for few seconds in newly formed pseudopods. In a population of vegetative cells, most cells are polarised and make protrusions in one or two directions, whereas about 5–15 % of the cells are round and do not show any polarity. Generally the fluorescent signal of the newly formed pseudopodia was higher than that of the surrounding cortex. Biochemical studies estimate that roughly 20 % of ddfilamin is associated with the cortical actin cytoskeleton whilst around 80 % remain unbound in the cytosol, the role of which has remained unclear. Though our results are mostly based on the visual observation of the expression of the GFP fusion proteins we found that the C terminal rod domain allows the cytosolic location of ddfilamin. The removal of the dimerisation domain did not affect the localisation of the protein, as it was identical to that of full-length ddfilamin. Our visual observation of the S174AFLC-GFP was also identical to that of FLC-GFP.

In the mammalian system it has been found that filamin binds to several proteins. Two proteins, Ral1 (Ohta *et al.* 1999) and protein kinase A (Prat *et al.* 1999) have been implicated in regulation of filamin's actin crosslinking activity. Ral1 is a small G protein of the Rho family, which binds in a GTP dependent manner to filamin. The induction of filopods in Swiss 3T3 cells requires both filamin and Ral1, suggesting that Ral1 is essential for regulation of the filamin function. Protein kinase A (PKA) has been shown to phosphorylate the human filamin at S2152 *in vitro*. This serine residue resides at the proposed dimerisation domain, suggesting that PKA may regulate the actin crosslinking activity and its translocation from the periphery to the cytosol. Bonner and Williams (1994) suggest that in *Dictyostelium* in addition to its role in cellular differentiation, PKA is required for several important aspects of slug behaviour (Bonner and Williams, 1999).

In AX2 cells expressing the RN-GFP protein it forms heterodimers with the endogenous protein, which brings the fusion protein into the actin cytoskeleton. The formation of isoform specific heterodimers can also occur in mammalian and *Drosophila* cells. Himmel et al. (2003) found that heterodimer formation is possible between filamins b and c but not between filamin a, and the other two filamins. Heterodimerisation might link the ligand of one filamin

isoform to the ligand of the second isoform, which would increase the complexity of the filamin family and its possible functions.

2. F-actin crosslinking by ddfilamin is essential for the rescue of the phototaxis defect in ddfilamin⁻ mutants

Phototactic migration in *Dictyostelium* is a natural behavior to migrate towards the light (Wallraff and Wallraff, 1997) in order to disperse the spores to a favourable environment. The formation of slugs and fruiting bodies is a complex process, which involves wide varieties of signaling within the cells and among groups of cells. This phenomenon can be compared with the development of higher eukaryotes. Before forming a motile slug, single cells from starving populations become activated. Stimulated cells produce cAMP pulses and other cells in the population respond by migrating towards the signal. This process is called cAMP relay. The cells organise into a multicellular aggregate (about 10^5 cells) where they differentiate into prestalk and prespore cells, and form the motile slug. The cells in the anterior 20 % portion become the tip consisting of mostly prestalk cells, which controls the migration of the slug. With the help of available reliable prestalk specific genes it has become possible to subdivide the tip cells into pstA, pstAB, and pstO cells. These subtypes are marked by the expression of the ecmA, ecmB and ecmO genes, respectively. PstA cells comprise the anterior 10 % of the slug; pstAB cells form a central core in the anterior tip, while a layer of pstO cells follows the pstA cells (Abe *et al.* 1994). It has been shown that the cells in the front move in a scroll wave, twisting around the pstAB cone (Seigert and Weijer, 1992 and Seigert and Weijer 1995). This circumferential movement continues in the pstO area. Cells continue to move straight forward in columns with a periodic increase or decrease of speed in the prespore zone.

To explore whether the phototactic defect in ddfilamin minus mutants is because of the lack of filamin-mediated F-actin crosslinking, or whether this protein controls the phototactic signalling pathway, we expressed different domains of the protein in the mutant HG1264 and in wild type AX2 cells. AX2 cells overexpressing RN-GFP performed normal phototaxis although the ddfilamin mediated F-actin crosslinking may have been disturbed to a large extent because of the formation of heterodimers. Western blot analysis of immunoprecipitated GFP fusion protein revealed that roughly 50 % of the protein formed heterodimers (data not shown). The amount of correct filamin dimers might therefore be sufficient to fulfill filamin's function in phototaxis. The expression of single domains in HG1264 cells such as the rod domain or the ABD and physically separated ABD and rod domain did not rescue the defect.

Summarising these results we may conclude that though the ddfilamin mediated F-actin crosslinking is necessary for the phototaxis rescue, partial disruption of this function did not alter the accuracy of the phototaxis.

RN-GFP alone and even when co-expressed with the ABD in HG1264 did not localise in the actin cortex. This observation led us to generate a deletion construct of ddfilamin that should localise normally but should not allow actin crosslinking. Ddfilamin having GFP fused to its C-terminus was still able to form homodimers and thus contributes its F-actin crosslinking function. We therefore generated a ddfilamin GFP fusion protein without the sixth rod domain, which could no longer dimerise. We found that it localised as the wild type protein and partially rescued the phototaxis defect in HG1264 such that the slugs migrated over longer distances, however they did not migrate towards the light in a directed fashion. This result suggests that full-length ddfilamin is necessary for the phototactic rescue where it plays a role as F-actin crosslinking protein and transduces signals to the photo/thermosensory machinery. Alternatively the dimerisation domain could provide the binding site for the proteins crucial for phototaxis.

Miura and Siegert (2000) found that light acts directly on the cAMP-signalling system and cell movement. Upon light irradiation, aggregating cells change their periodicity of cAMP signalling and cells in the slug tip release cAMP. They also found that concomitant changes in cell movement also occurred in slug cells. Our results with solitary amoebae in a cAMP gradient show that the filamin minus mutant cells HG1264 and GHR ($10.97 \pm 2.18 \mu\text{m}/\text{min}$) can migrate with equal speed as wild type AX2 cells ($11.32 \pm 1.23 \mu\text{m}/\text{min}$). It appears that ddfilamin does not play a key role in chemotactic migration of the single cells or that other proteins can compensate its loss. Association of filamin with membrane receptors such as β -integrins, its actin crosslinking function and lipid membrane insertion can be controlled by phosphorylation. Ohta and Harwig (1995) reported that upon phosphorylation with CaM kinase II, the dissociation constant for the binding of filamin to the actin filament increases approximately by two folds in vitro. The expression of point mutated full-length ddfilamin at the potential phosphorylation site in the ABD rescued the phototaxis defect in HG1264 mutant in that far, that slugs traveled over shorter distances but oriented correctly towards the light indicating that phosphorylation at this site could play a regulatory role in phototactic signaling. This partial rescue is not similar to that of Fil5. The latter slugs do not orient properly but migrate over longer distances than the parent mutant strain, HG1264. Thus the

photodetection i.e. orientation of slugs towards the light source and phototactic migration are two independent mechanisms. Several mutants have been reported, for example GRP125 (Stocker *et al.* 1999) and RasD (Wilkins *et al.* 2000), which have a defect in photodetection but migrate as far as the wild type slugs in the dark. For the photodetection of the slug, F-actin crosslinking by ddfilamin is essential, which may control the shape of the pseudoplasmodia that act as a cylindrical lens and the migration of the slug could be controlled by signal transduction mechanisms where ddfilamin plays a central role. Häder and Burkart (1983) stained wild type slug with Neutral Red and found that slugs eventually migrated away from the light. This also underlines that any alteration in the optical properties of the cylindrical lens leads to negative phototaxis. Summarising these results we conclude that for the proper orientation of the slug towards the incoming light, crosslinking of F-actin into three-dimensional arrays by full-length ddfilamin is essential.

Dictyostelium filamin is a phosphoprotein. We identified the potential phosphorylation site by *in vivo* phosphorylation. To study the biochemical significance of this phosphorylation, we introduced a point mutation and studied the localisation of the protein and rescue activity in the phototaxis in HG1264. As discussed before, there was partial rescue for the HG1264 slugs expressing the mutated protein. Therefore, we gave priority to identify the kinase responsive for this phosphorylation. This is a difficult task because *Dictyostelium* has several kinases among them are homologs of the Ste20p. The Ste20p (sterile 20 protein) is a putative yeast mitogen-activated protein kinase kinase kinase kinase (MAP4K) involved in the mating pathway. The Ste20 group is further divided into the p21-activated kinase (PAK) and germinal center kinase (GCK) families (Dan *et al.* 2001). The PAK family of serine/threonine kinases comprises at least four isoforms that are differentially expressed in mammalian tissues (Knaus *et al.* 1998). PAKa localises in the posterior end of polarised chemotaxing *Dictyostelium* cells. Overexpression of activated PAKa leads to an upregulated assembly of F-actin and results in multiple actin crowns. Human filamin is phosphorylated at S2152 by PAK1, which exhibits 59% sequence identity to the kinase domain of PAKa and Myosin I Heavy Chain Kinase (MIHCK) of *Dictyostelium*. Therefore we have chosen as candidate kinases of the STE20/PAKa family proteins to check for a probable kinase phosphorylating ddfilamin. Attempts to phosphorylate ddfilamin *in vitro* with a 'kinase responsive to stress 1 like kinase' from *Dictyostelium*, a member of the Ste20/Pak protein kinases, were however not successful (R. Arasada, personal communication). In continuation of this work we have

also isolated the kinase domain of PAKa and Myosine I Heavy Chain Kinase (MIHCK) (data not shown) to pursue the in vitro phosphorylation.

3. Filamin in the tip region is essential for slug movement and phototaxis

It has been shown that the tip region is responsible for directing slug motility and phototaxis. Grafting of a tip from a wild-type slug to a non-phototactic mutant allows the slug to move directionally (Fisher *et al.* 1984). To test whether the presence of ddfilamin at the anterior tip region of the slug is necessary and sufficient for the phototaxis rescue we expressed ddfilamin under the control of cell type specific promoters. The cells that occupy the anterior tip of the slug express the *ecmA* gene most strongly and are called *pstA* cells (Morrison *et al.* 1994). *PstO* cells follow the *pstA* region where the *ecmA* gene is expressed at a low level. *PstAB* cells occupy the central core of the anterior tip and express both *ecmA* and *ecmB* genes (Jermyn *et al.* 1989). Expression of *ecmA::FLC-GFP* in HG1264, where the fusion protein was found expressed at the anterior tip of slugs, corrected the phototaxis defect completely.

The *cotB* gene, exclusively expressed in the spore coat, is a reliable marker for prespore cells (Fosnaugh *et al.* 1994). Expression of *cotB::FLC-GFP* in HG1264 led to expression of the fusion protein at the posterior $\frac{3}{4}$ th part of the slug and did not rescue the phototaxis defect. Summarizing these results we may conclude that expression of ddfilamin at the anterior tip of the slug is necessary for the normal phototactic migration of the slug where full-length ddfilamin may control the quality of the cylindrical lens formed by pseudoplasmodia. Wallraff and Wallraff (1997) suggested that absence of ddfilamin alters the shape of the lens, which is formed by the cells at the front and/or enhances the internal light scattering via abrogation of intercellular coherence.

4. Interaction partners of filamin suggest a diverse function for the protein

Immunoprecipitation of ddfilamin from AX2 cells overexpressing *FLC-GFP* revealed an interaction with TipA. MALDI-MS analysis gave a score as high as 305 for the protein band at around 90 kDa, the predicted molecular weight for the protein, and a 83 kDa and 60 kDa protein which may represent degradation products of TipA. Stege *et al.* (1999) found four *Dictyostelium* tip genes, *tipA*, *tipB*, *tipC*, and *tipD*, by REMI analysis. All mutants showed a primary defect in cell sorting and the formation of tips in the developing mound; the strains aggregated into larger than average mounds, which split up and formed many lips on their surfaces. Furthermore, each mutant exhibited cell autonomous defects such as reduced or

aberrant cell-sorting behavior, never made migrating slugs, and had severely reduced fruiting body and spore production (Stege *et al.* 1997 and Stege *et al.* 1999). The tip genes function in parallel pathways of early *Dictyostelium* development. Overexpression of one gene in the background of others significantly improves the morphogenesis. The authors furthermore found that prespore and prestalk gene expression was reduced or delayed in the tip mutants. The tipA gene is expressed in pstO cells where the ecmA gene is expressed at low levels. When ddfilamin is expressed under the control of the ecmA promoter, low levels of the protein expressed in pstO cells may interact with TipA that may contribute to the functions of TipA. The sequence analysis of the tipA gene fails to exhibit its biochemical function. A SMART search shows the PP2Cc Ser/Thr phosphatase domain but when using blast, this domain does not show the sequence homology with any such proteins. According to the NCBI blast search engine, the PP2C domain does not share homology with the PP1, PP2A, PP2B family of protein Ser/Thr phosphatases.

The second protein in the co-immunoprecipitation experiment was identified by matrix-assisted laser desorption–ionization mass spectrometry (Maldi-MS) and peptide microsequencing as GAPA. The peptide score in this case was 48. *D. discoideum* has two IQGAP-related proteins that are about 50 % identical. Both DGAP1 and GAPA are involved in cytokinesis. GAPA⁻ cells can initiate the formation of a cleavage furrow, but often fail to complete cytokinesis (Adachi *et al.* 1997). Despite their homology to GTPase-activating proteins (GAPs), IQGAP-related proteins do not possess GAP activity (Faix *et al.* 1998). Sucurai *et al.* (2001) demonstrated that almost the entire region of GAPA homologous to IQGAP. At least one of the GAPs is essential for the formation of a quaternary complex consisting of Rac1, cortexillin I and II. GAPA forms a complex with cortexellins and localises them into cleavage furrow functioning in cytokinesis (Faix *et al.* 2001). Cortexillins of *D. discoideum* are actin-bundling proteins that organise actin filaments preferentially into anti-parallel bundles and associate them into three-dimensional meshworks. Cortexillins are enriched in the cortex of interphase cells, translocate to the equatorial region of dividing cells and are required for the correct positioning of the cleavage furrow (Weber *et al.* 1999). Mutants lacking both isoforms, cortexillin I (CI) and II (CII), are severely impaired in cytokinesis and form large multinucleate cells. Ddfilamin resembles the cortexillins in that far, that it similarly associates with F-actin filaments to form three-dimensional arrays and this activity might be subject to GAPA regulation.

SapA, another probable binding partner for ddfilamin pulled down with mAb 82-421-5, has several Sap B domains. Saposin (B) domains are present in multiple copies in prosaposin and in pulmonary surfactant-associated protein B. In plant aspartic proteinases, a saposin domain is circularly permuted (Taylor, 2000). Not much is known about this protein in *Dictyostelium*.

5. FIP may function in membrane traffic

Elucidating the interaction partners of filamin is critical for our understanding of the molecular mechanisms that regulate the diverse cellular functions of this actin cytoskeleton associated protein. Proteins involved in actin polymerisation and crosslinking the filaments into bundles or networks support a broad range of functions. Findings from interaction studies with vertebrate filamins indicate an involvement of this protein family in such diverse processes as mechanical stability, intracellular trafficking and signal transduction. Vesicle transport is a cellular process important in the trafficking of lipids and proteins between intracellular organelles. Genetic and biochemical approaches in yeast and mammalian cells have identified a large number of proteins that are involved in the various steps of vesicle transport including the production of vesicles from donor compartments, the transport and docking of these vesicles, and the fusion of vesicles with acceptor membranes (Rothman, 1994). FIP, the filamin interacting protein, which we have identified in a yeast-two-hybrid screen, appears to be a vesicle associated protein. Immunostaining with fluorescently labeled antibodies and TRITC-phalloidin however showed that FIP colocalises also to some extent with F-actin (Knuth, 2001). Additional information about its association with the actin cytoskeleton was gathered from studies using DMSO.

DMSO has long been known to lead to a reversible rearrangement of actin filaments and has been used to assess the role of microfilaments in mediating motility and maintenance of cell structure (Osborn and Weber, 1980). Redistribution of FIP upon a treatment with DMSO indicates that FIP is associated with F-actin, but it is not clear whether this is due to a general collapse of cellular structures or whether this is due to specific interactions between FIP containing membrane structures and the actin network

6. Microarray analysis suggests that the phototaxis defect in ddfilamin⁻ mutants may be due to reduced cell adhesion and defective cAMP wave propagation

During the first 8-10 h of the developmental cycle, cells in the population come together and form a loose aggregate and behave in this structure as identical single-celled organisms whose behaviour is coordinated by a complex signalling system. Several genes functioning in

adhesion, cell type differentiation and cAMP/cGMP signalling are expressed at this stage. Therefore we decided to use RNA isolated at 10 h of development for our microarray analysis to understand the global genes involved in the process of phototaxis.

With our microarray data analysis we found that a gene for cAMP phosphodiesterase (PDE) was down regulated. PDE is expressed in prestalk cells as a result of the activity of a specific promoter. This PDE is a class II phosphodiesterase (psdA) that functions extracellularly, and is analogous to the class I cAMP PDE, RegA, which functions within the cell. The extracellular PDE can have two roles: it degrades the background cAMP between the pulses that are produced every 6 minutes, and plays a role in modulating the gradient as it passes the cells (Nanjundiah and Malchow 1976). Overexpression of PDE leads to rapid development, presumably because cells spend less time to adapt (Kessin, 2001). The low levels of PDE in the GHR mutant may result in elevated levels of cAMP that may cause the cells to adapt and the gradient to become less steep.

The level of extracellular cAMP is controlled selectively by PDI, the PDE inhibitor. PDI competes with cAMP for binding to PDE. PDI is a glycoprotein and like PDE it is secreted during development. Its regulation is precisely opposite to that of the PDE, as it is repressed by high levels of extracellular cAMP. Wu and Franke (1990) showed that removing cAMP from the developing population of cells leads to a dramatic synthesis and secretion of PDI. Our microarray result shows that expression of PDI in GHR is upregulated.

A decrease in PDE expression and an increase in PDI expression in GHR could cause an elevation in the cAMP level that in turn activates the PKA. But this presumably moderate activation of PKA may not cause any alteration in development as reported by Wang and Kupsa (1997). However, the increase in extracellular cAMP concentration in the GHR mutant might interfere with the formation of the three-dimensional scroll wave by increasing the length of the adaptation. The tip dominance properties of the slug are also disrupted when slugs are placed on cAMP. New organizing centers appear along the length of the slug and fruiting bodies arise along its length (Nestle and Sussman, 1972 and Schaap and Wang 1985). The phototactic turning in case of the GHR mutant could also be explained by elevated levels of cAMP at the tip but the question remain unanswered why they turn only clockwise.

The majority of genes down regulated can be grouped as genes coding for calcium binding proteins like Calcium Binding Protein (CBP), CBP2, CBP4a, CBP7 and additional ones that are homologous to CBP3 and some unknown proteins with EF hands, and cell adhesion molecules. Prestalk and prespore cells possess qualitatively different, high-capacity stores containing distinct amounts of calcium and probably being involved in regulation of the anterior-posterior $[Ca^{2+}]_i$ -gradient. Micromolar amounts of calcium inhibit the cross-linking activity of α -actinin and 34kDa actin bundling protein (Fechheimer *et al.* 1982) and promote the severing activity of severin and gelsolin. Ca^{2+} induces K^+ channels, which increases the pH. At pH <7.2, α -actinin, hisactophilin, ADF, and cofilin will bind actin. At pH >7.2, α -actinin and hisactophilin dissociate from actin, while ADF and cofilin depolymerize the actin filament. From this information we may conclude that down regulation of several Ca^{2+} sequestering proteins may increase the intracellular Ca^{2+} concentration, which could then activate several Ca^{2+} -dependent kinases, which might negatively regulate the slug migration (Endl *et al.* 1996). Interestingly amounts of the α -actinin and hisactophilin mRNAs were increased. The major F-actin crosslinker in wild type cells is α -actinin, whose activity *in vitro* is at least five times greater than that of ddfilamin (Fechheimer *et al.* 1982 and Condeelis and Vahey, 1982). Its function in F-actin crosslinking could be impaired because of the probable increase of the intracellular Ca^{2+} -level. This result underlines our finding that F-actin crosslinking by ddfilamin is essential for the phototactic rescue of GHR mutant.

During development, *Dictyostelium* cells express several adhesion systems that allow cells to adhere to each other as they aggregate. We found that several genes functioning as adhesion molecules like contact site A (gp80), Csb A (gp24) and the putative adhesion molecule CAD2 were down regulated.

Early studies by Gerisch distinguished two major classes of cell adhesion sites (Gerisch, 1980). One class is sensitive to low concentrations of EDTA, while the other is stable in EDTA up to a concentration of 15 mM. The EDTA-sensitive cell adhesion sites can be divided into two subtypes, the EDTA/EGTA-sensitive adhesion sites and the EDTA-sensitive/EGTA-resistant adhesion sites (Beug *et al.* 1973). The glycoprotein gp24, the product of the csbA gene, has been implicated in cell-cell adhesion of *D. discoideum*. There are two proteins named gp24a and gp24b, which are 85% identical. Their genes are expressed within a few hours of the initiation of development; their mRNAs accumulate to a peak at 12 hr and persist until culmination. Two independent adhesion mechanisms, contact sites A and

contact sites B, function during the aggregation stage. Our microarray results suggest that both mechanisms are partially impaired in the GHR mutant resulting in reduced cell-cell adhesion. Further down regulation of the putative adhesion molecule CAD2 supports earlier findings with gp80 and gp24a.

The majority of the genes that are down regulated are predominantly expressed in the prestalk region. The function of some of the DIF (differentiation inducing factor) regulated genes like pst-cathepsin, a papain like cysteine protease is unknown but can be correlated with the function of earlier genes found down regulated. Another gene, fatty acid desaturase gene, was significantly upregulated. Li *et al.* (2001) investigated the role of Sphingosine-1-phosphate (S-1-P) lyase, an enzyme that functions in fatty acid metabolism and catalyses Sphingosine-1-phosphate degradation, and found that it also controls the slug migration.

The acetylornithine deacetylase mRNA was also found to have increased levels. This is an enzyme important in the ammonia metabolism. Ammonia, the major component of the amino acid catabolism, regulates the migration of the slug indirectly. As long as ammonia levels are high, the slugs will not culminate and form fruiting bodies rather, they will continue to migrate as slug. Acetylornithine deacetylase is involved in arginine biosynthesis. Arginine along with ornithin in human can be used for ammonia detoxification. Significant induction of this gene in the ddfilamin minus mutant could explain the reduced migration of the slug and early formation of fruiting bodies.

We also found that profilin, a ubiquitous G-actin sequestering protein (Karakesisoglou *et al.* 1999) in eukaryotic cell is down regulated. Its regulation is controlled by membrane phospholipids like PIP₂ or its precursor PIP. Profilin binds to several proteins that include actin related protein or VASP. The profilin-minus mutant showed a severe and complex phenotype: single cells were up to 10 times larger than wild-type cells, the F-actin content was increased, motility decreased, and development ceased at early culmination. Profilin-minus cells were impaired in cytokinesis and formed multinucleated cells that grew on surfaces but could not withstand the shearing forces in shaking culture. The down regulation of the profilin along with reduced cell adhesion might be more relevant to our findings regarding the enhanced phagocytosis of the GHR cells than the defect in phototaxis. Genes encoding hypothetical proteins of unknown function and genes coding for proteins whose function cannot be correlated with phototaxis and phagocytosis are not discussed here.

V. Summary

Dictyostelium discoideum is a soil-living social amoeba, feeds on bacteria and lives as a solitary unicellular organism when food is plentiful. However, when cells undergo starvation, the programmed expression of various genes allows the cells in the population to aggregate and differentiate into a motile multicellular organism, the slug. Slugs sense smallest difference in temperature and migrate towards the light. Phototaxis is a complex phenomenon where several genes have been suggested to be involved, but filamin emerged as the first cytoskeletal protein, whose absence led to a severe defect in phototactic migration of slugs without any alteration in development. Filamin⁻ slugs migrate less distance with an angle of about 45⁰ towards either side of the incoming light and almost every trail of phototaxing slugs ends up with a typical clockwise turn, similar turns are also observed when wild type slug migrate in dark. During our investigation we have tried to find out how a single cytoskeletal protein controls a complex phenomenon like phototaxis.

In an attempt to understand, whether the defect is due to the actin crosslinking activity of filamin we expressed the actin binding domain and the rod domain of ddfilamin fused to GFP in HG1264 and GHR (these filamin⁻ mutants, respectively generated by chemical mutagenesis and homologous recombination, show a similar phenotype). We found that both the

domains were unable to rescue the phototaxis indicating that filament crosslinking by filamin might be important for phototaxis. RN-GFP when expressed in AX2 cells forms a heterodimer with the endogenous protein and can interfere with the crosslinking function of endogenous filamin. The results from the phototaxis analysis however indicated that partial disruption of this function did not alter the phototaxis. To follow up this question, we expressed a filamin lacking the region responsible for dimerisation in HG1264 cells. Slugs expressing this protein, migrate longer distances but were impaired in sensing the light as their parent strain, suggesting that actin crosslinking by filamin controls the phototactic turning of the slugs. We detected and generated a point mutation at a potential phosphorylation site, which was located in the actin binding domain of filamin. This mutation did not affect the localisation of the protein at the subcellular level but it affected the rescue potential of the protein. The HG1264 slugs expressing the mutated protein were oriented accurately but traveled less distance as compared to wild type slugs. Several researchers have shown that the anterior tip of the slug controls the migration of the slug. Accordingly, expression of the full-length filamin in cells at the anterior tip was essential and sufficient to rescue the phototactic defect of the mutant.

The confocal microscopic study of RN-GFP expressing cells suggests that the fusion protein does not localise properly in mutants whilst when expressed in AX2 cells it localises at the cell cortex and the phagocytic cup. Expression of RN-GFP affected the phagocytosis in both mutants as well as wild type cells and led to a significant reduction. Our studies also revealed that the rate of phagocytosis in the mutant was higher as compared to that of AX2 cells.

Chemotaxis towards cAMP plays a pivotal role during *Dictyostelium* development including the slug migration. Detailed analysis of LIM protein mutants for chemotaxis revealed that LimD controls the cell migration by affecting the formation of lateral pseudopods as the cells lacking LimD form a higher number of pseudopods and migrate less persistent towards the cAMP gradient. The phototactic behavior of this mutant was indistinguishable from wild type cells indicating that the chemotactic migration of cells within the slug might not be controlled by this protein although the possibility of the mutant cells performing a normal chemotaxis at the higher concentration of cAMP within the slug environment cannot be ignored.

To understand the involvement of filamin in signal transduction controlling the slug migration and phototaxis we identified proteins interacting with filamin by biochemical methods. TipA, a protein, which controls the tip formation of the slug and has a role in pattern formation, along with GAPA, an IQGAP family protein, and SapA, a SapB domain containing protein with unknown function in *Dictyostelium*, were found as potential interacting partners. The significance of these interactions is currently under investigation.

Finally, the microarray analysis results suggest that the phototactic defect in the mutant slugs may be due to elevated levels of extracellular cAMP, which may disturb the generation of the wave by increasing the adaptation of cells to cAMP. The down regulation of several calcium binding protein genes and adhesion molecules such as csA, gp24 and ddCAD2 might also be of relevance in this process. Though expression levels of α -actinin, a major actin crosslinking protein and hisactophilin, a pH-dependent actin crosslinking protein, are elevated, their functions might be impaired because of increased levels of intracellular calcium.

V. Zusammenfassung

Das Zytoskelett einer Zelle ist in vielfältige Prozesse involviert. Es ist wichtig für die Bewegung, für Zell-Zell-Kontakte, Zell-Substrat-Anhaftung, für die Zellteilung und für intrazelluläre Transportprozesse. Für die Aufrechterhaltung dieser verschiedenen Funktionen sind neben den Hauptkomponenten des Zytoskeletts, Aktin, Tubulin und Intermediärfilamente, die akzessorischen Proteine der Filamentsysteme von entscheidender Bedeutung wie vor allem Mutantanalysen gezeigt haben. Die hier vorgestellten Arbeiten sind in *Dictyostelium discoideum* durchgeführt worden, einem eukaryontischen Mikroorganismus mit einzelligen und mehrzelligen Entwicklungsstadien, der zur Analyse von verschiedenen zellbiologischen Fragestellungen wie der Rolle und Funktion des Zytoskeletts hervorragend geeignet ist.

Filamin (Gelationsfaktor, ABP120 oder ddFilamin) gehört zur Gruppe der aktinbindenden Proteine, die Aktinfilamente quervernetzen und den Aufbau von dreidimensionalen Aktinstrukturen ermöglichen. Es besteht aus einer aktinbindenden Domäne und sechs Wiederholungseinheiten von je einhundert Aminosäuren, die für die Ausbildung seiner stäbchenförmigen Struktur verantwortlich sind und über deren letzte Einheit die Dimerisierung des Moleküls erfolgt, die die Grundlage für die Quervernetzungsaktivität von Filamin bildet. *Dictyostelium* Mutanten, denen Filamin fehlt, sind im multizellulären Slugstadium beeinträchtigt. Slugs orientieren sich normalerweise auf das einfallende Licht hin

und wandern darauf zu, während Filamin⁻ Mutanten eine veränderte phototaktische Reaktion aufweisen und in einem Winkel zum Licht hin und über kürzere Strecken wandern.

Um zu verstehen, welche Eigenschaft von Filamin für diese veränderte Reaktion verantwortlich ist, sind einzelne Domänen in der Mutante exprimiert und auf ihre Fähigkeit hin, den Phototaxisdefekt zu kompensieren, getestet worden. In diesen Untersuchungen konnte der Phototaxisdefekt vom Motilitätsdefekt getrennt werden, wobei für eine verbesserte Motilität die Expression eines verkürzten Proteins ausreichend war, das aus aktinbindender und verkürzter stäbchenförmiger Domäne bestand und das auf Grund der fehlenden letzten Wiederholungseinheit nicht mehr in der Lage war zu dimerisieren. Der Phototaxisdefekt war dagegen nicht aufgehoben. Dies verweist auf die Bedeutung der Quervernetzungsaktivität des Proteins für diese Aktivität. Eine Mutation in einer potentiellen Phosphorylierungsstelle in der aktinbindenden Domäne korrigierte dagegen den Phototaxisdefekt, beeinträchtigte aber die Slugmotilität. Schliesslich konnte gezeigt werden, dass eine Filaminexpression in den Zellen an der Spitze des Slugs, den sogenannten Tipzellen, ausreicht, um den Phototaxisdefekt vollständig aufzuheben. Diese Daten in Kombination mit Daten aus anderen Gruppen lassen darauf schliessen, dass die Qualität der Spitze entscheidend für die Wirkung des Lichtes ist. Weitere Daten zur Genexpression in der Mutante und die Identifizierung von Filamin-Bindeproteinen weisen auf Veränderungen in der cAMP Signaltransduktion in der Mutante, die die Ursache für die veränderte Slugmotilität sein können

VI. Bibliography

Abe T, Early A, Siegert F, Weijer C, Williams J, Patterns of cell movement within the *Dictyostelium* slug revealed by cell type-specific, surface labeling of living cells. *Cell*. 1994, **77** 687-699.

Adachi H, Takahashi Y, Hasebe T, Shirouzu M, Yokoyama S and Sutoh K, *Dictyostelium* IQGAP-related protein specifically involved in the completion of cytokinesis. *J Cell Biol*. 1997, **137** 891-898.

Allen E, Zicha D, Ridley J and Jones G, A role for Cdc42 in macrophage chemotaxis. *J Cell Biol*. 1998, **141** 1147-1157.

Andrews R and Fox J, Interaction of purified actin-binding protein with the platelet membrane glycoprotein Ib-IX complex, *J. Biol. Chem*. 1991, **266** 7144-7147.

Bellanger J, Astier C, Sardet C, Ohta Y, Stossel T and Debant A, The Rac1- and RhoG-activating domain of the bifunctional guanine nucleotide exchange factor Trio targets filamin to remodel cytoskeletal actin. *Nature Cell Biol*. 2000, **2** 888-892.

Bennett H and Condeelis J, Isolation of an immunoreactive analogue of brain fodrin that is associated with the cell cortex of *Dictyostelium* amoebae. *Cell Motil. Cytoskel*. 1988, **11** 303-317.

Bertholdt G, Stadler J, Bozzaro S, Fichtner B. and Gerisch G, Carbohydrate and other epitopes of the contact site A glycoprotein of *Dictyostelium discoideum* as characterized by monoclonal antibodies. *Cell Differ*, 1985, **16** 187-202.

Beug H, Katz F and Gerisch G, Dynamics of antigenic membrane sites relating to cell aggregation in *Dictyostelium discoideum*. *J Cell Biol*. 1973, **56** 647-658.

Bishop A and Hall A, Rho GTPases and their effector proteins. *Biochem. J*. 2000, **348** 241-255.

Bonner J, Evidence for the formation of cell aggregates by chemotaxis in development of the slime mold *Dictyostelium discoideum*. *J. Exp. Zool*. 1947, **106** 1-26.

Bonner J, *The Cellular Slime Molds* (Princeton Univ. Press, Princeton, 1967).

Bonner J and Williams J, Inhibition of cAMP-dependent protein kinase in *Dictyostelium* prestalk cells impairs slug migration and phototaxis. *Dev Biol*. 1994, **164** 325-327

Borisy G and Svitkina T, Actin machinery: pushing the envelop. *Curr. Opin. Cell Biol.* 2000, **12** 104-112.

Brier J, Fechheimer M, Swanson J and Taylor D, Abundance, relative gelation activity, and distribution of the 95,000 dalton actin-binding protein from *Dictyostelium discoideum*. *J. Cell Biol.* 1983, **97** 178-185.

Brink A, Gerisch M, Isenberg G, Noegel A., Schleicher M, Segall J. and Wallraff E, A *Dictyostelium* mutant deficient in severin, an F-actin fragmenting protein, shows normal motility and chemotaxis. *J Cell Biol*, 1989, **108** 985-995.

Brink M, Gerisch G, Isenberg G, Noegel A, Segall JE, Wallraff E and Schleicher M, A *Dictyostelium* mutant lacking an F-actin crosslinking protein, the 120 kD gelation factor. *J. Cell Biol.* 1990, **111** 1477-1489.

Brown S, A calcium insensitive actin-crosslinking protein from *Dictyostelium discoideum*. *Cell Motil.* 1985, **5** 29-543.

Bullock W, Fernandez J and Short J, XL1-blue: A high efficiency plasmid transforming *recA Escherichia coli* strain with beta-galactosidase selection. *BioTechniques*, 1987, **5** 376-378.

Carroll R and Gerrard J, Phosphorylation of platelet actin-binding protein during platelet activation. *Blood* 1982, **59** 466-471.

Chien S, Chung C, Sukumaran S, Osborne N, Lee S, Ellsworth C, McNally J and Firtel R, The *Dictyostelium* LIM domain-containing protein LIM2 is essential for proper chemotaxis and morphogenesis. *Mol Biol Cell.* 2000, **11** 1275-1291.

Chung C and Firtel R, PAKa, a putative PAK family member, is required for cytokinesis and the regulation of the cytoskeleton in *Dictyostelium discoideum* cells during chemotaxis. *J Cell Biol.* 1999, **147** 559-576.

Chung C, Lee S, Briscoe C, Ellsworth C and Firtel R, Role of Rac in controlling the actin cytoskeleton and chemotaxis in motile cells. *Proc Natl Acad Sci U S A.* 2000, **97** 5225-5230.

Chung C, Funamoto S and Firtel R, Signaling pathways controlling cell polarity and chemotaxis. *Trends Biochem. Sci.*, 2001, **26** 557-566.

Claviez M, Pagh K, Maruta H, Baltes W, Fisher P and Gerisch G, Electron microscopic mapping of monoclonal antibodies on the tail region of *Dictyostelium* myosin. *EMBO J.* 1982, **1** 1017-1022.

Condeelis J, Salisbury J and Fujiwara K, A new protein that gels F-actin in the cell cortex of *Dictyostelium discoideum*. *Nature* 1981, **292** 161-163.

Condeelis J and Vahey M, A calcium and pH-regulated protein from *Dictyostelium discoideum* that cross-links filaments. *J. Cell Biol.* 1982, **94** 466-471.

Cox D, Condeelis D, Wessels D, Soll H, Kern and Knecht D, Targeted disruption of the ABP-120 gene leads to cells with altered motility. *J. Cell Biol.* 1992, **116** 943-955.

Cox D, Ridsdale J, Condeelis J, Hartwig J, Genetic deletion of ABP-120 alters the three-dimensional organization of actin filaments in *Dictyostelium* pseudopods. *J Cell Biol.* 1995, **128** 819-835.

Cox D, Wessels D, Soll D, Hartwig J and Condeelis J, Re-expression of ABP-120 rescues cytoskeletal, motility and phagocytosis defects of ABP-120⁻ *Dictyostelium* mutants. *Mol. Biol. Cell* 1996, **7** 803-823.

Dan I, Bosgraaf L, Russcher H, Smith J, Wessels D, Soll D and Van Haastert P, A novel cGMP signalling pathway mediating myosin phosphorylation and chemotaxis in *Dictyostelium*. *EMBO J.* 2002, **21** 4560-4570.

Daniel J, Spiegelman GB, and Weeks G, Characterization of a third ras gene, *rasB*, that is expressed throughout the growth and development of *Dictyostelium discoideum*. *Oncogene* 1993, **8** 1041-1047.

Daniel J, Bush J, Cardelli G, Spiegelman and Weeks G, Isolation of two novel ras genes in *Dictyostelium discoideum* evidence for a complex, developmentally regulated ras gene subfamily. *Oncogene* 1994, **9** 501-508.

Darcy P, Wilczynska Z and Fisher P, The role of cGMP in photosensory and thermosensory transduction in *Dictyostelium discoideum*. *Microbiology* 1994, **140** 1619-1632.

de Hostos E, Rehfuss C, Bradtke B, Waddell D, Albrecht R, Murphy J. and Gerisch G, *Dictyostelium* mutants lacking the cytoskeletal protein coronin are defective in cytokinesis and cell motility. *J. Cell. Biol.* 1993, **120** 163-173.

De La Roche M, Lee S, Cote G, The *Dictyostelium* class I myosin, MyoD, contains a novel light chain that lacks high-affinity calcium-binding sites. *Biochem J.* 2003, **374** 697-705.

Demma M, Warren V, Hock R, Dharmawardhane S and Condeelis J, Isolation of an abundant 50,000 dalton actin filament bundling protein from *Dictyostelium discoideum*. *J. Biol. Chem.* 1990, **265** 2286-2291.

Devereux J, Haerberli P and Smithies O, A comprehensive set of sequence analysis programs for the VAX. *Nucleic Acids Res.* 1984, **12** 387-397.

Dormann D, and Weijer C, Propagating chemoattractant waves coordinate periodic cell movement in *Dictyostelium* slugs. *Development.* 2001, **128** 4535-4543.

Edwards D, Towb P and Wasserman S, An activity-dependent network of interactions links the Rel protein Dorsal with its cytoplasmic regulators. *Development.* 1997, **124** 3855-3864.

Edwards D, Sanders L, Bokoch G and Gill G, Activation of LIM-kinase by Pak1 couples Rac/Cdc42 GTPase signalling to actin cytoskeletal dynamics. *Nat Cell Biol.* 1999, **1** 253-259.

Eichinger L, Köppel B, Noegel A, Schleicher M., Schliwa M, Weijer K, Witke W. and Janmey P, Mechanical perturbation elicits a phenotypic difference between *Dictyostelium* wild-type cells and cytoskeletal mutants. *Biophys. J.* 1996, **70** 1054-1060.

- Elble R**, A simple and efficient procedure for transformation of yeasts. *Biotechniques*. 1992, **13** 18-20.
- Endl I, Konzok A and Nellen W**, Antagonistic effects of signal transduction by intracellular and extracellular cAMP on gene regulation in *Dictyostelium*. *Mol Biol Cell*. 1996, **7** 17-24.
- Faix J, Steinmetz M, Boves H, Kammerer R, Lottspeich F, Mintert U, Murphy J, Stock A, Aebi U and Gerisch G**, Cortexillins, major determinants of cell shape and size, are actin-bundling proteins with a parallel coiled-coil tail. *Cell* 1996, **86** 631-642.
- Faix J, Clougherty C, Konzok A, Mintert U, Murphy J, Albrecht R, Muhlbauer B and Kuhlmann J**, The IQGAP-related protein DGAP1 interacts with Rac and is involved in the modulation of the F-actin cytoskeleton and control of cell motility. *J Cell Sci*. 1998, **111** 3059-3071.
- Faix J, Weber I, Mintert U, Kohler J, Lottspeich F and Marriott G**, Recruitment of cortexillin into the cleavage furrow is controlled by Rac1 and IQGAP-related proteins. *EMBO J*. 2001, **20** 3705-3715.
- Fechheimer M, Brier J, Rockwell M, Luna E and Taylor D**, A calcium and pH regulated actin binding protein from *D. discoideum*. *Cell Motil*. 1982, **2** 287-308.
- Fechheimer M and Taylor D**, Isolation and characterization of a 30,000-dalton calcium-sensitive actin cross-linking protein from *Dictyostelium discoideum*. *J. Biol. Chem*. 1984, **259** 4514-4520.
- Fechheimer M**, The *Dictyostelium discoideum* 30,000 Dalton calcium-sensitive actin-bundling protein is selectively present in filopodia. *J. Cell Biol*. 1987, **104** 1539-1551.
- Fechheimer M, Murdock D, Carney M and Glover CVC**, Isolation and sequencing of cDNA clones encoding the *Dictyostelium discoideum* 30,000 dalton actin bundling protein. *J. Biol. Chem*. 1991, **266** 2883-2889.
- Fisher P, Dohrmann and Williams K** Signal processing in *Dictyostelium discoideum* slugs. *Modern Cell Biol*. 1984, **3** 197-248.
- Fisher PR**. Genetics of phototaxis in a model eukaryote, *Dictyostelium discoideum*. *Bioessays* 1997a, **19** 397-407.
- Fisher P, Noegel A, Fechheimer M, Rivero F, Prassler J and Gerisch G**, Photosensory and thermosensory responses in *Dictyostelium* slugs are specifically impaired by absence of the F-actin cross-linking gelation factor (ABP-120). *Curr Biol* 1997b, **7** 889-892.
- Flick JS, and Johnson M**, Two systems of glucose repression of the *Gall* promotor in *Saccharomyces cerevisiae*. *Mol. Cell Biol*. 1990, **10** 4757-4769.
- Flick M and Konieczny S**, The muscle regulatory and structural protein MLP is a cytoskeletal binding partner of β I-spectrin. *J. Cell Sci*. 2000, **113** 1553-1564.
- Fontana D**, Two distinct adhesion systems are responsible for EDTA-sensitive adhesion in *Dictyostelium discoideum*. *Differentiation*. 1993, **53** 139-147.

Francis D, *J. Cell. Compar. Physiol.* 1964, **64** 131-138.

Freyd G, Kim S and Horvitz H, Novel cysteine-rich motif and homeodomain in the product of the *Caenorhabditis elegans* cell lineage gene *lin-11*. *Nature* 1990, **344** 876–879.

Fucini P, Renner C, Herberhold C, Noegel AA and Holak T, The repeating segments of the F-actin crosslinking gelation factor (ABP-120) have an immunoglobulin-like fold. *Nature Struct. Biol.* 1997, **4** 223-230.

Fucini P, Köppel B, Schleicher M, Lustig A, Holak T, Müller R, Stewart M and Noegel A, Molecular architecture of the rod domain of the *Dictyostelium* gelation factor (ABP120). *J Mol Biol* 1999, **291** 1017-1023.

Gerisch G, Univalent antibody fragments as tools for the analysis of cell interactions in *Dictyostelium*. *Curr Top Dev Biol.* 1980, **14** 243-270.

Gerisch G and Keller H, Chemotactic reorientation of granulocytes stimulated with micropipettes containing fMet-Leu-Phe. *J. Cell Sci.* 1981, **52** 1-10.

Glogauer M, Arora P, Chou D, Janmey P, Downey G and McCulloch C, The role of actin-binding protein 280 in integrin-dependent mechanoprotection, *J. Biol. Chem.* 1998, **273** 1689-1698.

Gloss A, Ravero F, Khaire N, Müller R, Loomis W, Schleicher M and Noegel A, Villidin, a novel WD-repeat and villin related protein from *Dictyostelium* is associated with membrane and the cytoskeleton. *Mol Biol Cell.* 2003, **14** 2716-2727.

Goldmann W, Phosphorylation of filamin (ABP-280) regulates the binding to the lipid membrane, integrin, and actin. *Cell Biol Int.* 2001, **25** 805-808.

Gorlin J, Yamin R, Egan S, Steward M, Stossel T, Kwiatkowski D and Hartwig J, Human endothelial actin-binding protein (ABP-280, nonmuscle filamin): a molecular leaf spring. *J. Cell Biol.* 1990, **111** 1089-1105.

Guo Y, Zhang S, Sokol N, Cooley L and Boulianne GL, Physical and genetic interaction of filamin with presenilin in *Drosophila*. *J. Cell Sci.* 2000, **113** 3499-3508.

Gronborg M, Kristiansen T, Stensballe A, Andersen J, Ohara O, Mann M, Jensen O and Pandey A, A mass spectrometry-based proteomic approach for identification of serine/threonine-phosphorylated proteins by enrichment with phospho-specific antibodies: identification of a novel protein, Frigg, as a protein kinase A substrate. *Mol Cell Proteomics.* 2002, **1** 517-527.

Gross JD, Developmental decisions in *Dictyostelium discoideum*. *Microbiol. Rev.* 1994, **58** 330-351.

Häder D and Burkart U, *Exp. Mycol.* 1983, **7** 1-8.

Hader D and Lebert M, Analysis of photoreceptor proteins of microorganisms by gradient gel electrophoresis and other biochemical separation methods. *Electrophoresis* 1994, **15** 1051-1061.

Hall A, Franke J, Faure M, Kessin R, The role of the cyclic nucleotide phosphodiesterase of *Dictyostelium discoideum* during growth, aggregation, and morphogenesis: overexpression and localization studies with the separate promoters of the pde. *Dev Biol.* 1993, **157**, 73-84.

Hall A, Rho GTPases and actin cytoskeleton. *Science* 1998, **279** 509-514.

Häder D and Burkart U, Optical properties of *Dictyostelium descoideum* pseudoplasmodia responsible for phototactic orientation. *Exp. Mycol.* 1983, **7** 1-8.

Hanahan D, Studies on transformation of *Escherichia coli* with plasmids. *J.Mol. Biol.* 1983, **166** 557-580.

Harper J, Adami G, Wei N, Keyomarsi K and Elledge S The p21 Cdk-interacting protein Cip1 is a potent inhibitor of G 1 cyclin-dependent kinases. *Cell* 1993, **75** 805-816.

Hartwig J, Spectrin Superfamily. In Protein Profile. 1994. P. Shelterline, editor. Academic, London. 711-778.

He H, Kole S, Kwon Y, Crow M and Bernier M, Interaction of filamin A with the insulin receptor alters insulin-dependent activation of the mitogen-activated protein kinase pathway. *J Biol Chem.* 2003, **278** 27096-27104.

Himmel M, Van Der Ven P, Stocklein W, Furst D, The limits of promiscuity: isoform-specific dimerization of filamins. *Biochemistry.* 2003, **42** 430-439.

Hiroak I, Hiroshi N. and Hiroto O, High efficiency transformation of *Escherichia coli* with plasmids. *Gene.* 1990, **96** 23-28.

Hock R and Condeelis J, Isolation of 240-kilodalton actinbinding protein from *Dictyostelium discoideum*. *J. Biol. Chem.* 1987, **262** 394-400.

Hoffmann C. and Winston F, A ten-minute DNA preparation from yeast efficiently releases autonomous plasmids for transformation of *Escherichia coli*. *Gene* 1987, **57** 267-272.

Hofmann A, Eichinger L, André E, Rieger D and Schleicher M, Cap100, a novel phosphatidylinositol 4, 5-bisphosphate-regulated protein that caps actin filaments but does not nucleate actin assembly. *Cell Motil. Cytoskel.* 1992, **23** 133-144.

Holmes D. and Quigley M, A rapid boiling method for the preparation of bacterial plasmids. *Analyt. Biochem.* 1981, **114** 193-197.

Hong C and Loomis W, Regulation of SP60 mRNA during development of *Dictyostelium discoideum*. *Biochim Biophys Acta.* 1988, **950** 61-66.

Jermyn KA, Duffy K, Williams J, A new anatomy of the prestalk zone in *Dictyostelium*. *Nature.* 1989, **340** 144-146.

Karakesisoglou I, Janssen K, Eichinger L, Noegel A, Schleicher M, Identification of a suppressor of the *Dictyostelium* profilin-minus phenotype as a CD36/LIMP-II homologue. *J Cell Biol.* 1999, **145** 167-181.

Katanaev V, Signal transduction in neutrophil chemotaxis. *Biochemistry*, 2001, **66** 351-368.

Kawamoto S and Hidaka H, Ca²⁺-activated, phospholipiddependent protein kinase catalyzes the phosphorylation of actin-binding proteins, *Biochem. Biophys. Res. Commun.* 1984, **118** 736-742.

Kessin R, Evolutionary biology: Cooperation can be dangerous *Nature* 2000 408 917-919.

Kessin R, *Dictyostelium*, Evolution, Cell Biology, and the Development of Multicellularity. Cambridge University Press 2001

Khurana B, Characterization of DLIM1, a novel cytoskeleton-associated LIM domain containing protein of *Dictyostelium discoideum* Ph.D. Thesis, 2001.

Kharana T, Characterization of DLIM2, a LIM domain containing protein, from *Dictyostelium discoideum*. Ph.D. Thesis, 2001.

Khurana B, Khurana T, Khaire N and Noegel A, Functions of LIM proteins in cell polarity and chemotactic motility. *EMBO J.* 2002, **21** 5331-5342.

Kimmel A and Parent C, The signal to move: *D. discoideum* go orienteering. *Science.* 2003, **300** 1525-1527.

Kopan R and Goate A, A common enzyme connects notch signaling and Alzheimer's disease. *Genes Dev.* 2000, **14** 2799-2806.

Knaus U and Bokoch G The p21Rac/Cdc42-activated kinases (PAKs). *Int J Biochem Cell Biol.* 1998 30 857-862.

Knecht D, Cohen S, Loomis W and Lodish H, Developmental regulation of *Dictyostelium discoideum* actin gene fusions carried on low-copy and high-copy transformation vectors. *Mol. Cell Biol.* 1986, **6** 3973-3981.

Knuth Monika, Identifizierung und Charakterisierung von FIP, einem neuen Filamin-bindenden Protein. Ph.D. thesis, 2001.

Kuspa A, and Loomis W, Tagging developmental genes in *Dictyostelium* by restriction enzyme-mediated integration of plasmid DNA. *Proc. Natl. Acad. Sci. USA.* 1992, **89** 8803-8807.

Laemmli U, Cleavage of structural proteins during the assembly of the head of bacteriophage T4. *Nature.* 1970, **227** 680-685.

Laevsky G and Knecht D, Cross-linking of actin filaments by myosin II is a major contributor to cortical integrity and cell motility in restrictive environments. *J Cell Sci.* 2003, **116** 3761-3770.

Lehrach H, Diamond D., Wozney J and Boedtke H, RNA molecular weight determinations by gel electrophoresis under denaturing conditions, a critical reexamination. *Biochemistry* 1977, **16** 4743-4751.

Leonardi A, Ellinger-Ziegelbauer H, Franzoso G, Brown K and Siebenlist U, Physical and functional interaction of filamin (actin-binding protein-280) and tumor necrosis factor receptor-associated factor 2. *J Biol Chem.* 2000, **275** 271-278.

Li M, Bermak J, Wang Z, and Zhou Q, Modulation of dopamine D(2) receptor signaling by actin-binding protein ABP-280. *Mol. Pharmacol.* 2000, **57** 446-452.

Li G, Foote C, Alexander S and Alexander H, Sphingosine-1-phosphate lyase has a central role in the development of *Dictyostelium discoideum*. *Development.* 2001, **128** 3473-3483.

Loo D, Kanner S and Aru A, Filamin binds to the cytoplasmic domain of the β 1-integrin. Identification of amino acids responsible for this interaction, *J. Biol. Chem.* 1998, **273** 23304-23312.

Louis S, Speigelman G and Weeks G, Expression of an activated RasD gene cell fate decision during *Dictyostelium* development. *Mol. Biol. Cell.* 1997, **8** 303-312.

Maeda Y, Inouye K, & Takeuchi I, (eds) *Dictyostelium--A Model System for Cell and Developmental Biology* (Universal Academy, Tokyo, 1997).

Machesky L, and Insall R, Scar1 and related Wiskott-Aldrich syndrome protein, WASP, regulate the actin cytoskeleton through Arp2/3 complex. *Current Biol.* 1998, **8** 1347-1356.

Malchow D, Nagele B, Schwarz H, and Gerisch G, Membrane-bound cyclic AMP phosphodiesterase in chemotactically responding cells of *Dictyostelium discoideum*. *Eur. J. Biochem.* 1972, **28** 136-142.

Maniak M, Rauchenberger R, Albrecht R., Murphy J. and Gerisch G, Coronin involved in phagocytosis: dynamics of particle-induced relocalization visualized by green fluorescent protein tag. *Cell* 1995, **83** 915-924.

Marti A, Luo Z, Cunningham C, Ohta Y, Hartwig J, Stossel T, Kyriakis J and Avruch J ABP-280 binds the SAPK activator SEK-1 and is required for TNF α activation of SAPK in melanoma cells. *J. Biol. Chem.* 1997, **272** 2620-2628.

Matsudaira P Modular organization of actin crosslinking proteins. *Trends Biochem. Sci.* 1991, **16** 87-92.

McCoy A, Fucini P, Noegel A and Stewart M, Structural basis for dimerization of the *Dictyostelium* gelation factor (ABP120) rod. *Nat Struct Biol* 1999, **6** 836-841.

McGough A, F-actin-binding proteins. *Curr Opin Struct Biol.* 1998, **8** 166-176.

McRobbie S and Newell P, Changes in actin associated with the cytoskeleton following chemotactic stimulation of *dictyostelium discoideum*. *Biochem Biophys Res Commun.* 1983, **115** 351-359.

Mejan C, Lebart M, Boyer M, Roustan C and Benyamin Y, *Eur. J Biochem.* 1992, **209** 555-562.

Miura K and Siegert F, Light affects cAMP signaling and cell movement activity in *Dictyostelium discoideum*. *Proc Natl Acad Sci U S A.* 2000, **97** 2111-2116.

Morio T, Urushihara H, Saito T, Ugawa Y, Mizuno H, Yoshida M, Yoshino R, Mitra BN, Pi M, Sato T, Takemoto K, Yasukawa H, Williams J, Maeda M, Takeuchi I, Ochiai H, Tanaka Y, The *Dictyostelium* developmental cDNA project: generation and analysis of expressed sequence tags from the first-finger stage of development. *DNA Res.* 1998, **5** 335-340.

Morrison A, Blanton R, Grimson M, Fuchs M, Williams K and Williams J, Disruption of the gene encoding the EcmA, extracellular matrix protein of *Dictyostelium* alters slug morphology. *Dev Biol.* 1994, **163** 457-466.

Nanjundiah V and Malchow D, A theoretical study of the effects of cyclic AMP phosphodiesterases during aggregation in *Dictyostelium*. *J Cell Sci.* 1976, **22** 49-58.

Nestle M and Sussman M, The effect of cyclic AMP on morphogenesis and enzyme accumulation in *Dictyostelium discoideum*. *Dev Biol.* 1972, **28** 545-554.

Newell PC, Telser A. and Sussmann M, Alternative developmental pathways determined by environmental conditions in the cellular slime mold *Dictyostelium discoideum*. *J. Bacteriol.* 1969, **100** 763-768.

Noegel A, Witke W and Schleicher M, Calcium-sensitive nonmuscle alpha-actinin contains EF-hand structures and highly conserved regions. *FEBS Lett.* 1987, **221** 391-396.

Noegel A, Rapp S, Lottspeich F, Schleicher M and Stewart M, The *Dictyostelium* gelation factor shares a putative actin-binding site with alpha-actinin and dystrophin and also has a rod domain containing six 100 residue motifs that appear to have a cross-beta conformation. *J. Cell Biol.* 1989, **108** 607-618.

Noegel A and Luna E, The *Dictyostelium* cytoskeleton. *Experientia* 1995, **51** 1135-1143.

Otto J, Actin-bundling proteins, *Curr. Opin. Cell. Biol.* 1994, **6** 105-109.

Ohta Y and Hartwig J, Actin filament cross-linking by chicken gizzard filamin is regulated by phosphorylation in vitro, *Biochemistry* 1995, **34** 6745-6754.

Ohta Y and Hartwig J, Phosphorylation of actin-binding protein 280 by growth factors is mediated by p90 ribosomal protein S6 kinase, *J. Biol. Chem.* 1996, **271** 11858-11864.

Ohta Y, Suzuki N, Nakamura S, Hartwig J and Stossel T, The small GTPase RalA targets filamin to induce filopodia. *Proc Natl Acad Sci U S A.* 1999, **96** 2122-2128.

Osborn M, Weber K, Dimethylsulfoxide and the ionophore A23187 affect the arrangement of actin and induce nuclear actin paracrystals in PtK2 cells. *Exp Cell Res.* 1980, **129** 103-114.

Ott I, Fischer E, Miyagi Y, Mueller B and Ruf W, A role for tissue factor in cell adhesion and migration mediated by interaction with actin-binding protein 280, *J. Cell Biol.* 1998, **140** 1241-1253.

Pang K, Lee E and Knecht D, Use of a fusion protein between GFP and an actin-binding domain to visualize transient filamentous-actin structures. *Curr Biol.* 1998, **26** 405-408.

Prassler J, Murr A, Stocker S, Faix J, Murphy J and Marriott G, DdLim is a cytoskeleton-associated protein involved in the protrusion of lamellipodia in *Dictyostelium*. *Mol. Biol. Cell* 1998, **9** 545–559.

Prat A, Cunningham C, Jackson G Jr, Borkan S, Wang Y, Ausiello D and Cantiello H, Actin filament organization is required for proper cAMP-dependent activation of CFTR. *Am J Physiol.* 1999, **277** C1160-C1169.

Parent C and Devreotes P, A cell's sense of direction. *Science* 1999, **284** 765-770.

Perez-Alvarado G, Miles C, Michelsen J, Louis H, Winge D, Beckerle M and Summers M Structure of the carboxy-terminal LIM domain from the cysteine rich protein CRP. *Nat. Struct. Biol.* 1994, **1** 388–398.

Pi M, Spurney R, Tu Q, Hinson T and Quarles L, Calcium-sensing receptor activation of rho involves filamin and rho-guanine nucleotide exchange factor. *Endocrinology.* 2002, **143** 3830-3838.

Poff K and Loomis WF Jr, Control of phototactic migration in *Dictyostelium discoideum*. *Exp Cell Res* 1973a, **82** 236-240.

Poff L, Butler W and Loomis WF Jr, Light-induced absorbance changes associated with phototaxis in *Dictyostelium*. *Proc Natl Acad Sci U S A* 1973b, **70** 813-816.

Poff K and Butler W, Spectral characteristics of the photoreceptor pigment of phototaxis in *Dictyostelium discoideum*. *Photochem Photobiol* 1974a, **20** 241-244.

Poff K, Loomis W Jr. and Butler W, Isolation and purification of the photoreceptor pigment associated with phototaxis in *Dictyostelium discoideum*. *J Biol Chem* 1974b, **249** 2164-2167.

Pyne S and Pyne N, Sphingosine 1-phosphate signalling via the endothelial differentiation gene family of G-protein-coupled receptors. *Pharmacol Ther.* 2000, **88** 115-131.

Raper KB, *Dictyostelium discoideum*, a new species of slime mould from decaying forest leaves. *J. Agr. Res.* 1935, **50** 135-147

Raper KB, Pseudoplasmodium formation and organization in *Dictyostelium discoideum*. *Journal of the Elisha Mitchell Scientific Society* 1940, **56** 241-282.

Raper KB, *The Dictyostelids* (Princeton Univ. Press, Princeton, 1984).

Reymond CD, Gomer RH, Mehdy MC and Firtel RA, Developmental regulation of a *Dictyostelium* gene encoding a protein homologous to mammalian Ras protein. *Cell* 1984 **39** 141-148.

Reymond C, Gomer R, Nellen W, Theibert A, Devreotes P and Firtel R, Phenotypic changes induced by a mutated Ras gene during the development of *Dictyostelium* transformants. *Nature* 1986, **323** 340-343.

Rivero F, Köppel B, Peracino B, Bozzaro S, Siegert F, Weijer CJ, Schleicher M, Albrecht R and Noegel A, The role of the cortical cytoskeleton: F-actin cross-linking proteins protect against osmotic stress, ensure cell size, cell shape and motility, and contribute to phagocytosis and development. *J. Cell Sci.* 1996, **109**, 2679-2691.

Rivero F, Furukawa R, Fechheimer M and Noegel A, Three actin cross-linking proteins, the 34 kDa actin-bundling protein, alpha-actinin and gelation factor (ABP-120), have both unique and redundant roles in the growth and development of *Dictyostelium*. *J Cell Sci.* 1999, **112** 2737-2751.

Robbins S, Williams J, Jermyn K, Spiegelman G and Weeks G, Growing and developing *Dictyostelium* cells express different ras genes. *Proc. Natl. Acad. Sci.* 1989, **86** 938-942.

Rothman J, Mechanisms of intracellular protein transport. *Nature.* 1994, **372** 55-63.

Sakurai M, Adachi H and Sutoh K, Mutational analyses of *Dictyostelium* IQGAP-related protein GAPA: possible interaction with small GTPases in cytokinesis. *Biosci Biotechnol Biochem.* 2001, **65** 1912-1916.

Sambrook J, Fritsch EF, and Maniatis T, *Molecular Cloning: A Laboratory Manual. 2nd ed.* 1989, Cold Spring Harbor Laboratory Press, Cold Spring Harbor, New York.

Scägger H, Native gel electrophoresis. In *A Practical Guide to Membrane protein purification.* 1994, 81-104 Academic Press, San Diego.

Schaap P and Wang M, cAMP induces a transient elevation of cGMP levels during early culmination of *Dictyostelium* minutum. *Cell Differ.* 1985, **16** 29-33.

Schindler J and Sussman M, Ammonia determines the choice of morphogenetic pathways in *Dictyostelium discoideum*. *J Mol Biol.* 1977, **116** 161-169.

Schleicher M, Gerisch G. and Isenberg G, New actin binding proteins from *Dictyostelium discoideum*. *EMBO J.* 1984, **3** 2095-2100.

Schlenkrich T, Porst M and Hader D, A rapid, simple method for the isolation and characterization of the photoreceptor of *Dictyostelium discoideum* amoebae. *FEBS Lett* 1995a, **364** 276-278.

Schlenkrich T, Fleischmann P and Hader DP, Biochemical and spectroscopic characterization of the putative photoreceptor for phototaxis in amoebae of the cellular slime mould *Dictyostelium discoideum*. *J Photochem Photobiol B* 1995b, 139-143.

Schmeichel K and Beckerle M, The LIM domain is a modular protein-binding interface. *Cell* 1994, **79** 211-219.

Schneider S, Buchert M and Hovens CM, An *in vitro* assay of β -galactosidase from yeast. *BioTechniques* 1996, **20** 960-962.

Schleicher M, and Noegel AA, Dynamics of *Dictyostelium* cytoskeleton during chemotaxis. *New Biol.* 1992, **4** 461-472.

Schleicher M, Andre B, Andreoli C, Eichinger L, Haugwitz M, Hofmann A, Karakesisoglou J, Stockelhuber M and Noegel A, Structure/function studies on cytoskeletal proteins in *Dictyostelium* amoebae as a paradigm. *FEBS Lett* 1995, **369** 38-42.

Schwarzman A, Singh N, Tsiper M, Gregori L, Dranovsky A, Vitek M, Glabe C, St George-Hyslop P and Goldgaber D, Endogenous presenilin 1 redistributes to the surface of lamellipodia upon adhesion of Jurkat cells to a collagen matrix. *Proc Natl Acad Sci U S A.* 1999, **96** 7932-7937.

Shaffer B, Q. *J. Microb. Sci.* 1957, **98** 393-405.

Sharma C, Ezzell R and Arnaout M Direct interaction of filamin (ABP-280) with the β 2-integrin subunit CD18. *J. Immunol.* 1995, **154** 3461-3470.

Siegert F and Weijer C, Three-dimensional scroll waves organize *Dictyostelium* slugs. *Proc Natl Acad Sci U S A.* 1992, **89** 6433-6437.

Siegert F and Weijer C, Spiral and concentric waves organize multicellular *Dictyostelium* mounds. *Curr Biol.* 1995, **5** 937-943.

Simpson P, Spudich J. and Parham P, Monoclonal antibodies prepared against *Dictyostelium* actin: characterization and interaction with actin. *J. Cell. Biol.* 1984, **1** 287-295.

Smith E, Fisher P, Grant W and Williams K, Sensory behaviour in *Dictyostelium discoideum* slugs: Phototaxis and thermotaxis are not mediated by a change in slug speed. *J. Cell Sci.* 1982, **54** 329-339.

Soll D, Wessels D, Voss E. and Johnson O, Computer-assisted systems for the analysis of amoeboid cell motility. *Methods Mol. Biol.* 2001, **161** 45-58.

Stahlhut M and van Deurs B, Identification of filamin as a novel ligand for caveolin-1: evidence for the organization of caveolin-1-associated membrane domains by the actin cytoskeleton. *Mol Biol Cell.* 2000, **11** 325-337.

Stege J, Shaulsky G and Loomis W, tip genes act in parallel pathways of early *Dictyostelium* development. *Dev Biol.* 1997, **185** 34-41.

Stege J, Laub M and Loomis W, Sorting of the initial cell types in *Dictyostelium* is dependent on the tipA gene. *Dev Genet.* 1999, **25** 64-77.

Stocker S, Hiery M and Marriott G, Phototactic migration of *Dictyostelium* cells is linked to a new type of gelsolin-related protein. *Mol Biol Cell.* 1999, **10** 161-178.

Studier F and Moffatt B, Use of bacteriophage T7 RNA polymerase to direct selective high level expression of cloned genes. *J. Mol. Biol.* 1986, **189** 113-130.

Sussman M, The origin of cellular heterogeneity in the slime molds, *Dictyosteliaceae*. *J. Exp. Zool.* 1951, **118** 407-417.

Takafuta T, Wu G, Murphy G and Shapiro S, Human β -filamin is a new protein that interacts with the cytoplasmic tail of glycoprotein IbK, *J. Biol. Chem.* 1998, **273** 17531-17538.

Taylor W Protein structure comparison using SAP. *Methods Mol Biol.* 2000, **143** 19-32.

Thompson T, Chan Y, Hack A, Brosius M, Rajala M, Lidov H, McNally E, Watkins S and Kunkel L Filamin 2 (FLN2): A muscle-specific sarcoglycan interacting protein, *J. Cell Biol.* 2000, **148** 115-126.

Tigges U, Koch B, Wissing J, Jockusch B and Ziegler W. The F-actin cross-linking and focal adhesion protein filamin A is a ligand and in vivo substrate for protein kinase C alpha. *J Biol Chem.* 2003, **278** 23561-23569.

Towbin H, Staehelin T. and Gordon J. Electrophoretic transfer of proteins from polyacrylamide gels to nitrocellulose sheets: procedure and some applications. *Proc. Natl. Acad. Sci. USA.* 1979, **76** 4350-4354

Troys V, Vandekerckhove J and Ampe C Structural modules in actin-binding proteins: towards a new classification. *Biochim. Biophys. Acta* 1999, **1448** 323-348.

Tu Y, Li F, Goicoechea S and Wu C, The LIM-only protein PINCH directly interacts with integrin-linked kinase and is recruited to integrin-rich sites in spreading cells. *Mol. Cell. Biol.*, 1999, **19** 2425-2434.

Ueda M, Oho C, Takisawa H and Ogihara S, Interaction of the low-molecular-mass, guanine-nucleotide-binding protein with the actin-binding protein and its modulation by the cAMP-dependent protein kinase in bovine platelets, *Eur. J. Biochem.* 1992, **203** 347-352.

Vadlamudi R, Li F, Adam L, Nguyen D, Ohta Y, Stossel T and Kumar R, Filamin is essential in actin cytoskeletal assembly mediated by p21-activated kinase 1. *Nat Cell Biol.* 2002, **4** 681-690.

van der Flier A and Sonnenberg A, Structural and functional aspects of filamins. *Biochim Biophys Acta.* 2001, **1538** 99-117.

Vardar D, Chisti A, Frank B, Luna E, Noegel A, Oh S, Schleicher M and McKnight C, Villin-type headpiece domains show a wide range of F-actin binding affinities. *Cell Motil. Cytoskel.* 2002, **52** 9-21.

Vieira J. and Messing J, The pUC plasmid, a M13mp7-derived system for insertion mutagenesis and sequencing with synthetic universal primers. *Gene* 1982, **19** 259-268.

Wallach D, Davies P and Pastan I, Cyclic AMP-dependent phosphorylation of filamin in mammalian smooth muscle, *J. Biol. Chem.* 1978, **253** 4739-4745.

Wallraff E and Wallraff H, Migration and bidirectional phototaxis in *Dictyostelium discoideum* slugs lacking the actin cross-linking 120 kDa gelation factor. *J Exp Biol* 1997, **200** 3213-3220.

Wang B and Kupsa A, *Dictyostelium* development in absence of cAMP. *Science* 1997, **277** 251-254.

Wang F, Van Brocklyn JR, Edsall L, Nava V and Spiegel S. Sphingosine-1-phosphate inhibits motility of human breast cancer cells independently of cell surface receptors. *Cancer Res.* 1999, **15** 6185-6191.

Watanabe N and Kusumi A. The Ste20 group kinases as regulators of MAP kinase cascades. *Trends Cell Biol.* 2001, **11** 220-230.

Weber I, Gerisch G, Heizer C, Murphy J, Badelt K, Stock A, Schwartz J and Faix J Cytokinesis mediated through the recruitment of cortexillins into the cleavage furrow. *EMBO J.* 1999, **18** 586-594.

Weiner O, Murphy J, Griffiths G, Schleicher M and Noegel A The actin-binding protein comitin (p24) is a component of the Golgi apparatus. *J. Cell Biol.* 1993, **123** 23-34.

Westphal M, Jungbluth A, Heidecker M, Mühlbauer B, Heizer C, Schwarz J, Marriot G and Gerisch G. Microfilament dynamics during cell movement and chemotaxis monitored using a GFP-actin fusion. *Curr. Biol.* 1997, **7** 176-183.

Wilkins A, Khosla M, Fraser D, Spiegelman GB, Fisher P, Weeks G and Insall R, *Dictyostelium* RasD is required for normal phototaxis, but not differentiation. *Genes Dev.* 2000, **14** 1407-1413.

Williams K and Newell P, A genetic study in the cellular slime mold *Dictyostelium discoideum* using complementation analysis. *Genetics.* 1976, **82** 287-307.

Wu L and Franke J, A developmentally regulated and cAMP-repressible gene of *Dictyostelium discoideum*: cloning and expression of the gene encoding cyclic nucleotide phosphodiesterase inhibitor. *Gene.* 1990, **91** 51-56.

Yada Y, Okano Y and Nozawa Y, Enhancement of GTP Q Sbinding activity by cAMP-dependent phosphorylation of a filamin-like 250 kDa membrane protein in human platelets, *Biochem. Biophys. Res. Commun.* 1990, **172** 256-261.

Yumura S and Fukui Y, Filopodelike projections induced with dimethyl sulfoxide and their relevance to cellular polarity in *Dictyostelium*. *J Cell Biol.* 1983, **96** 857-865.

Zhang W, Han S, McKeel D, Goate A and Wu J, Interaction of presenilins with the filamin family of actinbinding proteins. *J. Neurosci.* 1998, **18** 914-922.

Zent R, Fenczik C, Calderwood D, Liu S, Dellos M and Ginsberg M, Class- and splice variant-specific association of CD98 with β integrin cytoplasmic domains. *J. Biol. Chem.* 2000, **275** 5059-5064.

Zhuang Q, Rosenberg S, Lawrence J and Stracher A, Role of actin binding protein phosphorylation in platelet cytoskeleton assembly. *Biochem. Biophys. Res. Commun.* 1984, **118** 508-513.

VII. Abbreviations

APS	ammonium persulphate
bp	base pair(s)
BSA	bovine serum albumin
Bsr	blasticidin resistance cassette
cAMP	cyclic adenosine monophosphate
CCD	charge-coupled device
cDNA	complementary DNA
CIAP	calf intestinal alkaline phosphatase
dNTP	deoxyribonucleotide triphosphate
DMSO	dimethylsulphoxide
DNA	deoxyribonucleic acid
DNase	deoxyribonuclease
DTT	1,4-dithiothreitol
ECL	enhanced chemiluminescence
EDTA	ethylenediaminetetraacetic acid
EGTA	ethyleneglycol-bis (2-amino-ethylene) N,N,N,N-tetraacetic acid
G418	geneticin
GFP	green fluorescent protein
GST	glutathione S-transferase
HEPES	N-(2-hydroxyethyl) piperazine-N'-2-ethanesulphonic acid
HRP	horse radish peroxidase
IgG	immunoglobulin G
IPTG	iso-propylthio-galactopyranoside
Kb	kilobase pairs
KD	kilodalton
MES	morpholinoethansulphonic acid
β -ME	beta-mercaptoethanol
MOPS	Morpholinopropanesulphonic acid

MW	molecular weight
NP-40	nonylphenylpolyethyleneglycol
OD	optical density
PAGE	polyacrylamide gel electrophoresis
PCR	polymerase chain reaction
PIPES	piperazine-N,N'-bis(2-ethanesulphonic acid)
PMSF	phenylmethylsulphonyl fluoride
RNA	ribonucleic acid
RNase	ribonuclease
rpm	rotations per minute
SDS	sodium dodecyl sulphate
TEMED	N,N,N',N'-tetramethyl-ethylendiamine
TRITC	tetramethylrhodamine isothiocyanate
UV	ultraviolet
vol.	volume
v/v	volume by volume
w/v	weight by volume
X-gal	5-bromo-4-chloro-3-indolyl-D-galactopyranoside

Units of Measure and Prefixes

Unit Name

°C	degree Celsius
D	Dalton
g	gram
h	hour
L	litre
m	metre
min	minute
ng	nanogram
sec.	second
µg	microgram
V	volt

Erklärung

Ich versichere, dass ich die von mir vorgelegte Dissertation selbständig angefertigt, die benutzten Quellen und Hilfsmittel vollständig angegeben und die Stellen der Arbeit - einschließlich Tabellen und Abbildungen -, die anderen Werke im Wortlaut oder dem Sinn nach entnommen sind, in jedem Einzelfall als Entlehnung kenntlich gemacht habe; dass diese Dissertation noch keiner anderen Fakultät oder Universität zur Prüfung vorgelegen hat; dass sie - abgesehen von unten angegebenen beantragten Teilpublikationen - noch nicht veröffentlicht ist, sowie, dass ich eine Veröffentlichung vor Abschluss des Promotionsverfahrens nicht vornehmen werde. Die Bestimmungen dieser Promotionsordnung sind mir bekannt. Die von mir vorgelegte Dissertation ist von Frau Prof. Dr. Angelika A. Noegel betreut worden.

Köln, den 18.09.2003

Nandkumar Krishna Khaire

Teilpublication:

1. Gloss A, Rivero F, **Khaire N**, Müller R, Loomis W, Schleicher M and Noegel A, Villidin, a novel WD-repeat and villin related protein from Dictyostelium is associated with membrane and the cytoskeleton. *Mol Biol Cell*. 2003, **14** 2716-2727.
2. Khurana B, Khurana T, **Khaire N** and Noegel A, Functions of LIM proteins in cell polarity and chemotactic motility. *EMBO J*. 2002, **21** 5331-5342.

Curriculum Vitae

Name	Nandkumar Krishna Khaire
Date of birth	03.03.1972
Place of birth	Solapur, India
Nationality	Indian
School education	
1977-1990	School education from 1st to 12th class
06.1988	10th class examination, Maharashtra, India
06.1990	12th class examination, Maharashtra, India
University Studies	
1991-1993	Bachelor of Science D.B.F. Dayanand College of Arts and Science Solapur, Shivaji University, Kolhapur, India
1994-1995	Master of Science Major subject: Biochemistry Department of Biochemistry Shivaji University Campus, Shivaji University, Kolhapur, India
Doctoral Studies	
10.2000 -12.2003	Advisor: Prof. Dr. Angelika A. Noegel, Institute of Biochemistry I, Medical Faculty, University of Cologne, Cologne, Germany Title of the Ph.D. thesis: 'Functional studies of phototaxis in mutants of <i>Dictyostelium discoideum</i> '.

Lebenslauf

Nandkumar K. Khaire,
Doctoral Student,
Prof. Angelika Noegel's Lab,
Institut für Biochemie I,
Medizinische Fakultät,
Universität zu Köln,
Joseph-Stelzmann-Strasse 52,
D50931 Köln
Ph. +49-221-478-6988,
Fax. +49-221-478-6979.
Email: khaire.nandkumar@uni-koeln.de



Geburtsdatum	03.03.1972
Geburtsort	Solapur, India
Staatsangehörigkeit	Indisch
Schulbildung	
1977-1990	Schulbildung 1. bis 12. Klasse
06.1988	Abschlußprüfung 10. Klasse, Maharashtra, Indien
06.1990	Abschlußprüfung 12. Klasse, Maharashtra, Indien
Studium	
1991-1993	Bachelor of Science D. B. F. Dayanand College of Arts and Science Solapur, Shivaji University, Kolhapur, India
1994-1995	Master of Science Hauptfach: Biochemie Department of Biochemistry Shivaji University Campus, Shivaji University, Kolhapur, India
Promotionsstudium	
10.2000 -12.2003	Betreuerin: Prof. Dr. Angelika A. Noegel, Institut für Biochemie I, Medizinische Fakultät der Universität zu Köln. Thema: 'Functional studies of phototaxis in mutants of <i>Dictyostelium discoideum</i> '.